Nuclear receptor co-repressor actions in bladder cancer

By

Syed Asad Abedin

A thesis presented to the School of Clinical and Experimental Medicine,

University of Birmingham,

For the degree of Doctor of Medicine (MD).

School of Clinical and Experimental Medicine

College of Medical and Dental Sciences

University of Birmingham

September 2009

Summary

Nuclear receptors are ligand dependent transcription factors and have defined expression patterns in classical tissues for example the Vitamin D receptor is expressed in small bowel, kidney and skin, as related to its function in maintaining serum calcium levels. However, nuclear receptor expression has also been demonstrated in non classical tissues for example VDR expression in the prostate and breast. Differential expression of a panel of nuclear receptors in bladder cancer cell lines (RT-4, RT-112, HT1376 and EJ-28 cells) at mRNA level and VDR and FXR expression at protein level has ben demonstrated. These cell lines demonstrate a range of anti-proliferative responses upon treatment with ligands to the panel of nuclear receptors ($1\alpha,25(OH)_2D_3$, 9 cis RA, EPA, ETYA, CDA, LCA, 22HC, GW3965 and DHA). EJ-28 cells are the least sensitive to the anti-proliferative effects of 5 of these ligands ($1\alpha,25(OH)2D3$, LCA, EPA, ETYA, CDA). EJ-28 cells also have the highest expression of the co-repressor NCoR1; this may be partly responsible for the reduced sensitivity displayed by EJ-28 cells by maintaining a closed chromatin structure around the nuclear receptor response elements. To test this, NCoR1 has been stably over-expressed in RT-4 cells which have the lowest relative expression of this co-repressor. This led to a statistically significant reduction in anti-proliferative response to CDA, LCA and the histone deacetylase inhibitor SAHA.

To further test the hypothesis that raised NCoR1 expression and hence a predominance of the co-repressor complex in EJ-28 cells was affecting the sensitivity to NR ligands, the four bladder cancer cell lines were co-treated with the NR ligands and the HDAC inhibitor SAHA. This demonstrated a strongly additive anti-proliferative response in RT-112 and E-28 cells which have raised NCoR1 expression. This may be due increased HDAC association with NRs at their respective response elements which may make these particular cells more susceptible to co-treatment with ligand and SAHA. The possible mechanism of the anti-proliferative response within EJ-28 cells is demonstrated to be a G1/S phase cell cycle arrest upon treatment with LCA +/- SAHA.

The expression of putative target genes was investigated using Q-RT-PCR, Q-RT-PCR$_m$ and Affymetrix human U133 genechip arrays upon treatment with LCA +/- SAHA. RT-4 and EJ-28 cells

express *CDKN1A* upon combined treatment with LCA + SAHA. LCA treatment leads to expression of the cytochrome P450 enzyme CYP3A4 mRNA in RT-4, RT-112 and HT1376 cells. However, the combined treatment with LCA + SAHA leads to CYP3A4 expression in EJ-28 cells.

RT-4 cells stably transfected to over-express NCoR1, were treated with LCA and the target transcriptome investigated using Q-RT-PCR$_m$. Three predominant groups of genes were induced; ABC transporter family of trans-membrane efflux pumps, detoxifying enzymes and cell cycle arrest proteins. EJ-28 cells were treated with LCA +/- SAHA and the target transcriptome investigated by hybridisation of cRNA to U133 Affymetrix genechip arrays. This yielded 3 predominant groups of targets; genes which drive cell proliferation and cell cycle progression, genes involved in transcription and post translational mRNA processing and genes involved in repair of damaged cellular components. Taken together, these two target transcriptomes suggest the presence of a xenobiotic protective response within the bladder urothelium which upon exposure to toxic compounds such as LCA inhibits cell division, expresses trans-membrane transporters and detoxifying enzymes to rid the cell of the toxin and finally initiates cellular repair. These findings may be harnessed for chemoprevention of bladder cancer by enhancing resistance to xenobiotics such as those derived from cigarette smoke.

<u>Acknowledgements</u>

I would like to thank my supervisor, Dr Moray Campbell for appointing me to a research position in his group, for his constant support, encouragement and help without which this thesis would not have been completed.

My deepest thanks and gratitude go to my wife, children, parents and in laws who have sacrificed enormously in supporting me through my years in research.

I have been particularly fortunate in having a fantastic group of scientists around me who have been friends and key supporters of my research. In particular, I would like to thanks Serena Rakha, Sebastiano Battaglia and James Thorne who were all members of the Campbell Group. Amongst the other scientists who I would like to thank in particular are Chris Bruce and Ashraf Dallol from the Department of Medical Genetics and Katie Evans, Helen Pemberton, Dai Kim, Anna Stratford and Farhat Khanim from the Departments of Endocrinology and Biosciences.

I have received vital help and support in the Affmetrix genechip experiments from Sim Sahota and Dr John Arrand from the Institute of Cancer Studies for which I am very grateful.

I am indebted to the Department of Urology at the Queen Elizabeth Hospital, Birmingham for their vital support, in particular for appointing me to the research post jointly with Dr Moray Campbell and for organising research funding. I am particularly indebted to Messrs Mike Wallace, Andrew Arnold and Alan Doherty.

This work was supported by the Department of Urology of the University Hospital Birmingham Foundation NHS Trust.

Abbreviations:-

ABC	**ATP-binding cassette**
AIF	apoptosis inducing factor
AMV	avian myeloblastosis virus
AR	Androgen receptor
ATP	Adenosine triphosphate
ATRA	All-trans retinoic acid
9 cRA	9 *cis* retinoic acid
22-HC	22-hydroxycholesterol
cAMP	cyclic adenosine monophosphate
CAR	Constitutive androsterone receptor
CBP	cAMP response element binding protein binding protein
CDA	chenodeoxycholic acid
CDC25	cell division cycle 25
CDK	cyclin dependent kinase
CDKI	cyclin dependent kinase inhibitor
cDNA	complimentary deoxyribonucleic acid
ChIP	chromatin immunoprecipitation
CHO	Chinese hamster ovary
CIS	Carcinoma in situ
CoA	co-activator

CoR	co-repressor
cRNA	complimentary ribonucleic acid
CYP	cytochrome p450 enzyme
CYP3A4	cytochrome p450 enzyme, family 3, subfamily A, polypeptide 4
CYP24	cytochrome p450 enzyme, 24-hydroxylase
DBD	DNA binding domain
DEX	dexamethasone
DHA	Cis 4,7,10,13,16,19 Docosahexaenoic acid
DMEM	Dulbecco's modified Eagle's medium
DNA	deoxyribonucleic acid
DRIP	vitamin D receptor interacting protein
DTT	Dithiothreitol
ED_{25}	Dose required to inhibit cell proliferation by 25%
ED_{50}	Dose required to inhibit cell proliferation by 50%
EDTA	ethylenediaminetetraacetic acid
EGFR	epidermal growth factor receptor
ER	estrogen receptor
EPA	Eicosapentaenoic acid
ETYA	5,8,11,14-eicosatetraenoic acid
FACS	fluorescence activated cell sorter
FXR	Farnesoid X-activated receptor
GAG	Glycosaminoglycans
GR	glucocorticoid receptor

GSTM1	Glutathione-S-transferase M1
HAT	histone acetyltransferase
HDAC	histone deacetylase
HDACi	histone deacetylase inhibitor
HIV	human immunodeficiency virus
HNF4α	hepatocyte nuclear factor 4α
HRP	horseradish peroxidase
Kb	kilo base
KD	kilo Dalton
LCA	Lithocholic acid
LCOR	Ligand-dependent nuclear receptor corepressor
LBD	ligand binding domain
LXR	Liver X receptor
MMLV	Moloney murine leukemia virus
MNAR	modulator of non-genomic action of estrogen receptor
MR	mineralocorticoid receptor
mRNA	messenger ribonucleic acid
NAT2	N-acetyltransferase 2
Na Cl	Sodium chloride
NCOR1	Nuclear receptor co-repressor 1
NCOR2/SMRT	Silencing mediator of retinoid and thyroid hormone receptors/Nuclear receptor co-repressor 2
NR	nuclear receptor
OD	optical density

PAGE	polyacrylamide gel electrophoresis
PBS	phosphate buffered saline
PCN	pregnenalone-16α-carbonitrile
PCR	polymerase chin reaction
PI	Propidium iodide
PPAR	Peroxisome proliferator activated receptor
PR	progesterone receptor
PVDF	polyvinylidene difluoride
PXR	pregnane X receptor
Q-RT-PCR	quantitative real time, reverse transcription polymerase chain reaction
Q-RT-PCR$_M$	micro-fluidic quantitative real time, RT polymerase chain reaction
RAR	retinoic acid receptor
Rb	retinoblastoma protein
RE	response element
RT	reverse transcription
RXR	retinoid X receptor
SAHA	suberoylanilide hydroxamic acid or vorinostat
SDS	sodium dodecyl-sulphate
SEM	standard error of the mean
SLIRP	SRA stem loop-interacting rna-binding protein
TCC	Transitional cell carcinoma
TRIP15/Alien	Co-repressor Thyroid hormone receptor interactor 15/Alien
TSA	Trichostatin A
UV	ultra-violet

VDR   vitamin D receptor

$1\alpha,25(OH)_2D_3$ $1\alpha,25$dihydroxyvitaminD_3

XREM   xenobiotic response enhancer module

Table of Contents

Table of Figures

Table of Tables

Chapter 1 INTRODUCTION

1.1 Opening Statement

Bladder cancer is a common condition with 10,278 new cases diagnosed every year in the United Kingdom and is the fourth most common cancer in men (Office of National Statistics). This cancer has two broad forms of presentation; approximately 55-60% of tumours present as superficial bladder tumours which have excellent long term survival but are characterised by frequent recurrences (Messing et al., 1995; Prout, Jr. et al., 1992). Approximately 30 % present as muscle invasive disease which is lethal if untreated with the overwhelming majority of patients dying within two years (PROUT and MARSHALL, 1956). Due to the long survival and repeated recurrences in patients with superficial bladder cancer, repeated long term surveillance is necessary with cystoscopic examinations of the bladder. These morbidity and mortality figures are similar in much of Europe and North America. This results in bladder cancer being one of the most costly of all tumours for example with an estimated per patient cost from diagnosis to death at $ 96,000 to $ 187,000 amounting to a direct cost within the USA in 2001 of $ 3.7 billion (Stenzl et al., 2008). Therefore there is an acute need for research led efforts that can firstly distinguish accurately and early between superficial and invasive tumours and secondly generate treatments that can reduce the recurrence rate of these tumours.

1.2   Development and function of the urinary bladder

1.2.1 Human urinary bladder embryology

Development of the human urinary bladder originates from the embryonal hindgut. The terminal part of this structure is an expanded cavity called the cloaca and is lined by endoderm. The anterior aspect of the cloaca is continuous with the allantois, which is a fingerlike diverticulum of the yolk sac. The cloaca is partitioned into an anterior and posterior portion by a wedge of mesenchyme called the urogenital septum. This partitioning is complete by the seventh week of development. The anterior portion is called the urogenital sinus and is divided into a cranial *vesical* part which is continuous with the allantois, a middle *pelvic* part and a caudal *phallic* part. The vesical part gives rise to the urinary bladder. The pelvic part of the urogenital sinus gives rise to the prostatic glandular cells in males.

1.2.2 Transitional epithelium (Urothelium) and Barrier Function

The lining the bladder is described as transitional cell epithelium. This extends from the collecting system of the kidneys, along the ureters, through the bladder and extends to the prostatic urethra in men. This urothelium consists of three layers of cells; the superficial layer of large and flat umbrella shaped cells; an intermediate layer of upto four cells thick which have their long axis perpendicular to the basement membrane and finally a basal layer of cuboidal cells.
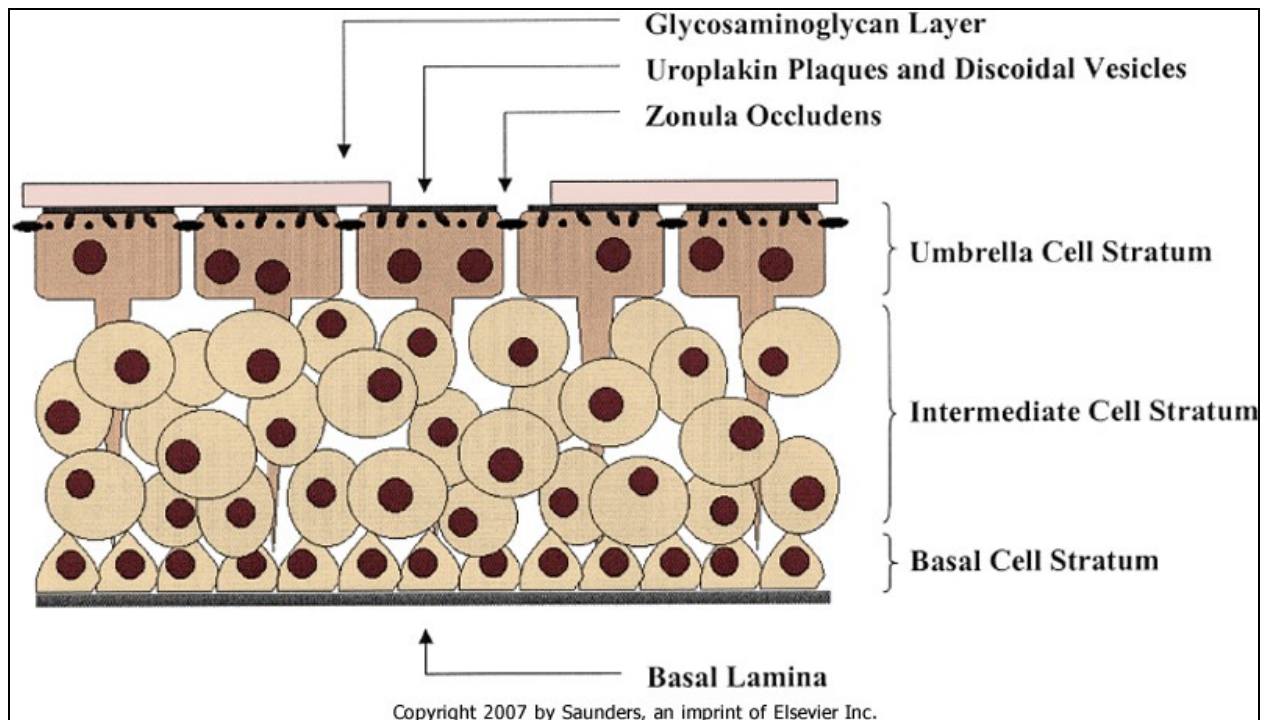
Figure 1.1: Diagram of the structure of the normal urothelium. (adapted from Campbell's Urology 2008, chapter 56). There are three layers of cells; the superficial layer of large and flat umbrella shaped cells; an intermediate layer of upto four cells thick which have their long axis perpendicular to the basement membrane and finally a basal layer of cuboidal cells.

On the luminal surface of the urothelium, there is a layer of glycosaminoglycans (GAGs). These consist of large polysaccharides which are normally found in the ground substance of connective tissue (Poggi et al., 2000). This GAG layer was proposed to be responsible for the "blood-urine barrier" (Parsons et al., 1975) however, this has been discredited due to a number of experimental findings. The GAG layer allows small molecules such as the drug amiloride to pass through it (Niku et al., 1994) and use of microelectrodes has revealed the first electrical resistive barrier to be upon entry into the umbrella cells rather than across the GAG layer.

The umbrella cells form the true blood-urine barrier in the urothelium. They have a uniquely asymmetric cell membrane structure composed of an outer leaflet of large protein plaques and

hinge like regions in between these proteins. The protein plaques are composed of four types of uroplakin proteins (type Ia, Ib, II and III). These proteins are thought to provide the barrier function of the bladder epithelium (Walz et al., 1995). This barrier is further strengthened by tight junctions between umbrella cells (Peter, 1978), these in combination with the protein plaques form the waterproof barrier in the urinary bladder.

The urinary bladder forms a classical epithelium that has significant barrier function as it is exposed to potentially harmful chemical and xenobiotics in the urine on the luminal side and which need to be contained and not allowed to leach into the blood. This is of key importance as much of our current understanding of bladder carcinogenesis is based on exposure of carcinogens carried in the urine, from industrial sources and from cigarette smoke.

1.3 Histopathology of Bladder Cancers

Transitional cell carcinoma (TCC) accounts for > 90% of bladder cancer. This is further divided by pathology into three main patterns. The majority are papillary TCCs, which appear as exophytic, frondlike structures. Second, are sessile TCCs , which are less frondular and have a more solid looking lesion with a broad base. A third form is the carcinoma *in situ* (CIS). This is characterised by flat, erythematous lesions, which may be multifocal and of a high grade. By definition, CIS is a pre-invasive form however, its presence indicates a higher degree of biological aggressiveness and hence a higher chance of progression to an invasive tumour.

Squamous cell carcinoma account for 7-8% of bladder cancer and is associated with chronic irritation of the bladder epithelium. Worldwide, the majority of these cases are linked with chronic Schistosomiasis infection. In the developed world, other causes include bladder calculi and long term urinary catheters.

Adenocarcinoma of the bladder accounts for 1-2 % of cases and is associated with either chronic infection, bladder extrophy or may develop in urachal remnants in the dome of the bladder. The urachus is a thick, fibrous cord which develops from the allantois (see embryology).

Rare types of bladder tumours consist of sarcoma, small cell carcinoma, melanoma and carcinoid tumour.

1.4   Histopathology, grades and staging of TCC

Transitional cell carcinoma is graded into well (G1), moderately (G2) and poorly differentiated (G3) tumours. Grade 1 tumours show increased number of urothelial layers with loss of orientation and hyperchromasia (dark staining nuclei indicative of an increased amount of chromatin). Grade 2 tumours show an increased degree of cell proliferation and loss of polarity within the epithelial layer. Grade 3 lesions are the least differentiated; in some cases it may be difficult to recognise the transitional nature of the epithelium (as described in section 1.2.2).

Bladder cancer is staged according to the 2002 TNM (tumour, lymph nodes and metastases) system. Tumours that have not invaded and breached the basement membrane are denoted pTa. Tumours that have breached through to the lamina propria are denoted pT1; pT2 tumours have invaded the muscularis mucosa; pT3 tumours have invaded the perivesical tissue and pT4 tumours have invaded neighbouring organs (prostate, uterus, vagina, pelvic and abdominal wall).

1.5   Epidemiology of Bladder Cancer

1.5.1 Incidence and Mortality

Bladder cancer is the fourth most common male malignancy and the tenth most common cancer in women in the western world. In Western Europe and the United States, bladder cancer account for 5-10 % of all malignancies in men. The risk of developing bladder cancer is quoted at 2-4 % for men and 0.5-1 % for women under the age of 75 years. The median age at diagnosis is between 65 and 70 years. Age standardised mortality rates globally, vary from 2-10 per 100,000 per year for men and 0.5-4 per 100,000 per year for women.

Bladder cancer has a clear preponderance for men; it is 3-4 times more common in men than women. This excess is not fully explained by the differences in smoking and occupational exposure, which are the two leading risk factors. Evidence from surveys of cancer incidence and mortality suggest that parous women have a lower risk of developing bladder cancer as compared to nulliaparous women. Furthermore, it appears the risk may reduce with increasing parity (Kirkali et al., 2005). Animal experiments suggest a role for androgenic exposure to increasing the risk of developing bladder cancer. Rats treated with androgens had a higher incidence of bladder tumours as compared to animals treated with estrogens. Certainly the reduced incidence in women and further in parous women, suggests a protective role for estrogens in humans too.
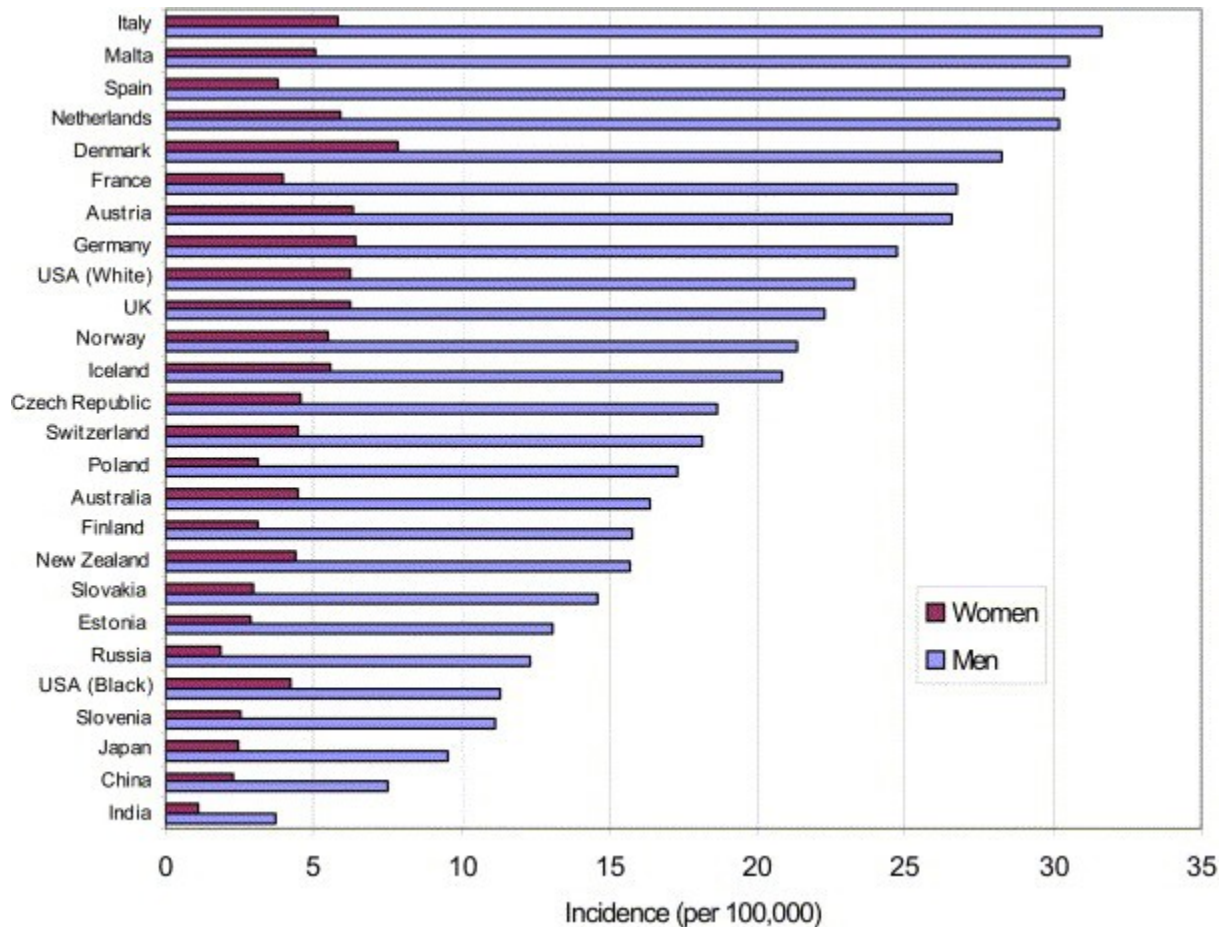
Figure 1.2: The incidence of bladder cancer per country. This illustrates the approximately 3:1 male : female ratio of bladder cancer. The UK has the 10th highest bladder cancer incidence amongst developed countries. (Cancer Research UK, http://info.cancerresearchuk.org/cancerstats/types/bladder/incidence/)

1.6 Pathology of bladder cancer

1.6.1 Bladder Cancer Risk Factors

The two largest groups of risk factors for the development of bladder cancer are industrial/occupational chemicals and smoking. These external carcinogens are likely to exert their effects via exposure of the urothelium to urine containing these carcinogens. Indeed, there is epidemiological evidence that passing urine at night is protective against bladder

cancer even in smokers (Silverman et al., 2008), suggesting that the urothelium's contact time with urine containing carcinogens is important in the pathogenesis of bladder cancer.

1.6.1.1 Occupational / Industrial and Recreational Carcinogens

Industrial bladder carcinogens are most often aromatic amines. As early as 1895, aniline dyes used in the textile industry were identified as bladder carcinogens (Rehn L, Ueber blasentrumoren bei fuchsinarbeitern. Arch Kind Chir 1895;50:588). Other chemicals, mainly used in the rubber and textile industries, also known to be bladder carcinogens are 2-naphthylamine, 4-aminobiphenyl and benzidine (Morrison and Cole, 1976). This occupational exposure is estimated to be responsible for 20 % of bladder cancers in the USA (Cole et al., 1972).

Cigarette smoking is also associated with a four fold increase in the risk of developing bladder cancer (Morrison, 1984; Burch et al., 1989). This risk decreases down to that of non-smokers after 20 years of cessation (Augustine et al., 1988). The exact identity of the bladder specific carcinogenic compounds in cigarette smoke is unknown; however, 4-aminobiphenyl, 2-naphthylamine and nitrosamine, all known carcinogens, are known to be present. The risk of the individual developing bladder cancer is not only dependent on exposure to carcinogens but also depends on genetic variation in xenobiotic metabolising enzymes, for example smokers (with > 30 year smoking history) homozygous for the NAT1*10 allele of the *N*-acetyltransferase, NAT1 gene have an 8.5 fold odds ratio of developing bladder cancer as compared to wild-type carriers (Taylor et al., 1998).

1.6.1.2 Xenobiotic metabolising enzymes and Bladder Cancer Risk

As an epithelial lining, the bladder urothelium is constantly exposed to a wide ranging milieu of chemicals in the urine. As noted above, chronic exposure to geno- and cellulo-toxic

compounds is likely to be a causative factor in bladder cancer initiation and progression. However, the epithelial lining has protective mechanisms against this potentially toxic milieu; genetic and epigenetic variation within the cells of this protective armamentarium most likely leads to variation in bladder cancer risk i.e. individuals who have a more effective protective response have a lower risk of developing bladder cancer that others.

4-aminobiphenyl, a bladder carcinogen in industrial chemicals and cigarette smoke, is detoxified via N-acetylation. N-acetyltransferase 2 (NAT2) is a major acetylating enzyme which exists predominantly in 6 different allelic forms in Caucasians. One particular allele leads to more rapid acetylation activity, hence, people who are homozygous for this allele may have the fastest acetylation activity. Risch et al (Risch et al., 1995) demonstrated that in a group of 189 bladder cancer patients in Birmingham, UK, slow acetylator genotypes predominated amongst bladder cancer patients in groups with industrial chemical and cigarette smoke exposure and without any carcinogenic exposure history at all. Okkels et al (Okkels et al., 1997) have similarly shown that smokers who carry the slow acetylator genotype have a higher risk of developing bladder cancer.

A second enzyme, CYP1A2, a member of the cytochrome P450 group is also implicated with bladder cancer risk. This enzyme de-methylates aromatic amines thereby activating potential carcinogens in urine. Brockmuller et al (Brockmoller et al., 1998) have demonstrated increased risk of bladder cancer in subjects with the highly inducible allele of CYP1A2 who were smokers or had the slow acetylator allels of the NAT-2 enzyme.

Glutathione-S-transferase M1 (GSTM1) is a key carcinogen detoxifying enzyme which conjugates polycyclic aromatic hydrocarbons in cigarette smoke to glutathione. The incidence of homozygous deletion of the gene for this enzyme in Caucasians is approximately 50 % (Bell et al., 1993b). Subjects who are homozygous for the absence of this gene are x1.8 more

likely to develop bladder cancer if they are smokers (Bell et al., 1993). Interestingly, the risk of bladder cancer is identical for non-smokers who are homozygous for GSTM1 absence as for non-smokers who have the allele. Therefore, this gene only seems to provide protection if the individual is exposed to cigarette smoke.

The above provides a second layer to the model of the bladder epithelium being bathed in a milieu of carcinogens in urine. The epithelium has different strategies to effect protection of urothelial integrity and the efficacy of these strategies combine to determine overall risk of malignant change. **Expression of detoxifying enzymes is a key epithelial protective strategy.**

1.6.2 Molecular Pathology of Bladder Cancer

Malignant transformation of a cell is modelled as a stepwise process of increasing genotypic and epigenetic accumulation of abnormalities which lead to the acquisition of a common set of phenotypic characteristics. Hanahan and Weinberg (Hanahan and Weinberg, 2000) elucidated this model in terms of six key phenotypic traits which could be acquired in any sequence but would allow the cell to behave in a transformed malignant manner. These traits are as follows:

1. Self sufficiency in growth signals.
2. Insensitivity to growth inhibitory signals.
3. Evasion of programmed cell death.
4. Limitless replicative potential.
5. Sustained angiogenesis.
6. Tissue invasion and metastasis.

Self sufficiency in growth signals is most commonly manifest by activating, dominant mutations in oncogenes.

1.6.2.1 Oncogenes in bladder cancer

The best characterised oncogene to be mutated in bladder cancer is H-RAS. This encodes a GTP-ase that is a key signal transduction molecule, allowing signals from activated cell membrane based receptors, such as epidermal growth factor receptor (EGFR), to be transmitted to the cell nucleus. H-RAS mutations have been detected in upto 45 % of bladder tumours and the frequency appears to be greater in higher grade tumours; upto 65 % in poorly differentiated bladder transitional cell cancers (Czerniak et al., 1992).

EGFR (ERBB1) is one of the family of growth factor receptors found to be overexpressed in bladder cancer patients. Neal et al (Neal et al., 1990) have demonstrated EGFR (ERBB1) positivity in 48 % of their series of bladder cancer patients and have shown a significant independent association of EGFR positivity with poor outcome i.e. risk of death from bladder cancer, risk of recurrence and shorter time to recurrence.

These are examples of self-sufficency in growth signals. Activating mutations of H-RAS allow a growth stimulatory signalling pathway to be constitutively switched on driving cell proliferation. This pathway would normally be turned on in response to ligand binding of a growth factor to its relevant receptor, however, mutations bypass this requirement and allow inappropriate signal transduction. Increased expression of growth factor receptors, such as EGFR (ERBB1) and ERBB2, a similar growth factor receptor (Sauter et al., 1993; Moch et al., 1993), allows the cancer cell to firstly be more sensitive to growth signals and in the case of constitutively active mutations, allow downstream growth signalling in the absence of appropriate growth factor binding.

1.6.2.2 Tumour Suppressor Gene defects in Bladder Cancer

Tumour suppressor genes encode for proteins which have a growth restricting role. The retinoblastoma gene was first described (Knudson, Jr., 1971) as requiring two hits or mutations for retinoblastoma to develop. Hence, tumour suppressor genes are recessive.

P53 is a key tumour suppressor gene which functions in three important ways to inhibit carcinogenesis. In the presence of DNA damage, it causes a G1/S cell cycle arrest which can progress into cellular senescence, it upregulates DNA repair enzymes and may also lead the cell down an apoptosis or programmed cell death pathway.

1.6.2.2.1 p53 and bladder cancer

P53 has long been associated with bladder cancer. Wild type p53 has a very short half life of 15 to 30 minutes (Oren et al., 1981). Mutations in the p53 gene lead to dysfunctional nuclear accumulation of the protein (Finlay et al., 1988) which is the basis of detection via immuno-histochemistry. Cote and co-workers have assessed the relative effects of gene mutations and altered p53 protein accumulation and outcomes in bladder cancer (George et al., 2007). Their sample population consisted of 150 radical cystectomy specimens from patients with muscle invasive or recurrent high grade, non-invasive bladder cancer. P53 gene mutations were detected using the Affymetrix® p53 gene chip; protein mutations were assessed by immuno-histochemistry. The authors divided samples in two groups; tumours with less than 10 % of tumour nuclei staining for p53 were designated wild type and tumours with 10% or greater nuclei staining were designated altered p53 protein status. 37 % of tumours were found to have p53 gene mutations and 36 % of tumours had nuclear accumulation of p53 protein. Mutations were associated with clinical stage of the tumours. Therefore, 26%, 42 % and 50 % of organ confined, locally advanced and lymph node positive tumours respectively had p53 gene mutations and 19%, 40% and 63% of organ confined, locally advanced and lymph node

positive tumours had p53 altered protein status. Interestingly, the p53 gene mutations were concentrated in exons 5-8 which represent the DNA binding domains.

Confirming the close relationship between abnormal p53 status and bladder cancer, both protein status and gene mutations have a correlation with clinical outcome. Tumours with wild type p53 protein have a 5 year recurrence free survival of 70 % as compared to 32 % for altered p53 protein. Similarly, patients with wild type p53 genes had a 5 year recurrence free survival of 66 % as compared to 44 % for patients with tumours with p53 gene mutations.

1.6.2.2.2 Retinoblastoma protein (Rb) and Bladder Cancer

Rb is the prototypical tumour suppressor gene. Its role is central in regulating the cell cycle.

Figure 1.3: Cell cycle control as exerted by cyclins, cyclin dependent kinases and Rb protein and E2F family of transcription factors (Kolch et al., 2002).

Regulation of the cell cycle is concentrated within the G1 phase. This phase is divided by the presence of a restriction point which behaves as a point of no return and is present after approximately 80-90 % of G1 has passed. The period of G1 preceding the restriction point is

characterised by the cell's dependence on constant extracellular mitogenic signals, usually via growth factors binding to cell membrane based receptors. Withdrawal of these mitogenic signals during this part of phase G1 would cease further passage of the cell through the remaining phases of the cell cycle. Once a cell passes the restriction point, it ceases to require any further extracellular growth signals to complete cell division and proceeds through the remaining phases of the cell cycle generally independent of the surrounding cell signalling milieu, whether pro- or anti-proliferative. Therefore, the restriction point is of fundamental importance to cell cycle regulation; Rb protein provides the molecular explanation of this aspect of the cell cycle. At a molecular level, the degree of phosphorylation of Rb protein molecules is key to its regulation. At the beginning of G1, D-type cyclins together with their partners, CDK4/6 (cyclin dependent kinase 4/6) initiate Rb phosphorylation. In this hypophosphorylated state, Rb continues to remain bound to the E2F family of transcription factors and inhibits their function as transcriptional activators of S-phase. As the cell approaches the restriction point, cyclin E levels rise and, together with its partner CDK2, further phosphorylate Rb to a hyper-phosphorylated state. In this state, Rb binding to E2F family members is inhibited and the unbound E2F transcription factors are free to initiate transcription of target genes which in turn act to drive the cell through the remaining phases of the cell cycle.

Rb gene mutations have been reported in all grades of urothelial cancer. Miyamoto investigated 30 primary bladder tumour samples using PCR based restriction fragment length polymorphism analysis (Miyamoto et al., 1995). Eight samples (27 %) were found to have Rb gene mutations which were spread across grades between superficial as well as muscle invasive bladder tumours. Therefore, 10 % of grade 1, 50 % of grade 2 and 25 % of poorly

differentiated grade 3 tumours had Rb mutations. 21 % of superficial tumours and 36 % of muscle invasive tumours had mutations.

Cote et al have correlated the expression of Rb with recurrence rate and survival in bladder cancer patients (Cote et al., 1998). They have analysed 185 radical cystectomy specimens in patients who have muscle invasive bladder cancer using immunohistochemistry to delineate nuclear expression of Rb protein. They divided the samples into 3 groups; patients with no expression, patients with moderate expression defined as 1%-50% of tumour cells showing Rb expression and finally patients with high levels of expression defined as >50 % of cells positive for nuclear Rb expression. Interestingly, both patients with no expression and those with high expression of Rb had similar rates of tumour recurrence (60% and 61 % respectively) and 5 year survival (33 % both groups). A possible explanation is provided by a later study of levels of Rb phosphorylation in bladder cancer (Chatterjee et al., 2004) by the same group. They studied 28 muscle invasive bladder cancer specimens and measured Rb and phosphorylated-Rb levels using Western blotting from frozen tumour specimens as well as using immunohistochemistry, using antibodies specific for the native as well as the phosphorylated forms of Rb protein. The authors demonstrated 71 % hyperphosphorylation of Rb in tumours with a high expression of total Rb as compared to 36 % hyperphosphorylation in tumours with moderate expression suggesting that constitutive hyperphosphorylation of the Rb protein may be a mechanism of Rb inactivation despite high overall expression. This is an interesting example of corruption of the normal cellular regulation mechanisms in cancer cells which afford a selective growth advantage to the cell. Therefore, as previously described, Rb hyperphosphorylation is involved in reversibly inactivating Rb at the restriction point of the cell cycle which leads to its detachment from members of the E2F family of transcription factors. The degree of hyperphosphorylation increases throughout S, G2 and M phases. At the

junction between mitosis and the onset of G1, Rb is dephosphorylated. It is the corruption of this process which may lead to constitutively hyperhosphorylated Rb in a subset of bladder cancer.

1.7 Nuclear Receptor Superfamily

1.7.1 Structure of Nuclear Receptors

Nuclear receptors (NR) constitute a family of transcription factors which mostly bind lipophilic molecules; thus becoming activated and binding particular response elements within the promoters of target genes and thereby regulating target gene transcription. Sequence homology studies have revealed 21 NR genes in *Drosophila melanogaster*, 48 in humans, 49 in mice and 270 in *Caenorhabditis elegans*. NRs have a common canonical structure; consisting of an N-terminal AF1 domain which behaves as a constitutively active transactivation domain. The DNA binding domain (DBD) is the most conserved region within NR structure. This contains a short motif called the P-box which is responsible for DNA binding specificity on sequences containing a hexameric nucleotide motif. A highly conserved feature of the DBD are two zinc fingers each containing four cystine amino acids which each chelate a zinc ion. This region is also involved in dimerisation of NRs.

After the DBD, NRs contain a D-domain which acts as a hinge region between the DBD and the ligand binding domain (LBD). The latter is the largest domain and contains a secondary protein structure of 12 α helices. As expected, the LBD is also responsible for trans-activation function of NRs following biding of ligand.

The nuclear receptor superfamily is divided into 7 subfamilies; within each subfamily NRs are classified into separate groups and individual genes within each group. The subfamilies are summarised below:

Subfamily 1: Thyroid Hormone Receptor-like

    Group A: Thyroid hormone receptor (Thyroid hormone)

    Group B: Retinoic acid receptor (Vitamin A and related compounds)

    Group C: Peroxisome proliferator-activated receptor (fatty acids, prostaglandins)

    Group D: Rev-ErbA (heme)

    Group F: RAR-related orphan receptor (cholesterol, ATRA)

    Group H: Liver X receptor-like (oxysterol)

    Group I: Vitamin D receptor-like

Subfamily 2: Retinoid X Receptor-like

    Group A: Hepatocyte nuclear factor-4 (HNF4) (fatty acids)

    Group B: Retinoid X receptor (RXRα) (retinoids)

    Group C: Testicular receptor

    Group E: TLX/PNR

    Group F: COUP/EAR

Subfamily 3: Estrogen Receptor-like

    Group A: Estrogen receptor (Sex hormones: Estrogen)

    Group B: Estrogen related receptor

    Group C: 3-Ketosteroid receptors

Subfamily 4: Nerve Growth Factor IB-like

        Group A: NGFIB/NURR1/NOR1

Subfamily 5: Steroidogenic Factor-like

        Group A: SF1/LRH1

Subfamily 6: Germ Cell Nuclear Factor-like

        Group A: GCNF

Subfamily 0: Miscellaneous

        Group B: DAX/SHP

        Group C: Nuclear receptors with two DNA binding domains (2DBD-NR)

           (A novel subfamily)

Figure 1.4: Canonical structure of NR domains. DBD – DNA binding domain, LBD – ligand binding domain.

1.7.2 Nuclear Receptor Signal Transduction

1.7.2.1 Classical signalling pathways

Nuclear receptors may be present in the cell cytoplasm, bound to chaperone heat shock proteins or alternatively may be present within the cell nucleus bound to a multimeric mega-

dalton co-repressor protein complex (see below). The dynamics of receptor distribution and re-distribution upon ligand activation are becoming increasingly apparent. NR ligands are lipid soluble small molecules which diffuse freely across the cell membrane and bind to the LBD of the relevant NR. This initiates a conformational change within the NR structure and leads to dissociation of either chaperone proteins or the co-repressor protein complex. Cytoplasmic NRs translocate to the nucleus and both types bind hormone response elements which are short DNA sequences within promoters of target genes. This binding is co-incident with the recruitment of a multimeric mega-dalton co-activator complex of proteins which associate with the ligand bound NR dimer. This complex contains co-activator proteins which have histone acetyltransferase activity; histone acetylation results in local uncoiling of DNA around structural histone proteins. The co-activator complex also recruits RNA polymerase II and the basal transcriptional machinery; chromatin uncoiling allows RNA pol II access to the transcriptional start site resulting in target gene transcription.
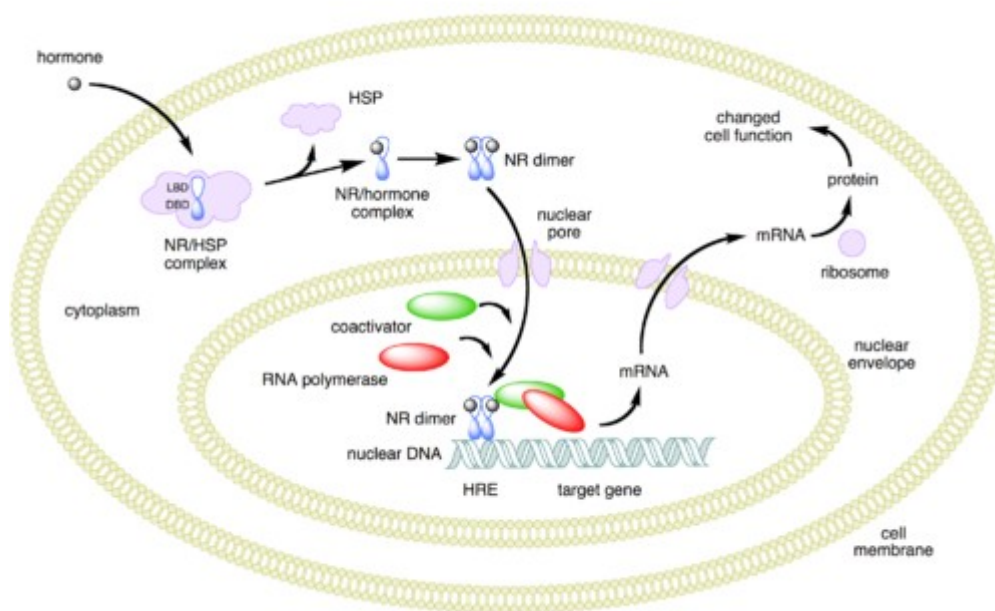
Figure 1.5: Diagram of the conventional model of NR signal transduction for a cytoplasmic located receptor such as AR. Most NR ligands are lipophilic, hence freely diffuse across the lipid bilayer cell membrane. The ligands bind NR either in the cytoplasm or the nucleus. This NR-ligand complex binds at relevant response elements in target gene promoters along with a multimeric mega-dalton co-activator complex which recruits the basal transcription machinery and hence target gene transcription is initiated.

Co-regulator complexes contain three broad groups of proteins. Firstly, there are proteins that covalently modify histones such as acetylases/deacetylases, methylases/demethylases, phosphorylases/dephosphorylases and ubiquitylases/deubiquitylases. The co-activators are associated with histone acetylases and the co-repressors with histone deacetylases. The second group of proteins in the co-regulatory complexes are involved with ATP dependent chromatin re-modelling. Thirdly, there are proteins which are involved in the recruitment and disassembly of co-regulator complexes (Perissi and Rosenfeld, 2005). Activation of receptor and gene transactivation involves highly choreographed and cyclical actions of components of all of these complexes.

1.7.2.2 Membrane bound rapid NR signalling

There is emerging evidence that nuclear receptors are involved in alternative signalling pathways other than that described in the previous section. These pathways involve NRs to be located at the cell membrane and involve cross-talk between NRs and other membrane localised receptors such as growth factor receptors and G-protein linked receptors.

The estrogen receptors ERα and β, progesterone receptors PRα and β and the androgen receptor (AR) have been demonstrated to be present at the plasma membrane in CHO (Chinese hamster ovary) and breast cancer cells (Pedram et al., 2007; Levin, 2008). These receptors require palmitoylation as a post translational modification onto a conserved motif on the E-domain of the nuclear receptors (Pedram et al., 2007); this leads to association with caveolin 1 proteins and transport to the cell membrane (Razandi et al., 2003). There is also evidence that ERα homodimerises upon exposure to 17β-estradiol at the plasma membrane to allow rapid signal transduction (Razandi et al., 2004).

Membrane localised nuclear receptors appear to cross-talk with well established membrane based signal transduction pathways, when exposed to ligand. Therefore, when ERα is exposed to 17β estradiol at the plasma membrane, it activates Gα proteins which leads onto a rise in calcium and cAMP levels in keeping with second messenger activation (Razandi et al., 1999). ERα also recruits and activates Gβγ proteins and stimulates downstream signal transduction (Kumar et al., 2007); an example being the stimulation of endothelial nitric oxide synthase and production of nitric oxide from endothelial cells which leads to vasodilation (Pedram et al., 2006).

ERα activates a number of kinase based signal transduction pathways via interactions involving different scaffold proteins. The MNAR protein (modulator of non-genomic action

of estrogen receptor) mediates the interaction between the E-domain of ERα and src tyrosine kinase which in turn leads to PI3 kinase pathway activation (Cheskis et al., 2008; Wong et al., 2002). ER, mineralocorticoid receptor (MR) and progesterone receptors (PR) also bind to and activate receptor tyrosine kinases such as epidermal growth factor receptor (EGFR) (Grossmann et al., 2008; Filardo et al., 2000; Razandi et al., 2003; Faivre and Lange, 2007). In response to ligand, membrane bound ERα again activates SRC kinases by activating G-proteins. In response, SRC activates cellular matrix metalloproteinases which lead to the release of heparin-binding EGF like growth factor (HB-EGF) which is an EGFR ligand (Filardo et al., 2000; Razandi et al., 2003).

Hence, there is mounting evidence of the presence of nuclear receptors, particularly the estrogen receptors, at the cell membrane and their responsiveness to ligand which stimulates downstream signalling events via cross-talk with established membrane based cellular signalling pathways.

1.7.3 Nuclear Receptors and Bladder Cancer Cells

There is evidence of expression of a number of NRs in bladder cancer cells. Hermann et al investigated the expression of VDR in normal and malignant bladder tissue from 26 patients by immunohistochemistry and demonstrated an increased expression with more advanced bladder tumours (Hermann and Andersen, 1997). Similarly, Sahin et al demonstrated VDR expression by immunohistochemistry, in 85.7 % of superficial TCC as compared to 66.6 % of control, normal bladder tissue. Patients with the highest VDR expression had the highest risk of tumour progression, the lowest disease free survival and the largest tumour size (Sahin et al., 2005). There is no identifiable published evidence of FXR expression in the urinary bladder.

1.7.4 Histone Deacetylase Inhibitors (HDACi)

1.7.4.1 Histone deacetylase enzymes

DNA is packaged in nucleosomes each of which is a repeating unit of DNA wound around an octamer of four pairs of core histone proteins. This compact structure places a barrier to the interaction of the multimeric basal transcription machinery with gene promoters. This barrier is overcome by local unwinding of the nucleosome which is enacted by covalent binding of moieties such as acetyl groups to the positively charged histone tails. This is catalysed by histone acetyltransferase (HAT) enzymes. The histone acetylation neutralises the positive charge on specific histone lysines which loosens their interaction with the negatively charged DNA and leads to a localised loosening of the nucleosome structure to allow gene transcription to occur (Pan et al., 2007). The converse process, histone deacetylation is catalysed by histone deacetylase enzymes (HDAC) which remove acetyl groups from histones which leads to transcriptional silencing of target enzymes.

HDACs are divided into four classes depending on their homology to yeast HDACs. Classes I, II and IV contain a Zinc ion and this is key to the mechanism of action of many HDAC inhibitors.

Classification			Location	Function
Zn^{2+} dependent	Class I	HDAC 1	Nucleus	Participate in Sin3, NuRD (nucleosome remodelling and deacetylation) and Co-REST complex
		HDAC 2	Nucleus	
		HDAC 3	Nucleus, rarely cyto	Participate in co-repressor SMRT and NCoR complexes
		HDAC 8	Nucleus	-
	Class IIa	HDAC 4	Nucleus, Cyto	Interaction with co-repressors SMRT, NCoR, BcoR and CtBP.
		HDAC 5	Nucleus, Cyto	
		HDAC 7	Nucleus, Cyto	
		HDAC 9	Nucleus, Cyto	Muscle differentiation
	Class IIb	HDAC 6	Cyto	Tubulin deacetylase
		HDAC 10	Nucleus, Cyto	Recruitment of other HDACs
	Class IV	HDAC 11	Nucleus, Cyto	-
Zn^{2+} independent	Class III	SIRT 1-7		

Table 1.1: Summary of HDAC classes, cellular location and function (Pan et al., 2007).

1.7.4.2 HDAC Inhibitors (HDACi)

HDACi can be classified into four groups according to their chemical class, as illustrated in the table below. The chemical interaction of TSA and the bacterial HDAC homologue HDLP (histone deacetylase-like protein) has been elucidated via x-ray crystallographic analysis (Finnin et al., 1999). The structure of the HDAC catalytic domain consists of a long tube equivalent of 4-6 straight carbon chain in length. The key part of the structure is a Zinc ion at the bottom of this catalytic tube. HDACi such as TSA and SAHA are divided into zinc chelating motif, an aliphatic linker and a polar cap group (Lin et al., 2006). The hydroxamate group has two functions; it acts to chelate the zinc ion and also forms a salt bridge, thereby forming a strong interaction between the HDACi and the catalytic domain of the HDAC. The NH-OH group in the hydroxamate motif transfers a proton to Histidine 131 thereby developing a negative charge. This allows the formation of a strong salt bridge between the positively charged Zinc ion and the negatively charged NH-OH group. This may be the reason for the high potency of hydroxamate based HDACi as compared to the other classes of HDACi, as they are able to form this strong interaction with the important zinc ion.
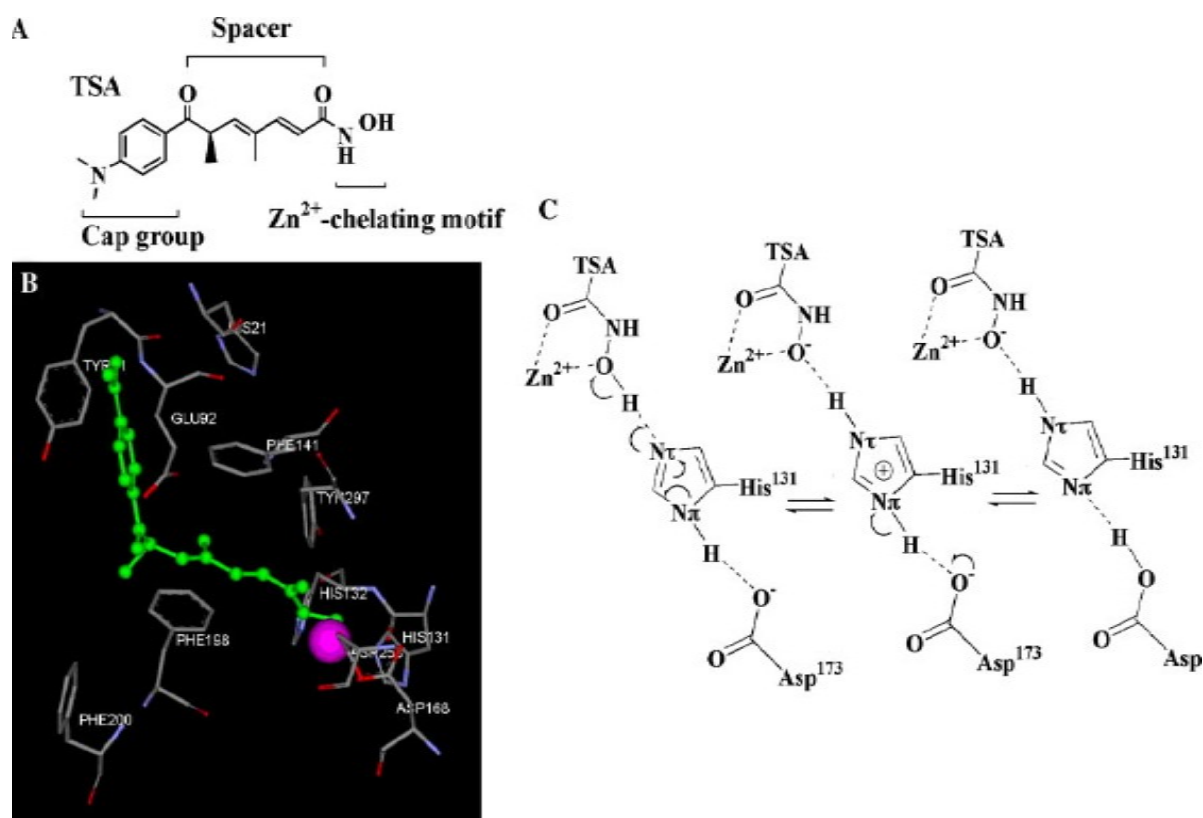
Figure 1.6: A:The structure of TSA demonstrating three functional motifs. B: The interaction between the Zinc ion (purple sphere) and the TSA hydroxamate motif. C: The proton transfer between the hydroxamate NH-OH group and Histidine 131 allows a salt bridge to form between the positively charged Zn^{2+} ion and the now negatively charged NH-O$^-$.

HDAC inhibitors cause both gene expression and repression in a panel of leukemia, multiple myeloma and solid tumour cell lines including bladder cancer cells (Chambers et al., 2003; Glaser et al., 2003; Mitsiades et al., 2004; Peart et al., 2005). Interestingly, HDACi are estimated to only alter expression of 7-10 % of genes as assessed by gene micro-arrays (Xu et al., 2007; Chambers et al., 2003; Glaser et al., 2003; Mitsiades et al., 2004; Peart et al., 2005; Sasakawa et al., 2005; Sasakawa et al., 2005). This pattern of gene regulation also reflects the multitude of anti-tumour responses elicited by HDACi treatment; cell may undergo growth arrest, terminal differentiation, apoptosis via intrinsic, extrinsic pathways, autophagic cell death and reactive oxygen species facilitated cell death (Xu et al., 2007).

Tumour cells treated with HDACi may undergo G1/S phase cell cycle arrest and this is frequently associated with a rise in p21$^{(wafl/cip1)}$ expression (Richon et al., 2000). Concomitantly, deletion of p21$^{(wafl/cip1)}$ abolishes the ability of the sodium butyrate to induce G1/S phase cell cycle arrest (Archer et al., 1998). However, these effects are cell and HDACi context dependent. Therefore, in the p21$^{wafl/cip1}$ deleted colon cancer cell line HCT116, TSA induces a G1/S cell cycle arrest by upregulating the expression of p15 (INK4b), which is an inhibitor of cyclin D dependent kinases (Hitomi et al., 2003). In other cell contexts, SAHA as well as TSA upregulate expression of p27, also a CDK inhibitor, in leukemia cell lines K562 and LAMA-84 (Nimmanapalli et al., 2003) and in breast cancer cell lines MCF-7 and MDA-MB-231 (Huang and Pardee, 2000; Xu et al., 2007).

Apoptosis may occur via extrinsic and intrinsic pathways. The extrinsic pathway occurs when death receptors such as FAS, TNFR1 and the TRAIL receptors DR4 and DR5 bind their respective ligands, FAS ligand, TNF and TRAIL. This leads to caspase activation and apoptosis. Nakata et al have demonstrated that both TSA and sodium butyrate increase the expression of the TRAIL death receptor DR5 (Nakata et al., 2004) in Jurkat acute lymphoblastic leukemia cells. They also demonstrate modest levels of apoptosis when Jurkat cells were treated with a minimal concentration TSA (0.5 μM) or 50 ng/ml of recombinant TRAIL. However, when both TSA and TRAIL were added together, there was a synergistic rise in apoptosis to 58 % of cells from 17 % and 12 % respectively; suggesting that TSA sensitises Jurkat cells to the apoptotic effects of recombinant TRAIL.

The intrinsic pathway of apoptosis is mediated by release of mitochondrial proteins such as cytochrome c, apoptosis inducing factor (AIF) and SMAC into the cytoplasm which leads to caspase activation and apoptosis. This process is regulated by the relative expression and function of pro- and anti-apoptotic members of the BCL-2 family of proteins. HDACi lead to

release of cytochrome c and activation of caspase 9 by unknown mechanisms (Xu et al., 2007). The HDACi suberic bishydroxamate, has also been shown to upregulate expression of pro-apoptotic members of the bcl-2 family, Bim, Bax and Bak and down-regulated expression of anti-apoptotic members Bcl-xL and Mcl-1 in melanoma cell lines (Zhang et al., 2004).

Class	Compound	HDAC target	Potency (cells)	Stage of development
Hydroxamate	SAHA	Classes I,II	µM	FDA approved
	Trichostatin A	NA	nM	-
	LBH589	Classes I,II	nM	Phase I
	PXD101	Classes I,II	µM	Phase II
	ITF2357	Classes I,II	nM	Phase I
	PCI-24781	Classes I,II	NA	Phase I
Cyclic peptide	FK228	HDAC 1,2	nM	Phase II
Benzamide	MS-275	HDAC 1,2,3	µM	Phase II
	MGCD0103	Class I	NA	Phase II
Aliphatic acid	Phenylbutyrate	Classes I, IIa	mM	Phase II
	Valproic acid	Classes I, IIa	mM	Phase II
	AN-9	NA	µM	Phase II
	Baceca	Class I	NA	Phase II
	Savicol	NA	NA	Phase II

Table 1.2: Summary table of current HDAC inhibitors in clinical development. NA–not available. Adapted from (Xu et al., 2007).

The urinary bladder is constantly exposed to toxins and xenobiotics within the urine and is likely to have protective mechanisms to ensure continued epithelial integrity. Nuclear receptors are involved in the execution of such a xenobiotic protective response in other organ systems, namely the liver and bowel. The liver is exposed to the toxic secondary bile acid, LCA; the levels of primary bile acids are sensed by the nuclear receptor FXR which in turn regulates the enzymes involved bile acid synthesis. Levels of LCA are further sensed by the nuclear receptor PXR which in turn switches on the expression of the xenobiotic metabolising enzymes CYP3A4 and SULT2A1 as well as the active cell membrane transporters MRP2 and MDR1 which actively excrete LCA out of hepatocytes (Elias and Mills, 2007). The urinary bladder may well require a similar xenobiotic protective response to maintain epithelial integrity in the face of constant exposure to xenobiotics. The bladder is known to express NRs such as VDR, which is a known inducer of both CYP3A4 (Matsubara et al., 2008; Jurutka et al., 2005) and SULT2A1 enzymes (Echchgadda et al., 2004); nuclear receptors may well act as the urinary bladder's xenobiotic sensors.

NRs, in particular VDR have been implicated in cancer (Thorne and Campbell, 2008) and hence, may be targeted with their respective ligands. However, despite the presence of functional NR, a cancer cell may exhibit resistance to the effects of NR ligands. Previously, our research group has demonstrated this resistance may be due to over-expression of the co-repressors NCoR2/SMRT in prostate cancer (Khanim et al., 2004) and NCoR1 in breast cancer (Banwell et al., 2006). With the above in mind, the aims of this thesis are follows:

1.8 AIMS

- To establish the expression pattern of a panel of nuclear receptors that bind dietary derived ligands and corresponding co-repressors in a panel of bladder cancer cell line models.

- To establish the sensitivity to the anti-proliferating effects of the nuclear receptor ligands in a panel of cell lines. To investigate the correlation between cell sensitivity with relative nuclear receptor and co-repressor expression and to what extent these effects can be enhanced by HDACi.

- To modulate co-repressors in relevant cell lines to investigate the effect of co-repressor expression on cell proliferation and sensitivity to NR ligands.

- To investigate target gene expression on treatment with NR ligands in wild type cells with either forced co-repressor overexpression or HDACi co-treatment.

Chapter 2 General Methods

This chapter describes the basic laboratory techniques used. Any modifications to these general methods have been specified in the relevant chapters.

2.1 NR ligands and HDAC inhibitors

$1\alpha,25(OH)_2D_3$, 9 cis RA and EPA (generous gift of Dr. Milan R. Uskokovic, Hoffman La Roche, Nutley, NJ 07110, U.S.A.) were stored as stock solutions of 1mM in ethanol at $-20^{\circ}C$. All trans retinoic acid (ATRA), Lithocholic acid (LCA), Chenodeoxycholic acid (CDA), Arachidonic acid (ETYA) were all stored as 1 mM stock solutions in ethanol at $-20^{\circ}C$. Suberoylanilide hydroxamic acid (SAHA) was provided by Dr Victoria Richon (Merck Research Laboratories, Boston, MA, United States) via a materials transfer agreement with Dr M.J. Campbell. This was stored in $-20^{\circ}C$ as a 1 mM stock solution. 22 (R) hydroxycholesterol (22HC) and GW3965 (both from Sigma-Aldrich) were stored as stock solutions in DMSO at 1mM at $-20^{\circ}C$. Cis 4,7,10,13,16,19 Docosahexaenoic acid (DHA) (Sigma- Aldrich) was stored as a 1 mM stock solution in chloroform at $-20^{\circ}C$.

2.2 Tissue culture techniques

All culture techniques were undertaken in a laminar flow cabinet to maintain a sterile environment. RT-4, HT-1376, RT-112 and EJ-28 bladder cancer cell lines were used *in vitro* to represent 3 different grades of bladder cancer; RT-4 is derived from G1 well differentiated bladder transitional cell papilloma, RT-112 is derived from a G2 moderately differentiated TCC and HT-1376 and EJ-28 are both derived from G3 poorly differentiated TCC. RT-4 and HT-1376 were obtained from the ATCC. RT-112 and EJ-28 were a kind gift from Professor David Neal's laboratory from the Department of Oncology at the University of Cambridge.

RT-4 was cultured in tissue culture flasks in McCoys 5a modified medium (Cambrex), HT-1376 was cultured with modified Eagle's medium, RT-112 and EJ-28 were cultured in Dulbecco's modified Eagle's medium; all with 10% FCS, 1% Penicillin and streptomycin (SIGMA), 1% L-glutamine (SIGMA) and incubated at 37°C with 5% CO_2.

Each cell line was washed with sterile PBS and split with 0.25% trypsin EDTA/PBS solution. Cells required for investigation were counted using a haemocytometer.

2.3 ATP bioluminescent proliferation assay

2.3.1 Assay Principle

All living cells require free energy in order to perform essential cellular functions; this free energy is carried in the form of Adenosine triphosphate (ATP). This molecule contains two energy rich phosphoanhydride bonds; free energy is released when ATP is broken down to adenosine di-phosphate which in turn regenerates further ATP as a result of cellular metabolism. Therefore, the levels of ATP within a cell are a close marker for cellular numbers and proliferation.

The ViaLight HS™ (Cambrex) kit was used to estimate relative cellular ATP levels. This utilises the following chemical reaction:

$$ATP + luciferin + O_2 \xrightarrow{\text{Luciferase, } Mg^{2+}} Oxyluciferin + AMP + CO_2$$
$$+ \text{LIGHT (at 565 nm)}$$
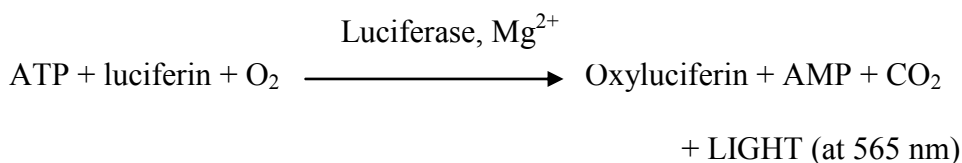
The emitted light intensity has a linear relationship to ATP concentration and is measured using a luminometer at 18-22°C (Crouch et al., 1993).

2.3.2 Assay method

This assay was developed to look at the proliferation of bladder cancer cell lines *in vitro* over a 96 hour time period. Each experiment was dosed at set up and re-dosed at 48hrs before results were obtained.

Cells were trypsinized and resuspended in culture media to yield a single cell suspension. They were then counted using a haematocrit slide, diluted in media and added to sterile white walled flat bottom 96-well plates to yield 2-4 $\times 10^3$ cells per well (depending on cell line – see figure legend below). Nuclear receptor ligands and/or SAHA were added to each well to make up a total volume of 100 µl per well. Each plate was then incubated at 37°C with 5% CO_2 for 96hrs, redosing with agent +/- SAHA at 48 hours. After the 96hrs incubation the plates were processed. This involved the addition of 100µl of nucleotide releasing reagent (Vialight HS, Cambrex) to the wells and incubation at room temperature for 15mins. During this time ATP monitoring reagent (Vialight HS, Cambrex), containing luciferin, luciferase and magnesium, was reconstituted with TRIS Acetate buffer (Vialight HS, Cambrex) and vortexed to equilibrate. Using the Orion Microplate Luminometer (Bethhold detection systems) 20µl of ATP monitoring reagent was added to each well and the luminescence measured with a 10 second exposure and recorded. ATP levels were recorded in relative light units and expressed as a percentage of untreated controls.

The sum of the individual mean effects for each compound acting alone was the *predicted* combined inhibition. The mean *observed* combined inhibition was then compared with this value using the Student's *t*-test. The inhibitory effects were designated as follows: strongly-additive effects were those with an observed value significantly greater than the predicted value, additive effects were those in which the observed value did not significantly differ

from the predicted value and sub-additive effects were those in which the observed value was significantly less than the predicted value (Khanim et al., 2004; Banwell et al., 2006).

2.4 Cell cycle analysis

2.4.1 Principle of assay

Cell cycle analysis measures DNA content of individual cells and conveniently reveals cell distribution against DNA content, which indicates the locations of cells in the cell cycle. G2 and M phase occur after DNA synthesis (S-phase), therefore cells in these phases contain twice as many chromosomes (and twice as much DNA) as cells in G1 and G0 phases. FACS analysis uses this feature to estimate the numbers of cells in a suspension that are within G2/M phases as compared to G1/G0 phases. Cells are treated with a fluorescent dye, propidium iodide which intercalates within the major groove of DNA. The cell suspension is passed through a FACS machine (fluorescence activated cell sorter) and is excited by light at a wavelength of 488 nm. The fluorochrome, propidium iodide, fluoresces and the intensity is measured by detectors. Cells in G2 and M phases will have twice as much fluorescence intensity as cells in G1/G0 phases. Cells in S phase are synthesising DNA, hence their DNA content and therefore fluorescence intensity will be intermediate between the two previous groups of cells.
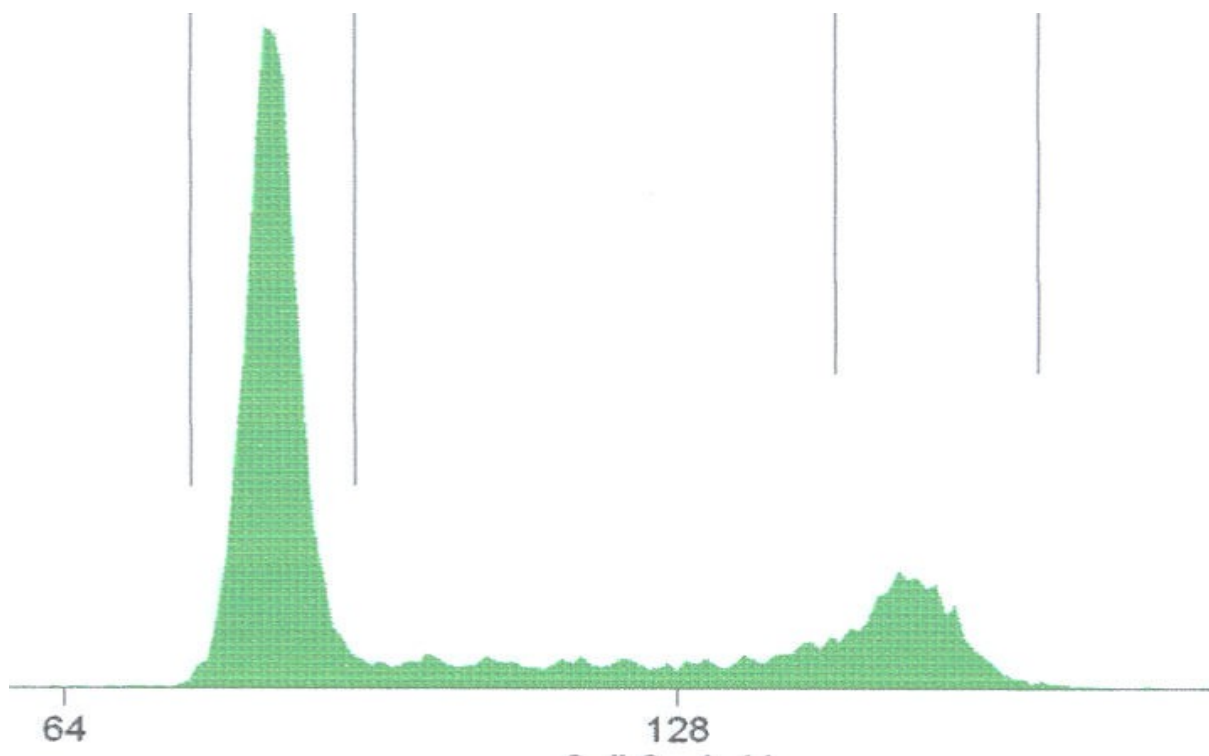
Figure 2.1: Representative copy of FACS histogram obtained. The x-axis represents intensity of fluorescence and the y-axis represents cell count. The peak labelled by R2 represents cell in G1 and G0. The much smaller peak labelled R3 represents cells in G2 and M phases. The area of the curve in between the peaks represents cells in S-phase.

2.4.2 Method

Cells (1.5×10^6) were plated in T75 flasks and incubated for 24 hrs to ensure mid-exponential proliferation and were dosed at 24 and 48 hrs with single or combination agents. Cells were harvested by trypsinisation at 72 hours, transferred into labelled tubes and centrifuged for 5 minutes at 1200 rpm to gather all of the cellular material into a pellet.

Detached cells were also included. The cells were resuspended in 1ml of PBS and transferred to a fluorescent activated cell sorter (FACS) tube (Becton Dickinson Labware). Cells were once again spun down before resuspension in 0.5ml of cell cycle buffer (5g sodium citrate, 0.5mls Triton X-100, 0.1mM sodium chloride, made up to 500mls with distilled water) containing fresh propidium iodide (2mg/ml). This buffer contains salt and detergent which disrupts the cell membrane and leaves nuclei intact. Cell membrane disruption is important to allow the propidium iodide access to DNA within the nuclei. Each sample was vortexed thoroughly, covered in foil (as propidium iodide is light sensitive) and incubated on ice (to minimum for 30mins) before being analysed in a Becton-Dickinson FACS machine using Cell-Cycle Analysis software. The effect on cell cycle distribution of each treatment was examined in triplicate.

2.5 RNA extraction protocols

2.5.1 Principle

RNA from cell lines was extracted using Tri-reagent (Sigma) which is an organic solution containing guanidine isocyanate and phenol. The guanidine isocyanate is a strong denaturant and the phenol acts to denature cellular RNAses and improve RNA yield. This method is a refinement on the single step method described by Chomczynski, P. and Sacchi, N (Chomczynski and Sacchi, 1987).

Cells are lysed by adding Tri-reagent. 1-Bromo-3-Chloropropane is added to this solution; this allows two layers form, an upper aqueous layer which is acidic and under these conditions dissolves RNA. The lower organic pink layer contains DNA and proteins. This step is called phase separation. This mixture is then centrifuged which leads to separation into

a lower organic phase containing proteins, the upper aqueous phase containing RNA and a cloudy interphase containing DNA. Chloroform may be used in place of 1-Bromo-3-Chloropropane however, is more toxic and is associated with a higher level of DNA contamination (Chomczynski and Mackey, 1995). The upper aqueous layer is separated carefully and isopropanol is added which causes RNA precipitation. Contaminants such as DNA are removed from the RNA pellet by washing with ice cold 70 % ethanol.

2.5.2 Method

Cells were prepared for total RNA extraction, by seeding $2x10^6$ cells per T25 flask. At indicated time points, 1 ml of Tri reagent (Sigma) was added and the plates swirled to mix for 5 minutes. This was transferred to labelled eppendorf tubes. Subsequently, 100μl 1-bromo-3-chloro propane (BCP) was added, mixed and left for 15 minutes at room temperature. The eppendorfs were then centrifuged at 12,000 x g for 15 minutes at 4°C and the upper phase transferred to a clean eppendorf. 500μl of isopropanol was then added, the tubes inverted to mix and then left for 15 minutes at room temperature. The eppendorfs were again centrifuged at 12,000 x g for 10 minutes at 4°C. The supernatant was aspirated with care to avoid disturbing the pellet, and 1ml of 75% ethanol added and centrifuged at 12,000 x g for 5 minutes at 4°C. The ethanol was then aspirated off and the pellet of purified RNA was resuspended in 30μl of nuclease-free H_2O.

The RNA was then quantified by diluting 4μl of purified RNA solution into 996μl dH_2O and the optical density (OD) measured at 260nm using the equation:

O.D. reading x ((40 μg/ 1000 μl)/ 1 O.D. unit) x dilution factor = concentration in μg/μl

(Gallagher and Desjardins, 2008)

RNA samples are stored at -80 °C to prevent degradation.

2.6 Reverse transcription polymerase chain reaction (RT-PCR)

2.6.1 Reverse transcription (RT) : Principle

Reverse transcription refers to the chemical reaction which results in single stranded RNA converted into complimentary DNA (cDNA). This process originates in RNA viruses or retroviruses which carry their genetic information as RNA, examples include the human immunodeficiency virus (HIV), Moloney murine leukemia virus (MMLV) and avian myeloblastosis virus (AMV). The key enzyme, reverse transcriptase catalyses this reaction and contains three enzymatic activities:

1. RNA dependent DNA polymerase.

2. Hybrid dependent exonuclease (RNase H)

3. DNA dependent DNA polymerase.

In vitro, only the first two functions are utilised to produce single stranded DNA. This is then used in downstream applications such as quantitative real-time PCR. The reaction has three phases. The RNA is heated at 70 $^{\circ}$C to denature the secondary structure. It is then incubated at 42 $^{\circ}$C for reverse transcription to occur, i.e. cyclical rounds of primer binding, elongation of the cDNA strand and degradation of the RNA template by the RNase H activity. Finally the sample is heated to 95 $^{\circ}$C to inactivate the reaction; this temperature degrades the reverse transcriptase enzyme and any remaining RNA fragments. Primers for this reaction may be a poly-T primer which will bind to the poly-A tails of the mRNA molecules, may be random hexamers which will bind to corresponding random complimentary sequences on RNA molecules, or lastly, may be a specific primer for a particular RNA species corresponding to expression of a particular gene.
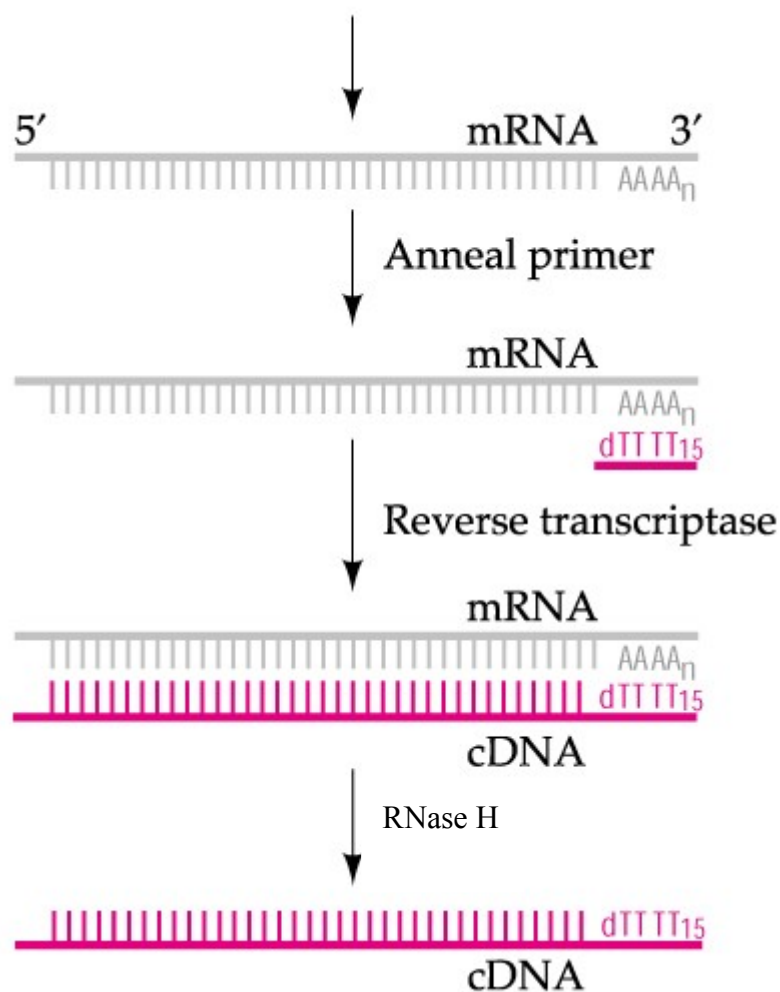
Figure 2.2: The key steps in reverse transcription. 1st step is primer annealing, then extension of the cDNA molecule and lastly degradation of the template RNA molecule. Downloaded from Google images (http://8e.devbio.com/images/ch04/0405fig2.jpg).

2.6.2 Method

Samples and reagents were allowed to thaw on ice. 1µg of RNA was prepared in 10µl of nuclease free water and incubated at 70°C for 5mins to allow degradation of the RNA secondary structure. 10µl of RT mastermix (2µ 10x reaction buffer (stratascript), 2µl 10mM dNTP's (Promega), 1µl RNAsin (40iu/µl, promega), random primers (250ng/µl, Promega), 1µl MLV-RT (10,000iu/µl, stratascript) and 4µl nuclease free water (promega) was prepared,

vortexed and spun down before being added to the reaction. Each reaction was vortexed, spun down and incubated at 42°C for 1hr to enable reverse transcription elongation to occur, 95°C for 5 mins to inactivate the reaction.

2.6.3 Polymerase chain reaction (PCR)

2.6.3.1 Conventional PCR: Principles

Conventional PCR is a chemical process employed to replicate a particular DNA sequence multiple fold. It is credited to Kay Mullis (Saiki et al., 1985) who used heat stable DNA polymerase enzyme from the Thermus aquaticus bacterium. Most enzymes would denature over a temperature of 50 $^{\circ}$C however, this DNA polymerase has an optimum working temperature of 72 $^{\circ}$C.

Conventional PCR has three basic steps; denaturation, annealing and elongation. Denaturation describes the separation of double stranded DNA into single strands by heating to 94 $^{\circ}$C; at this temperature the hydrogen bonds between complimentary DNA bases is disrupted. Annealing describes the binding of primers to the sequence of DNA which is to be amplified. Primers are short sequences of oligonucleotides which are complimentary to the 5' ends of the DNA sequence to be amplified and are required to allow DNA Taq polymerase to start the polymerisation reaction. Primers need to bind at the 5' ends of the DNA template as DNA polymerase only polymerises the new DNA strand in the 5' to 3' direction. The annealing temperature is usually 3-5 $^{\circ}$C below the melting temperature of the primers. The melting temperature refers to the temperature at which the primers dissociate from the DNA template. Clearly the annealing temperature needs to be below the melting temperature, however, as the annealing temperature is reduced the chances of non-specific primer binding increases.

Therefore, as a compromise, an annealing temperature 3-5 ^{o}C below the melting temperature is used. Elongation refers to the synthesis of the new DNA strand complementary to the template. The optimal temperature for Taq polymerase is 72 ^{o}C

2.6.3.2 Conventional PCR: Method

All samples and reagents were allowed thawed on ice. A 20µl PCR mastermix was prepared using the following reagents:

10x Reaction Buffer (Promega)	2µl
25mM MgCl$_2$ (Promega)	3.2µl
10mM dNTP's (Promega)	2µl
Forward Primer (30µM)	0.4µl
Reverse Primer (30µM)	0.4µl
5iu/µl Taq polymerase (Promega)	0.4µl
Nuclease free water (Promega)	9.6µl
Total	18µl

50ng of cDNA in 2µl of nuclease free water was added to the mastermix and vortexed. Using the Gene Amp PCR system 9700 thermal cycler, a sequence of denaturing (94°C) for 30 seconds, annealing at 60 ^{o}C for 30 seconds, and elongation (72°C) for 30 seconds cycled for 35 cycles prior to a 7 minute 72°C period of elongation at the end of the reaction. The product was then loaded onto a 1% agarose gel with 4x loading buffer alongside the 1Kb DNA ladder plus (Bioline) before development under UV light and annotation.
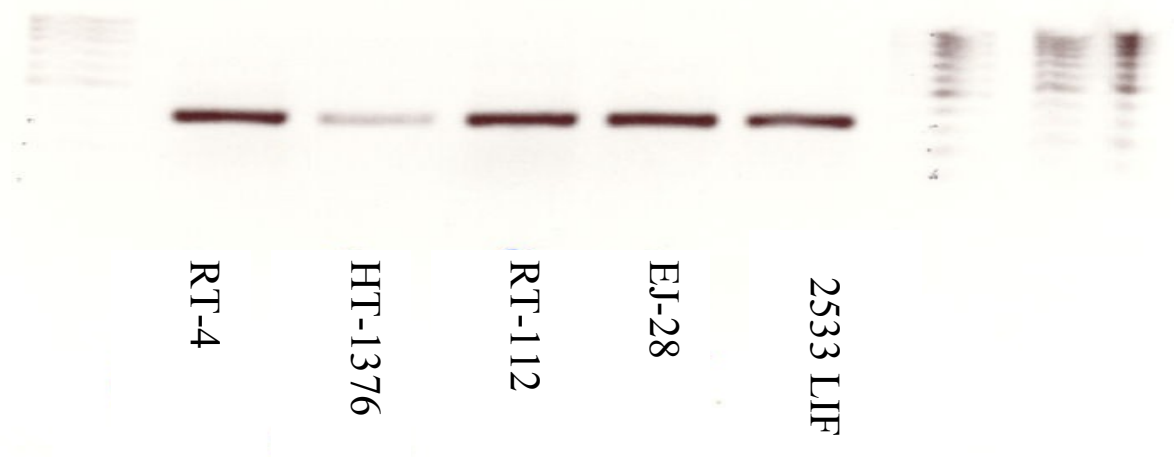
Figure 2.3: Conventional PCR gel image of 18 S ribosomal RNA reverse transcribed and amplified from RNA from bladder cancer cell lines.

2.6.3.3 Agarose gel electrophoresis of PCR products

1% agarose gels are used to resolve DNA PCR products by size using electrophoresis. 1g electrophoresis grade agarose (Sigma) was dissolved in 100 ml 1x Tris/Borate/EDTA (TBE) buffer (108g tris, 55g boric acid, 40ml 0.5M EDTA pH 8.0 in 10L H_2O) with 5 µl of 10mg/ml ethidium bromide (final concentration 1 µg/ml) to visualise cDNA. 1µl of the 1Kb plus DNA ladder (Bioline) was diluted in 9µl H_2O and 2µl 6x loading buffer (0.25% Bromophenol Blue, 0.25% xylene FF and 30% glycerol in H_2O). Samples in 6x loading buffer were prepared and loaded onto polymerised 1% agarose gels. Following electrophoresis at 55V for 20mins images were developed under UV light and annotated.

2.6.4 Quantitative RT-PCR (Q-RT-PCR)

2.6.4.1   Q-RT-PCR: Principles

Quantitative real time PCR is a technique which allows precise quantification of gene expression by performing a PCR reaction on cDNA, allowing measurement of changes in mRNA of a particular gene of interest from different samples. This is a highly sensitive technique which allows a high throughput of samples.

Taqman Q-RT-PCR involves a PCR reaction with two pairs of primers for a particular gene of interest, along with a probe. The probe is an oligonucleotide which is complementary to a sequence which is 3' downstream of the primer binding site. The probe should ideally bind a sequence which is at an exon-exon boundary. This will ensure that the probe only binds cDNA which does not contain introns as compared to contaminating genomic DNA. The probe contains a fluorophore reporter at its 5' end and a quencher molecule at its 3' end. The fluorophore is a chemical molecule such as 6-carboxyfluorescein (shortened to FAM) which fluoresces, however its proximity to the quencher results in inhibition of fluorescence. During a PCR cycle, DNA Taq polymerase causes polymerisation of the PCR product and when it arrives at the 5' end of the probe, its 5' to 3' exonuclease activity cleaves off the fluorophore which loses its proximity to the quencher and therefore can fluoresce which is detected and recorded by the real-time thermocyclers. Therefore, the amount of fluorescence recorded is directly proportional to the amount of PCR product.

The above PCR reaction allows quantification of the process unlike Northern or Southern blots. A Northern blot allows RNA to be electrophoresed on a gel, transferred onto a membrane and detected by hybridisation with a labelled oligoncleotide probe. This is a semi-quantitative method at best and is cumbersome and time consuming. A Southern blot in this

setting describes electrophorescing cDNA on a gel; it is also at best a semi-quantitative technique.

Q-RT-PCR is quantified by plotting the fluorescence or ΔRn (fluorescence detected – background) against cycle number on a logarithmic scale. The exponential phase of the PCR reaction is a straight line (as the plot is on a logarithmic scale); this is when the PCR reaction rate is the highest and there are no limiting factors such as primer availability. Hence, a sample which contains a higher concentration of a particular cDNA should achieve the exponential phase of reaction at an earlier cycle number as compared to a sample with a lower concentration of the cDNA species being investigated. This cycle number is denoted Ct and is normalised by subtracting it from the Ct of a housekeeping gene which should be abundantly expressed and this should not vary between different samples. This difference in Ct gives rise to the ΔCt. As the PCR product doubles per cycle, the fold difference in expression between samples is calculated as $2^{-(\Delta Ct1-\Delta Ct2)}$ where ΔCt1-ΔCt2 is the difference between the ΔCt of the two samples.
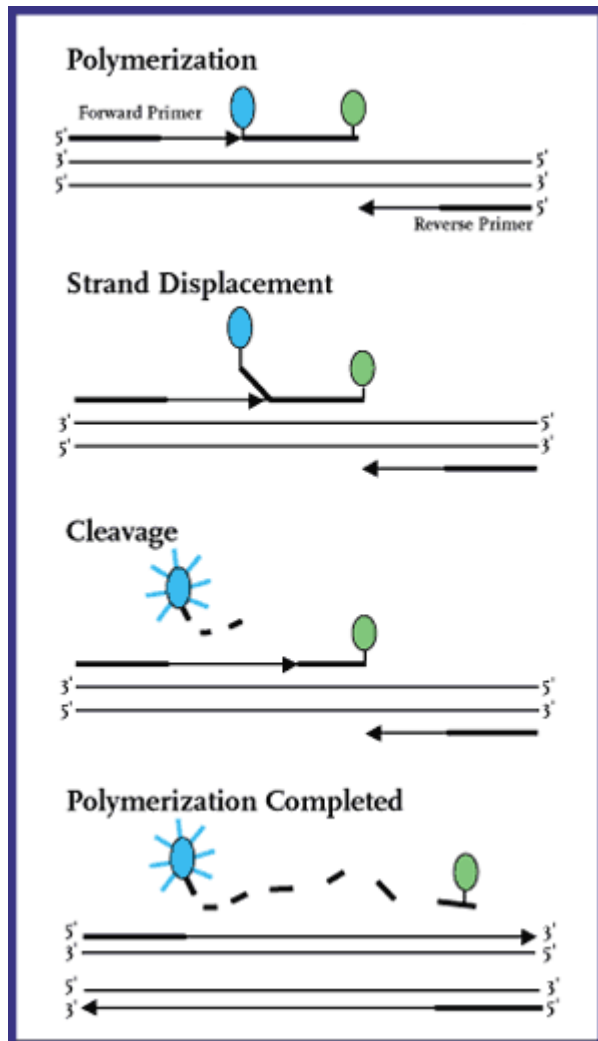
Figure 2.4: The principle of Taqman qRT-PCR. The probe binds its complementary sequence. As the Taq DNA polymerase forms the PCR product, it cleaves off the fluorochrome (blue) which releases fluorescence as it is detached from the quencher (green). This is detected by the real-time PCR thermal cycler. Diagram downloaded from Google Images.

2.6.4.2 Q-RT-PCR: Method

The sequences of the primers and probes used are shown below:

Sequences or primers and probes for Q-RT-PCR.

Primer	Sequence
TRIP15/Alien Forward primer TRIP15/Alien Reverse primer TRIP15/Alien Probe	CCTCATCCACTGATTATGGGAGT CATCATAATTCTTGAAGGCTTCA CCCTCAAGTGCATTTTACCACCACATTCTCT
NCoR1Forward primer NCoR1Reverse primer NCoR1Probe	TGAAGGTCTTGGCCCAAAAG TTTGTCTTGATGTTCTCATGGTA CTGCCACTGTATAACCAGCCATCAGATACCA
NCoR2/SMRT Forward primer NCoR2/SMRT Reverse primer NCoR2/SMRT Probe	CACCCGGCAGTATCATGAGA CGAGCGTGATTCCTCCTCTT CTTCCGCATCGCCTGGTTTATT
VDR Forward Primer VDR Reverse Primer VDR Probe	CTTCAGGCGAAGCATGAAGC CCTTCATCATGCCGATGTCC AAGGCACTATTCACCTGCCCCTTCAA
P21 Forward Primer P21 Reverse Primer P21 Probe	GCAGACCAGCATGACAGATTTC GGATTAGGGCTTCCTCTTGGA CCACTCCAAACGCCGGCTGATCTTT
	(Khanim et al. Oncogene 2004,23;40:6712)

Primers and probes for a further panel of nuclear receptors were ordered via the Applied Biosystems Assays on Demand service. The catalogue numbers are listed below as the primer and probe sequences are commercially restricted.

FXR	Hs00231968_m1
LXR α	Hs00172885_m1
LXR β	Hs00173195_m1
PPAR δ	Hs00602622_m1
RAR α	Hs00230907_m1
RAR β	Hs00233407_m1
RXR α	Hs00172565_m1
Cyp3A4	Hs00430021_m1
18S internal control	4308329

All samples and reagents were allowed to thaw on ice. A mastermix was prepared for each gene, depending on whether the reaction was singleplex (one gene per well, requiring an additional control well per sample for 18S VIC dye labelled probe) or duplex (18S VIC dye labelled probe and gene of interest, 6-FAM dye labelled probe in same well with different reporter dyes).

Each 20μl mastermix was prepared using the following reagents:

Singleplex 18S mastermix (housekeeping gene):

      2x Q-RT-PCR Mastermix (Applied Biosystems)   10μl

      18S ribosomal RNA control probe (Applied Biosystems)   0.1μl

      18S ribosomal RNA control forward primer (Applied Biosystems) 0.1μl
      18S ribosomal RNA control reverse primer (Applied Biosystems) 0.1μl

cDNA	1µl
Nuclease Free Water (Promega)	8.7µl
Total	20µl

Singleplex assays-on-demand mastermix:

2x Q-RT-PCR Mastermix (Applied Biosystems)	10µl
20x Assays-on-demand mastermix (Applied Biosystems)	1µl
cDNA	1µl
Nuclease Free Water (Promega)	8µl
Total	20µl

Duplex mastermix:

2x Q-RT-PCR Mastermix (Applied Biosystems)	10µl
Gene specific probe 1.25µM (Oswell)	2µl
Gene specific forward primer 9µM (Alta bioscience)	2µl
Gene specific reverse primer 9 µM (Alta bioscience)	2µl
18S ribosomal RNA control probe (Applied Biosystems)	0.1µl
18S ribosomal RNA control forward primer (Applied Biosystems)	0.1µl
18S ribosomal RNA control reverse primer (Applied Biosystems)	0.1µl
cDNA	1µl
Nuclease Free Water (Promega)	8.7µl
Total	20µl

19µl of mastermix is then loaded in 96 well plate format into each well and 200µg cDNA added in 1µl nuclease free water.

After setting up the ABI Prism 7500 sequence detector and loading the plate the standard cycling conditions were as follows:

2 mins	50oC	AmpErase UNG Activation	
10 mins	95oC	AmpliTaq Gold Enzyme Activation	
15 secs	95oC	Denature	} 44 cycles
1 min	60oC	Anneal, Extend	

Following the PCR run, data was downloaded and analyzed using the sequence detector software. Data was expressed as Ct values (the cycle number at which logarithmic PCR plots cross a calculated threshold line) and used to determine ΔCt values (ΔCt = Ct of the target gene minus Ct of the housekeeping gene). This value can then be compared to other control samples by subtracting, for example, the normal sample ΔCt from the cancer ΔCt to give the $\Delta\Delta Ct$. The fold increase in expression can then be calculated using the formula:

Fold Increase in expression   = $2^{-(\Delta\Delta Ct)}$

Data was then graphed using bar graphs of fold increase in expression. Each reaction was performed in triplicate and error bars calculated representing the SEM ($SEM = SD/\sqrt{n}$).

2.6.5   Microfluidic Q-RT-PCR$_M$

Simultaneous quantitative comparison of multiple gene transcripts was undertaken on the custom-designed TaqMan® Low Density Arrays (ABI 7900HT Fast Real-Time PCR System). The full list of gene targets is divided into nine functional groups whose expression together reflects nuclear receptor signaling capacity. These are 1. Cell surface transporters 2. Nuclear receptors 3. Nuclear receptor co-factors 4. Histone modifiers 5. Metabolic enzymes; 6. Cell death regulators; 7. Transcription factors; 8. Cell cycle regulators; 9. Signal transduction components.

Triplicate RNA samples from both RT4 pNCOR#7 and RT4 pcDNA#6 cells at different passage numbers and each treated plus or minus with LCA (10µM, 6 h.), were each measured in duplicate on each array. Total RNA was extracted using TriReagent (Sigma) as per section 2.5.2, and reverse transcribed to cDNA, and quantified using the one-step QuantiTect Probe

RT-PCR kit (Qiagen, http://www1.qiagen.com) directly on arrays. Data was normalized to the internal control 18S and the pNCOR samples calibrated to the pcDNA samples using the $\Delta\Delta$CT method as described above.

Statistical analysis was performed using TIGR MultiExperiment Viewer 4.0, MeV (freely available at www.tm4.org); fold change values, obtained comparing treated and untreated pNCOR#7 ΔCts versus pcDNA#6 ΔCts, were compared using a one sample t-test. Vectors containing gene expression values were tested against the predicted mean of 1 that indicates no changes in gene expression with cut-off (p<0.01).

2.7 Protein extraction

2.7.1 Protease inhibitor cocktail

Protease inhibitor cocktail (P8340, Sigma) was used for extraction of all cell protein lysate production. The inhibitor and final concentration used were AEBSF (104mM), Aprotinin (80μM), Leupeptin (2mM), Bestatin (4mM), Pepstatin A (1.5 mM) and E-64 (1.4mM). The protease inhibitor cocktail solution was stored at -20°C.

2.7.2 Extraction of cell protein

Treated cells were grown in T25 cell culture flasks (Greiner) until subconfluent. After aspiration of the media, cells were washed in PBS and trypsinised; 10 mls of fresh medium was added to halt the reaction. The cells were transferred to a 15 ml Falcon tube (Corning) and pelleted (x1500 rpm for 10 mins). The medium was aspirated off and discarded. 100μl of RIPA Buffer (1ml NP-40, 0.5g Sodium Deoxycholate, 1ml 10% SDS, 98ml $H_2$0 with 30μl Protease inhibitors (P8340, Sigma) per 300μl for each use) added to each flask, mixed, and

transferred to a 1.5ml eppendorf and incubated at -80 ^{o}C for 30mins. RIPA is a cell lysis buffer and denatures proteins i.e. unfolds the secondary, tertiary and quartenary structures as it contains the ionic detergents sodium dodecylsulphate and sodium deoxycholate. It does so by disrupting the non-covalent bonds in proteins as well as imparting a negative charge to proteins which is proportional to the mass of the protein. Cell lysis occurs by membrane disruption and by freezing. The preparation was allowed to thaw at room temperature, vortexed and briefly spun down. A further cycle of freezing at -80 ^{o}C was carried out. This was followed by centrifugation for 10mins at 12,000rpm to remove cellular debris the supernatant was transferred to new labelled eppendorf and stored at -20°C prior to ascertaining protein concentration.

2.7.3 Nuclear/Cytosolic Protein Fractionation

A commercially available kit (BioVision Nuclear/Cytosol Fractionation Kit) was employed to extract nuclear and cytosolic protein fractions from wild type bladder cancer cell lines as well as RT-4 cells stably transfected with pNCoR1 and pcDNA3 control plasmids. The protein fractions were used for Western blot analysis as described below.

Briefly, bladder cells were pelletted by centrifugation at 600 x g for 5 minutes at 4°C. These were resuspended in 200 µl of cytosol extraction buffer-A, containing protease inhibitors and 1mM DTT. 11 µl of ice cold cytosol extraction buffer-B was added and mixed. Nuclei were pelletted by centrifugation at 16,000 g for 5 minutes. The supernatant represented the cytosolic fraction. The nuclear pellet was resuspended in 100 µl of nuclear extraction buffer (containing protease inhibitors and 1mM DTT). This mix was repeatedly vortexed to ensure nuclear lysis. The mix was centrifuged at 16,000 g for 10 minutes; the supernatant represents the nuclear fraction.

2.7.4 Assay to determine protein concentration: Modified Lowry Assay

The Lowry assay is a calorimetric protein assay based on Copper (II) ions in alkaline solution forming complexes with protein. The amount of complex present is directly proportional to the amount of protein present. The complexes react with phosphotungstic and phosphomolybdic acids in phenol which are reduced to molybdenum/tungsten blue. The higher the concentration of protein the deeper the colour of blue obtained; the absorbance can be measured by a spectrophotometer at 690 nm (LOWRY et al., 1951). Proteins standards of differing concentrations of bovine serum albumin are also assayed to produce a standard curve which can then be used to estimate the concentration of protein in the samples.

Each protein sample to be tested and protein standards of 5.0, 1.0, 0.75, 0.5 and 0.25mg/ml were thawed and stored on ice. A 96 well clear, flat bottomed plate was labelled and 5µl of each standard or samples were added into allocated wells in triplicate. 25µl of protein determination solution A (BIORAD) was then added to each well followed by 200µl of protein determination solution B (BIORAD). The plate was then incubated at room temperature for 15 minutes before the absorbance at 690nm was read using a spectrophotometer. After plotting the standard's optical density vs concentration, the concentrations of each sample was then interpolated from their optical densities in mg/ml and recorded.

2.8 Western Blotting-Resolution of proteins by SDS-PAGE

2.8.1 Principle

Western blotting refers to a semi-quantitative technique to initially separate proteins followed by detecting particular proteins by applying specific antibody binding.

Proteins are separated by SDS-PAGE which refers to polyacrylamide gel electrophoresis. Protein samples are denatured initially by boiling in a solution containing sodium dodecyl sulphate and β-mercaptoethanol. The former applies a uniform negative charge to proteins in proportion to their molecular weight and thereby disrupts the secondary, tertiary and quartenary protein structures so they become rod-like. The latter disrupts disulphide bonds. When an electrical current is applied along the polyacrylamide gels containing the protein samples, they migrate towards the positive electrode and separate according to their molecular weight.

Detection of particular proteins by antibodies requires the proteins to be transferred to a nitrocellulose or PVDF (polyvinylidene difluoride) membrane. The gels are too fragile to handle and the protein epitopes are not adequately exposed to allow antibody binding. The membranes have good non-specific protein binding characteristics due to both hydrophobic and charged interactions. The proteins were transferred via electroblotting i.e. by applying a positive electric current across the gel and membrane. The membranes were incubated in a solution of fat-free milk powder to allow milk protein to bind to the remaining non-specific protein binding sites on the membrane to reduce the occurrence of non-specific antibody binding.

Antibody binding was a two step process. Initially a specific antibody against the protein in question was incubated with the membrane. Following this, a secondary antibody which binds the Fc or common domain of the primary antibody. The secondary antibody has a conjugated horseradish peroxidise enzyme which catalyses a chemiluminescent reaction when exposed to ECL reagent (Roche) which is detected on x-ray paper.

2.8.2 Western blotting: Method

Separation of proteins by size was achieved using SDS-PAGE prior to transfer to a PVDF membrane and exposure to primary and secondary antibodies.

Using Protogel reagents (Geneflow) an 8% resolving gel was prepared using 2.67ml protogel (30% w/v acrylamide), protogel resolving buffer 2.6ml (1.44M tris-HCl, 0.384% SDS, pH 8.8), H_20 4.62ml, Ammonium persulphate (10%) 100μl and TEMED 10μl and poured into a BIORAD gel apparatus and allowed to polymerise at room temperature. Stacking gel was prepared using 130μl Protogel (30% w/v acrylamide), 250μl protogel stacking buffer (0.5M tris-HCl, 0.4% SDS, pH 6.8), H_20 610μl, Ammonium persulphate (10%) 50μl and TEMED 10μl was then prepared, poured onto the set and allowed to polymerise at room temperature. Gel combs were used to allow well formation for loading.

Protein samples were then thawed on ice and diluted to give 30μg per sample with 10μl of 4x SDS loading buffer (3.75ml H_20, 1.25ml TRIS HCl pH 6.8, 2.5ml glycerol, 2ml SDS(10%), 0.5ml βmercaptoethanol, 0.5ml Bromophenol Blue, total volume 10mls) to a volume of 40μl. Samples were denatured by heating to 95°C for 10 mins and loaded, in parallel with a protein ladder in a separate well (Prestained Dual Color SDS Page Standards, BIORAD). SDS-PAGE running buffer (25mM TRIS, 192mM Glycine, 0.1% SDS, Geneflow) was added to the apparatus. Electrophoresis at 200V, 400mA then proceeded for approximately 50 minutes, or until the 120kDa Galactosidase marker was approaching the end of the gel.

Transfer of the separated protein onto a pre-hydrated polyvinylidene difluoride PVDF membrane (Immobilon P, Millipore) was undertaken using a BIORAD transfer apparatus and transfer buffer (TRIS 25mM, Glycine 192mM, 0.1% SDS and 20% methanol) for 1 hr at 100V, 400 mA using ice packs and a magnetic stirrer to prevent over heating of the apparatus.

Transfer of NCoR1 protein was performed as described above however, at 4°C, 10 V for 16 hours.

Transfer membranes were preblocked with 10% Blotto (Reconstituted milk powder) for 1hr, the membrane was incubated with primary antibody at varying concentrations (see table below) in TBST (50ml 1M TRIS HCl pH 7.6, 20g NaCl in 2.5l dH$_2$O). Each membrane was then washed in 10ml TBS-T (50ml 1M TRIS HCl pH 7.6, 20g NaCl, 0.1% TWEEN-20 and dH$_2$0 to 2.5l) for 3x 20 mins prior to exposure to the appropriate secondary antibody (HRP-conjugated, 1:10000 in TBS, Amersham). Following further washes with 10mls TBS-T for 3x 20mins membranes were incubated in 1ml ECL plus (Amersham Biosciences), at room temperature for 2 mins prior to exposure to film (Hyperfilm ECL, Amersham pharmacia biotech) prior to development and annotation.

Target	Manufacturer	Clone / Catalogue no	Dilution	Incubation time
VDR monoclonal	Chemicon International	MAB1360	1:500	2.5 hrs, 21 $^{\circ}$C
FXR monoclonal	R&D Systems	A9033A	1:500	2.5 hrs, 21 $^{\circ}$C
NCoR1 polyclonal	Abcam	ab24552	1:5000	24 hrs, 4°C
Nucleolin monoclonal	Abcam	ab13541	1:10,000	20 hrs, 4°C
B-actin	Sigma	AC15	1:10,000	1 hr, 21 $^{\circ}$C

Table 2.1: Details of various antibodies used for Western blotting. 21 $^{\circ}$C denotes room temperature.

2.9 Stable transfection of NCoR1 over-expressing plasmid

2.9.1 Transformation and maxi-prep: Principle

Transformation is a process whereby bacteria take up foreign DNA, a plasmid in this instance and replicate this plasmid with every round of bacterial cell division. The bacterial cells were chemically transformed by chilling the cells on ice in the presence of divalent ions followed

by providing a heat shock by immersing the cells in a water bath at 42 $^{\circ}$C. This allows the cells to take up the foreign plasmid. The purpose of transformation in this case is for the bacteria to synthesise massive amounts of plasmid as they divide so a significant amount can be recovered via the maxiprep to use in transfection.

The maxiprep is a commercial kit which allows chemical recovery of plasmid DNA from bacteria which have proliferated in culture having copied the plasmid as they have copied their genomic DNA before each cell division. The maxiprep starts by collecting all the bacterial cells by centrifugation at 5000 x g. The cellular pellet is treated with an alkali solution of detergents to lyse the cell walls. After lysis, the protein and membrane lipid are precipitated by adding potassium acetate; this mix is ultracentrifuged to separate the precipitate. The plasmid DNA remains in solution which is filtered through and is subsequently precipitated by adding isopropanol. This is ultracentrifuged to collect the plasmid DNA pellet. This pellet is subsequently purified by binding the plasmid DNA to a resin and passing solutions containing ethanol through columns to remove impurities. The plasmid is finally eluted by passing through hot water through the columns.

2.9.2 Transformation and maxi-prep: Method

I transfected a pcDNA3 expression plasmid (figure 6) with a full length NCoR1 insert into RT-4 cells. The plasmid was a generous gift from Dr. Johnson Liu (Mount Sinai School of Medicine, currently The Feinstein Institute of Medical Research, New York, USA).
E.Coli cells (α-select chemically competent cells, Bioline BIO-85026) were transformed with the plasmid as per the manufacturer's instructions. Briefly, 5 µl of plasmid, pcDNA-NCoR1 as well as control pcDNA3 blank plasmid was added separately to 50 µl of cells in a 15 ml

test tube and gently mixed. This was incubated on ice for 3 minutes. The tubes were placed in a 42 °C waterbath for 45 seconds and then placed on ice for 2 minutes. This solution was then diluted by adding 1 ml of LB medium (per litre: 10 g tryptone, 5 g yeast extract, 5 g Na Cl, 1 ml 1M Na OH). The tubes were shaken for 60 minutes at 200 rpm at 37 °C following which they were spread on LB agar plates (recipe as per LB medium but with additional 15 g agarose) with 100 μg/ml ampicillin and incubated overnight at 37 °C. As a control, 2 μl of puc19 plasmid was also used in separate transformations. The next morning, discrete colonies of E.Coli cells were picked which had grown on the ampicillin containing plates due to resistance afforded by the pcDNA3 plasmid. 300 mls of LB medium in 1 litre sterile conical flasks was inoculated with pcDNA3-NCoR1 and mock transformed colonies and cultured overnight on a shaker (200 rpm at 37 °C). The next morning, plasmid maxipreps were carried out as per the manufacturer's instructions (Promega Wizard plus maxipreps DNA purification system A7270, USA). The culture solution was pelletted by centrifugation at room temperature at 5000 g for 10 minutes. The supernatant was discarded and the pellet was resuspended in 15 mls of cell resuspension solution (50 mM Tris-HCL (pH 7.5), 10 mM EDTA and 100 μg/ml RNase A). The cells were lysed by adding 15 mls of lysis solution (0.2 M NaOH and 1 % SDS). This solution was neutralised by adding 15 mls of neutralisation solution (1.32 M potassium acetate pH 4.8). The resulting solution was centrifuged at 14,000 g for 15 minutes at room temperature; the clear supernatant filtered through Whatman paper. Plasmid DNA was precipitated by adding ½ volume of room temperature isopropanol and centrifuging at 14,000 g at room temperature for 15 minutes. The DNA pellet was resuspended in 2 mls of TE buffer (10 mM Tris-HCL pH 7.5, 1mM EDTA).

2.9.3 Plasmid DNA purification: Method

Purification resin (10 mls) was added to the plasmid DNA solution, mixed and run through a maxiprep column followed by 25 mls of column wash solution (80 mM potassium acetate, 8.3 mM Tris-HCL, 40 µM EDTA and 55 % ethanol). The columns were washed through with 5 mls of 80 % ethanol. The columns were centrifuged at 1300 g for 5 minutes, dried by applying a vacuum and the DNA eluted by passing 1.5 mls of preheated (65-70 $^{\circ}$C) water and centrifuging at 130 g for 5 minutes.

The plasmid DNA concentration was determined by measuring the absorbance at 260 nm using spectrometer and using the equation below:

Concentration of plasmid (µg/µl) = $\underline{\text{OD x 250 (dilution factor) x 50}}$

$$1000$$

2.9.4 Stable transfection of plasmid

5×10^5 RT4 cells per well (6 well plates) were allowed to adhere overnight. Per well, 3 µl of Fugene® 6 agent (Roche) was added to 97 µl of Optimem solution (Invitrogen) and after 5 minutes, 1 µg of plasmid DNA (pcDNA3-NCoR1 or pcDNA3 blank) was added. This was left at room temperature for 20 minutes and all of this solution was added per well to 2 mls of fresh medium (McCoy's 5a with serum). After 48 hours, McCoys 5a medium with selection antibiotic, G418 660 µg/ml was added in place of the regular culture medium. This concentration of G418 was chosen by previously incubating RT4 cells with a range of McCoys 5a medium with varying concentrations of G418 (100-1000 µg/ml in 100 µg/ml steps). A concentration of between 600 – 700 µg/ml led to cell death. Further titration led to a dose of 660 µg/ml as the threshold for RT-4 cell killing.

After 2 weeks of incubation, discrete cell colonies were growing in the G418 containing medium. These were isolated by placing sterile steel rings with paraffin wax at the base around each colony and by trypsinising and isolating each colony for further subculture, as a pure sub-clone. These were maintained in McCoys 5a medium with selection antibiotic G418 (660 µg/ml) with repeat passages as necessary.
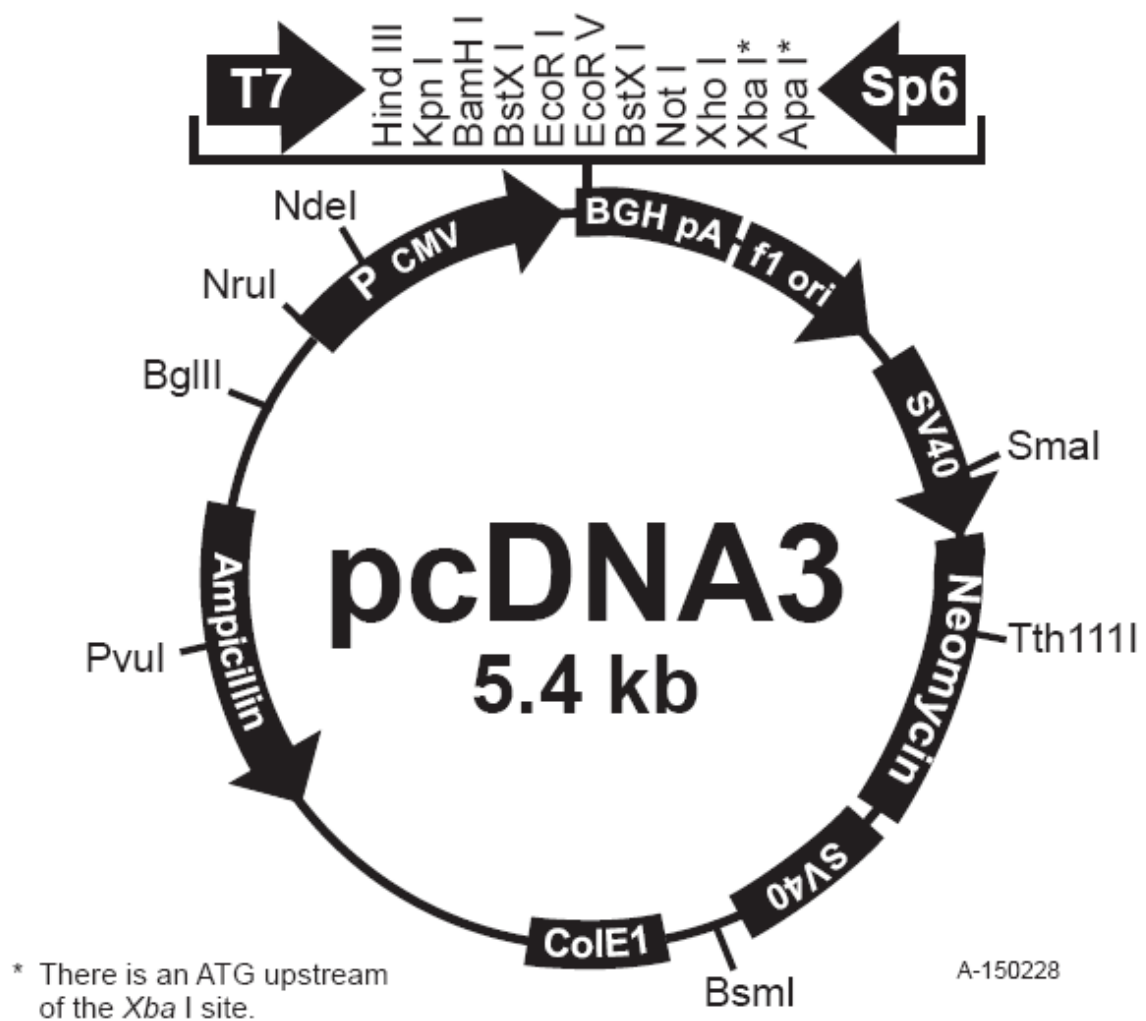
Figure 2.5: Structure of the empty pcDNA3 plasmid. The insert was the whole sequence of NCoR1; over-expressing vector obtained from Dr. Johnson Liu (Mount Sinai School of Medicine, currently The Feinstein Institute of Medical Research, New York, USA). Image downloaded from website http://www.molecularinfo.com/MTM/K/K2/K2-1/pcdna3.pdf.

2.10 Affymetrix® gene expression arrays

The target gene expression in EJ-28 cells was investigated after treatment with LCA, SAHA and the combination of the two ligands; total RNA was extracted at 6 hours post treatment. 2 x 10^6 cells were plated onto T75 (75 cm^3 surface area) culture flasks and left overnight (18 hours) to adhere. The cells were treated with the following concentrations of treatments: LCA = 100 μM, SAHA = 0.8 μM and negative control was treated with vehicle i.e. ethanol. At 6 hours post treatment, total RNA was extracted as described in section 2.5.1. The RNA was purified using the Qiagen® RNeasy mini kit as per the manufacturer's instructions. Briefly, the RNA samples were adjusted to 100 μl volume with RNAse free water. 350 μl of buffer RLT is added and mixed well. This is a guanidine isothiocyanate containing denaturing buffer which immediately inactivates RNAses. 250 μl of 100 % ethanol is added to this mixture. This optimises binding of RNA molecules longer than 200 bases to the silica-gel membrane within the mini columns. The mixture is added to the columns and centrifuged for 15 seconds at 8000 x g. The flow-through is discarded. We performed the optional on-column DNAse digestion step to further eliminate DNA contamination. Following this, 500 μl of RPE buffer is added to the column and the centrifugation step is repeated and the flow-through is discarded again. This is repeated with centrifugation for 2 minutes to ensure drying of the column and also so that ethanol is not carried over into the final RNA eluate. Finally, RNA is eluted by passing 30 μl of RNAse free water through the column.

The sample processing for the Affymetrix® has 5 steps before hybridisation of the cRNA to the oligonucleotides on the genechip®. The RNA is reverse transcribed to cDNA, this is put through a "clean up" process following which the cDNA is converted to biotin-labelled cRNA in a process called in vitro transcription (IVT). The cRNA is then put through a further "clean

up" process, followed by fragmentation. This fragmented cRNA is hybridised on to the genechips®.

2.10.1 Reverse transcription

Preparation of Poly-A RNA controls

The quality of the entire target RNA labelling process is monitored by a set of exogenous *Bacillus subtilis* poly-A RNA molecules added to the target total RNA samples at predetermined concentrations. Probes to these bacterial genes are on each of the GeneChip arrays; these genes are not found in eukaryotic samples. The poly-A controls are reverse transcribed, amplified and labelled together with the target RNA samples and hybridised onto the GeneChips. The intensity of hybridisation provides an independent control for the quality of pre-hybridisation processing of the target RNA.

Table 2.2: The following B subtilis genes are present in the poly-A control concentrate:

B subtilis genes	Final Dilution (estimated ratio of copy numbers)
Lys	1:100,000
Phe	1:50,000
Thr	1:25,000
Dap	1:6,667

(from GeneChip® Expression Analysis Technical Manual-Affymetrix®)

The starting RNA concentration for these reactions was 5 μg, hence the following serial dilutions were used to prepare the poly-A controls from stock concentrate:

1st dilution   1:20
2nd dilution   1:50
3rd dilution   1:10
2μl of the final dilution was used for each sample.

First Strand cDNA synthesis

5 µg of total RNA is used. The following mix is prepared for each specimen:

2 µl of diluted poly-A control RNA
1 µl (100 pmol/µl) T7 oligo dT primer
Made up to 12 µl with DEPC treated water.

The samples were incubated at 65-70 ^{o}C for 10 minutes to denature the RNA. The following mastermix was added to each sample: 4 µl (x5) first strand buffer, 2 µl DTT, 1 µl (10 mM) dNTPs. This mix is incubated for 42 ^{o}C for 1 hour. 200 IU of Superscript II Reverse Transcriptase (Qiagen) is added and the mix incubated at 42 ^{o}C for a further 1 hour.

Second Strand cDNA synthesis

At the end of first strand synthesis, RNA/DNA heteroduplex molecules are present. In order for the second strand of cDNA to be synthesised, the method first described by Gubler and Hoffman (Gubler and Hoffman, 1983) is used. RNAse H enzyme is an RNAse which hydrolyses the RNA strand so that short RNA primers are left bound to the cDNA molecule. DNA polymerase I then synthesises the second cDNA strand. T4 DNA polymerase is added which creates blunt DNA termini.

The following reaction mix is added to the samples from the last reaction: 91 µl of DEPC treated water, 30 µl of (x5) second strand buffer, 3 µl of (10mM) dNTPs, 1µl of E. Coli DNA ligase (10 U), 4µl of E. Coli DNA Polymerase I (40 U), 1 µl of E.coli RNAse H (2U). This mix is incubated at 16 ^{o}C for 2 hours; then 2 µl (10 U) of T4 DNA polymerase is added followed by incubation at 16 ^{o}C for 5 minutes. Then 10 µl of 0.5M EDTA is added.

Clean-up of Double Stranded cDNA

This procedure uses spin columns to selectively bind and then elute cDNA akin to the Qiagen RNeasy mini kit procedure explained earlier. Briefly, 600 µl of cDNA binding buffer is added to the cDNA reaction mix. 500 µl of this mix is added to the cDNA cleanup spin column and spun for 1 minute at full speed. This is repeated with the rest of the reaction mix. 750 µl of wash buffer is added to the column and spun through. The purified cDNA is eluted by adding 14 µl of elution buffer and spinning for 1 minute at 10,000 rpm.

Synthesis of cRNA - In vitro Transcription

This process converts cDNA to cRNA and labels the molecules with biotinylated ribonucleotides. The following mix (28 µl) is added to each cDNA sample: 8µl of DEPC treated water, 4 µl (10x) IVT labelling buffer, 12 µl of IVT labelling NTP mix and 4 µl of IVT labelling enzyme mix containing viral derived RNA polymerases. The samples are incubated overnight at 37 $^{\circ}$C.

cRNA Clean-up

This process utilises RNA binding columns. The IVT reaction is diluted with 60 µl of RNAse free water. 350 µl of cRNA binding buffer is added followed by 250 µl of 100 % ethanol. This mix is passed through the cleanup column and spun at 10000 rpm for 15 seconds; the flow through is discarded. The columns are washed with 500 µl of wash buffer solution and then with 500 µl of 80 % ethanol (centrifuged at 10,000 rpm for 15 seconds). The cRNA is then eluted with RNAse free water and the concentration is checked with a nanodrop spectrophotometer.

cRNA Fragmentation

The cRNA is fragmented before it can be hybridised to the GeneChips®. 25 µg of cRNA is mixed with 10 µl of (x5) fragmentation buffer and made upto 50 µl with DEPC treated water. The (x5) fragmentation buffer contains 200 mM Tris-acetate pH 8.1, 500 mM potassium acetate and 150 mM magnesium acetate. The reaction mix is incubated at 94 ^{o}C for 35 minutes to cause cRNA fragmentation.

Hybridisation to Affymetrix U133 Array

15 µg of fragmented and labelled cRNA is used to hybridise to the geneChips®. This cRNA is mixed with a hybridisation cocktail of control oligonucleotide B2 (3nM) 5 µl, 20 x eukaryotic hybridisation controls 15 µl, hybridisation mix 150 µl, 30 µl of DMSO and nuclease free water made upto 300 µl. The arrays are equilibrated to room temperature and the hybridisation cocktail is applied. The arrays are hybridised in a proprietary oven for 16 hours followed by staining and scanning as per The GeneChip Expresison Analysis Technical Manual (Affymetrix).

2.10.2 Microarray Statistical Analysis

The Affymetrix gene chip array contains multiple oligonucleotide probes per gene; hybridisation of labelled cRNA oligonucleotides from the experimental sample generates a signal, the intensity is proportional to the number of cRNA oligonucleotides that have been bound and hence the degree of expression of that particular gene.

The first process in microarray data analysis is normalisation. This aims to remove systematic errors or biases from the data. In theory, a particular cRNA sample hybridised to two separate

microarray chips should generate exactly the same signal density from each probe on the chip. However, this does not occur in practice. This is due to random as well as systematic errors or biases. Systematic biases may be due to human errors in experiment replication, pippetting errors or differences in experiment protocol, if results from microarray experiments conducted in different laboratories are being compared. Normalization aims eliminate these biases so data generated from separate microarray experiments may be compared.

The Affymetrix Array contains paired sets of probes for each RNA gene. One pair represents the perfect Watson-Crick oligonucleotide and the mismatch pair contains the same sequence except for a single mismatched base pair. The degree of signal from the mismatch pair is representative of non-specific binding of the cRNA sample. This is subtracted from the signal from the perfect pair to give an adjusted result.

The normalisation method used in the present microarray analysis is denoted as quantile normalisation. This method ranks all of the probe signals by intensity. It then calculates the mean intensity of each rank and replaces the signal intensity at each rank with this mean value. The dChip software (freely available on http://biosun1.harvard.edu/complab/dchip/), incorporates quantile normalisation.

After normalisation, an expression value is generated for each gene which can then be statictically compared between treatments (vehicle only vs LCA alone or SAHA alone or LCA + SAHA) using the Student's t-test with $p<0.01$ being statistically significant.

Chapter 3 : Expression profiling of nuclear receptors and co-repressors in bladder cancer cell lines.

3.1 Introduction:

Nuclear receptors have been described as having classical endocrinological actions such as the VDR regulating the uptake of calcium from the small intestine. However, NRs are expressed in tissues which are not related to their well described classical actions, for example VDR is expressed in the prostate (Kivineva et al., 1998) and FXR is expressed in the breast (Swales et al., 2006). It is postulated that these NRs may be involved in regulating growth and differentiation at these sites, possibly acting as a co-operative network to sense dietary and xenobiotic inputs. For example, FXR is known as a bile acid sensor in the hepato-biliary tract. However, bile acids have been detected in breast cyst fluid (Javitt et al., 1994) and FXR may be involved in sensing these potentially toxic compounds in the breast.

Nuclear receptor ligands elicit a spectrum of anti-proliferative responses in cancer cells. These responses are not fully explained by either the level of nuclear receptor expression alone or the presence of mutations within the NR gene. An example is the VDR and the anti-proliferative responses to $1\alpha25$ $(OH)_2D_3$ in prostate cancer cells; Zhuang has demonstrated that cellular VDR content does not explain the variety of anti-proliferative responses in a panel of prostate cancer cell lines (Zhuang et al., 1997). Also, the VDR is not found to be frequently mutated in cancers (Miller et al., 1997). A possible explanation proposed by Khanim et al and Banwell et al is the overexpression of the co-repressors SMRT/NCoR2 and NCoR1 in prostate and breast cancers changes the NR signalling equilibrium towards selective repression of potentially anti-proliferative target genes despite the presence of adequate ligand and VDR (Khanim et al., 2004; Banwell et al., 2006). They also describe the

frequent overexpression of SMRT/NCoR2 in prostate cancers and NCoR1 in breast cancers as measured by Q-RT-PCR compared to matched normal tissue.

The specific hypothesis is that dietary derived NRs are expressed in the bladder cancer cell lines and exhibit a spectrum of anti-proliferative responses towards ligands to these NRs. A role for co-repressor expression is explored to explain the anti-proliferative responses.

3.2 Materials and Methods

- Quantitative real-time PCR.

- Western blotting.

- ATP proliferation assay.

- Stable transcription of NCoR1 over-expressing pcDNA3 plasmid.

3.3 Results

3.3.1 Bladder Cancer Cell lines have a spectrum of anti-proliferative responses to nuclear receptor ligands

The four bladder cancer cell lines were treated with ligands to various nuclear receptors as listed below.

Ligand	Nuclear Receptor
1α25 (OH)$_2$D$_3$	Vitamin D receptor (VDR)
Lithocholic acid (LCA)	Farnesoid X receptor (FXR) and VDR
9 cis retinoic acid (9cis RA)	Retinoid X receptor α, β, γ (RXR α, β, γ)
Eicosapentanoiec acid (EPA)	Peroxisome proliferator activating receptor α (PPAR α)
5,8,11,14-eicosatetraenoic acid (ETYA)	Peroxisome proliferator activating receptor γ (PPAR γ)
Chenodeoxycholic acid (CDA)	Farnesoid X receptor (FXR)
GW3965	Liver X receptor α and β (LXR α and β)
22 (R) Hydroxy Cholesterol (22-HC)	Liver X receptor α and β (LXR α and β)
Docosahexanoic acid (DHA)	Retinoid X receptor α, β, γ (RXR α, β, γ)

Table 3.1: Nuclear receptor ligands and their respective receptors.

Cells were plated out at densities of 2-4 x 10^3 per well and allowed to adhere overnight. They were treated with the stated concentrations of ligand as listed in the graphs below. The cells were re-treated at 48 hours and the ATP levels were read at 96 hours as described in section 2.3.
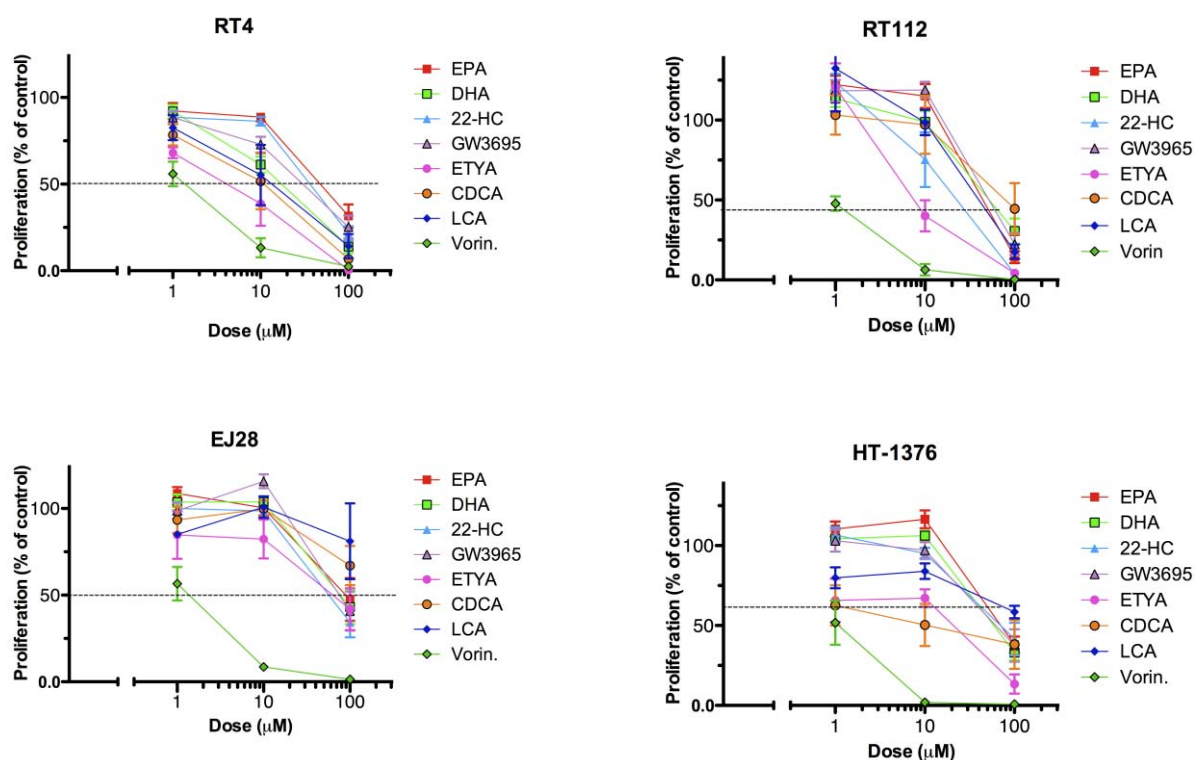
Figure 3.1: Cells were plated at the following densities into 96 well plates; RT-4 $2x10^3$ cells per well, HT-1376 $4x10^3$ per well, RT112 and EJ28 $3x10^3$ cells per well. These cell densities were pre-optimised to result in cells in the exponential phase of growth. The ATP levels were determined as per section 2.3 at 96 hours post treatment with an additional dose at 48 hours. The luminescence for the treatment wells was divided by that for the negative control to give a survival fraction. Therefore, survival >100 % denotes a pro-proliferative response and <100 % denotes an anti-proliferative response. The experiments were conducted in triplicate and were repeated three times. Error bars denote standard error of the mean.
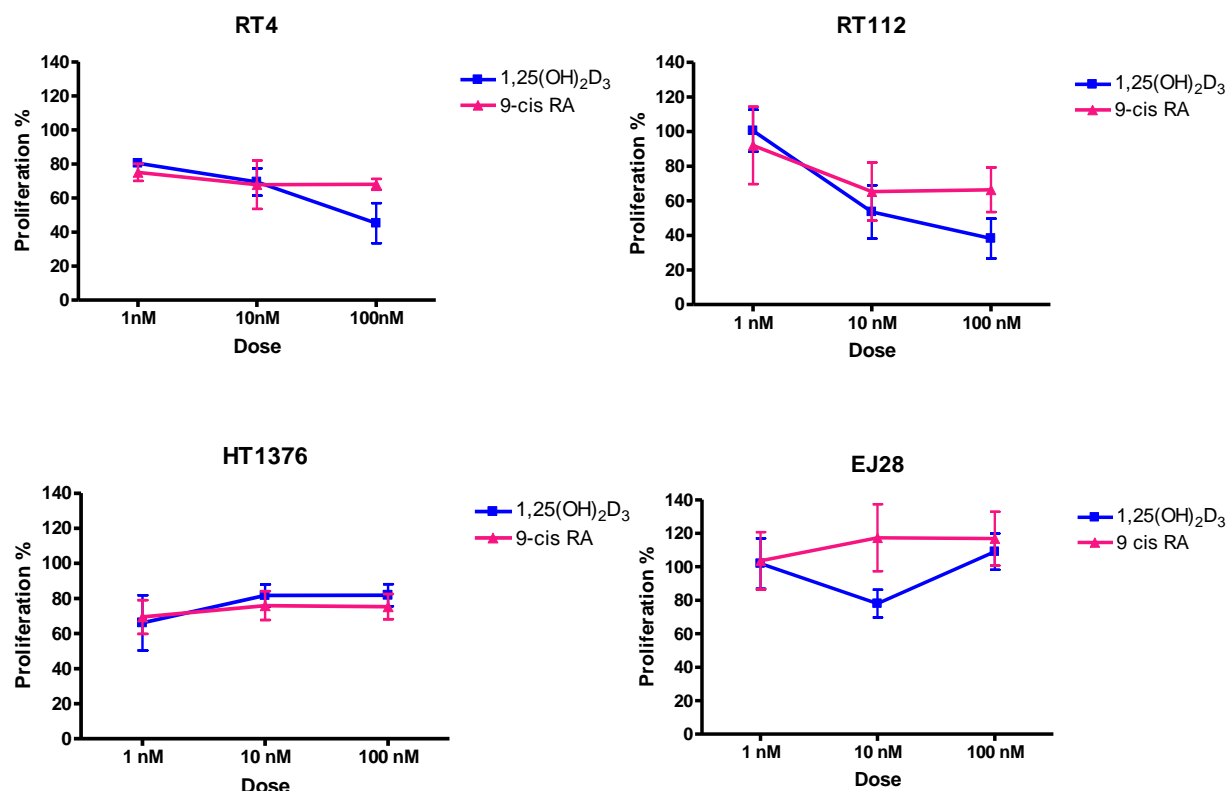
Figure 3.2: Cells were plated at the following densities into 96 well plates; RT-4 2x10³ cells per well, HT-1376 4x10³ per well, RT112 and EJ28 3x10³ cells per well. The ATP levels were determined as per section 2.3 at 96 hours post treatment with an additional dose at 48 hours. The luminescence for the treatment wells was divided by that for the negative control to give a survival fraction. Therefore, survival >100 % denotes a pro-proliferative response and <100 % denotes an anti-proliferative response. The experiments were conducted in triplicate and were repeated three times. Error bars denote standard error of the mean.

The above dose response graphs illustrate varying responses to treatment with the different nuclear receptor ligands and SAHA. ED50 doses, i.e. the estimated dose required to kill half the number of cells in comparison to vehicle only control, were calculated as a measure of cell sensitivity to the ligands. These are shown in table 3.2. There are two broad patterns which emerge from table 3.2. RT-4 cells appear to be the most sensitive i.e. have the lowest ED50 for all ligands except $1\alpha,25(OH)_2D_3$. Also, EJ-28 cells appear to be the least sensitive, i.e. have the highest ED50 for four ligands (EPA, ETYA, CDA and vorinostat). The dose response curve did not cross 50 % for $1\alpha25(OH)_2D_3$, LCA and 9-cis RA, hence, it is not

possible to comment on their sensitivity. The exceptions are DHA, GW3965 and 22 H Chol where EJ-28 is not the least sensitive cell line.

	Receptor	RT-4	RT-112	HT-1376	EJ-28
$1\alpha,25(OH)_2D_3$ (nM)	VDR	90	25	NC	NC
LCA (µM)	VDR, FXR	9.3	80	NC	NC
9-cisRA (nM)	RXR α,β,γ	NC	NC	NC	NC
DHA (µM)	RXR α,β,γ	89	90	110	95
EPA (µM)	PPAR α	105	110	110	130
ETYA (µM)	PPAR γ	3.6	12	20	85
CDA (µM)	FXR	8.9	105	45	862
GW3965 (µM)	LXR α, β	21	85	110	98
22HChol (µM)	LXR α, β	16	66	110	98
SAHA /Vorinostat (µM)	HDACi	1.2	0.9	1.0	1.3

Table 3.2: The ED50 values of the four bladder cancer cell lines when treated with the NR ligands listed in left hand column. ED50 values represent the concentration at which the dose response line crosses 50 %. NC-no convergence, describes ligands where dose response curve does not cross 50 %, therefore it is not possible to calculate an ED50 value.

3.3.2 Bladder Cancer cell lines display a spectrum of nuclear receptor and co-repressor expression.

Relative mRNA expression of a panel of nuclear receptors and co-repressors is shown in figure 3-1. These data are expressed relative to RT-4 cells. Unfortunately, a non-malignant bladder transitional epithelial cell line is not available for comparison. Hence RT-4 was used as a baseline because this cell line is the most sensitive to treatment with nuclear receptor ligands and it is the most differentiated cell line (derived from Grade 1 well differentiated transitional cell papilloma, ATCC number HTB-2).

Figure 3-3 reveals a spectrum of expression of nuclear receptors. The most clear pattern in terms of suppression of nuclear receptor expression is illustrated for the high grade bladder cancer cells, HT 1376 and EJ 28. Between the two of them, they have suppressed expression of 8 out of 10 nuclear receptors investigated (FXR, LXRα, PPARγ, PPARδ, VDR, RARα, RARβ, RXRα). EJ 28 alone expresses reduced levels of nuclear receptors as compared to the well differentiated RT4 cells in 7 out of the 10 nuclear receptors investigated (FXR, LXRα, PPARγ, PPARδ, VDR, RARβ, RXRα).

The pattern for nuclear receptor over-expression is less clear. The moderately differentiated RT-112 cell line expresses five nuclear receptors (LXRα,PPARδ,VDR, RARα and RXRα) at a higher level. The only co-repressor to be overexpressed is NCoR1 in RT-112 cells (1.59 fold, p=0.01) and EJ-28 cells (2.56 fold, p=2×10^{-5}).
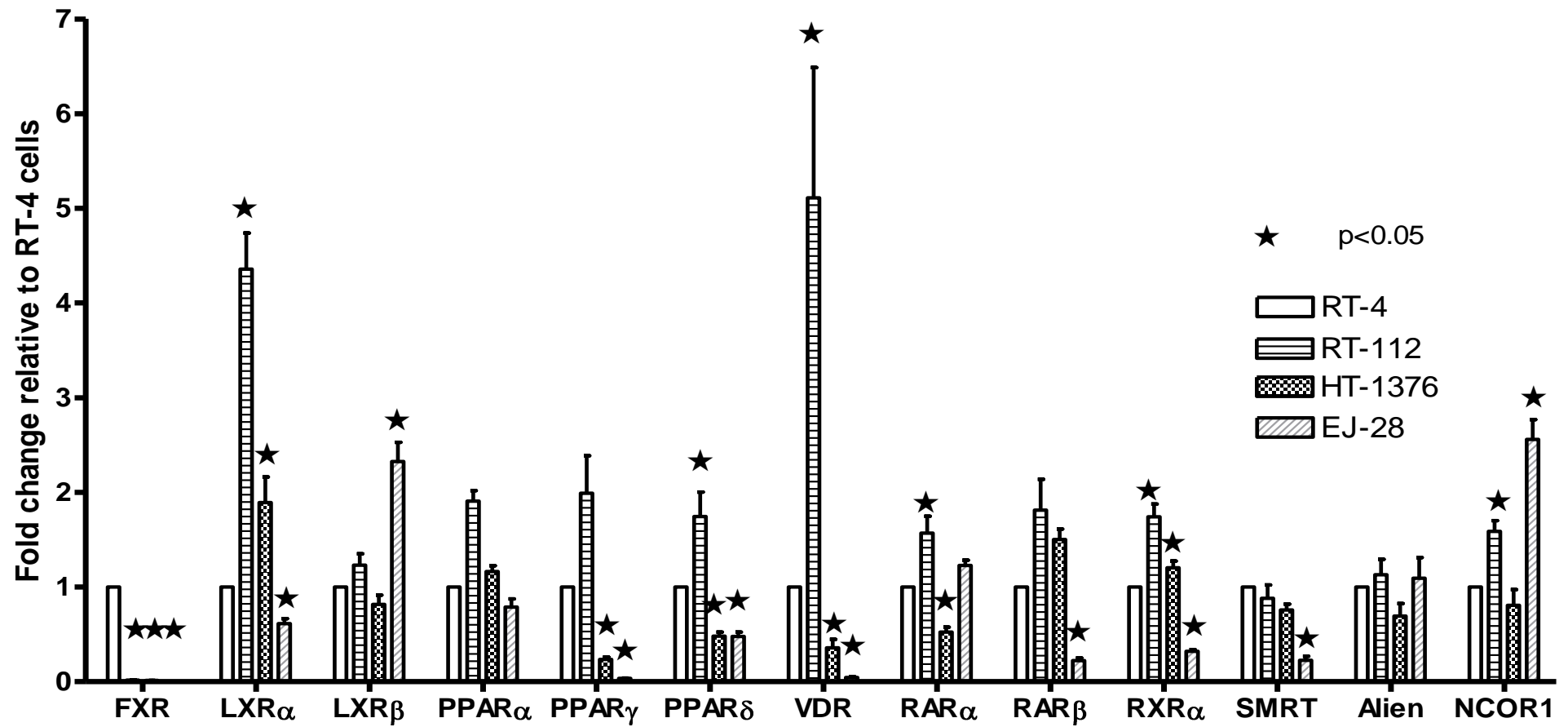
Figure 3.3: Relative expression of a panel of nuclear receptors and co-repressors (SMRT/NCoR2, NCOR1 and TRIP15/Alien) with respect to RT-4 cells. RNA was extracted from proliferating cells at sub-confluent levels (70 % confluence visually). RNA was reverse transcribed and Taqman qRT-PCR performed with primers for stated genes. Results stated relative to RT-4 cells and represent mean fold change from three separate experiments. Error bars represent S.E.M. of fold changes. * represents $p < 0.05$ i.e. statistical significance on a 2 tailed student's t-test.

3.3.3 VDR and FXR are expressed in bladder cancer cells at the protein level.

Two particular nuclear receptors, VDR and FXR, were investigated at the protein level by Western blotting.
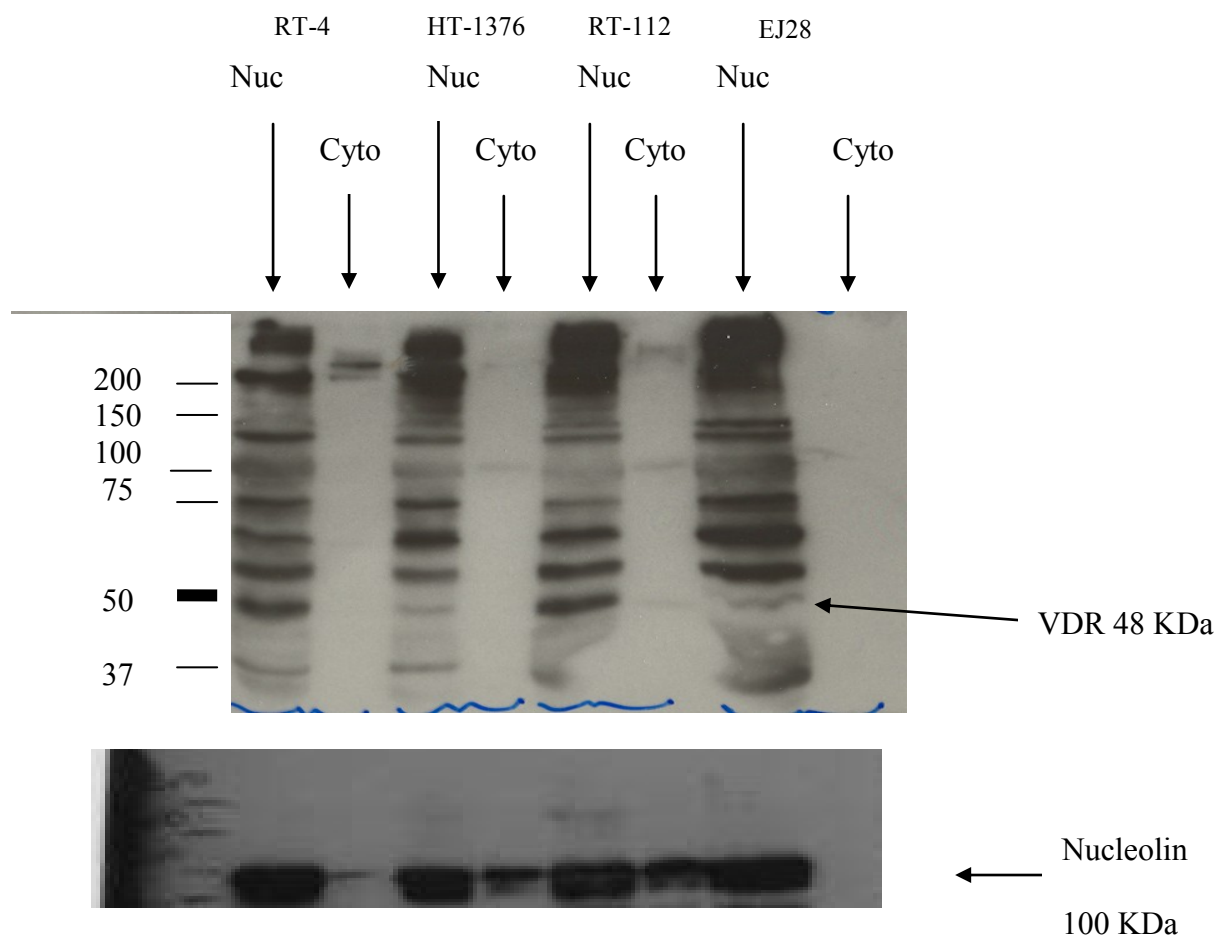
Figure 3.4: Western immunoblot of nuclear and cytoplasmic proteins extracted from the 4 bladder cell lines used (commercially available BioVision kit for the nuclear/cytoplasmic protein extraction was used). $2x10^6$ cells were seeded in T25 cell culture flasks and cells were harvested after they reached mid-exponential growth (~36 hrs). Monoclonal antibody against VDR clone MAB1360 was obtained from Chemicon International. Membranes were re-probed with a polyclonal antibody against nucleolin to ensure equal protein loading. Proteins were detected by chemiluminesence.

These particular nuclear receptor expression patterns were investigated at protein level because the action of LCA, a ligand for both VDR and FXR was further investigated on the panel of bladder cancer cell lines in terms of cell cycle FACS analysis, target gene expression via Affymentrix genechip microarray and Q-RT-PCR micro-fluidic genecard techniques as described in chapter 4. Hence, it is appropriate to confirm protein expression for these particular nuclear receptors.

The blot above illustrates that VDR is not expressed in the cytosolic protein fraction in the bladder cancer cell lines. It also broadly follows the same pattern as the real-time PCR receptor expression as shown in figure 3-1. Therefore, RT-112 and RT-4 appear to have significantly higher VDR expression as compared to HT-1376 and EJ-28 cells. The VDR blot has multiple bands in the nuclear protein fraction. This may be due to non-specific antibody binding however, this seems unlikely as there are very few bands within the cytosolic fraction. The lower nucleolin blot confirms the presence of protein within the nuclear lanes. Perhaps the VDR antibody would have been bound within these lanes had there been non-significant binding, An alternative explanation may be VDR protein with post translational modification for some of the bands. There is evidence of VDR binding to nuclear membrane proteins; these complexes may be giving rise to the multiple bands (Nangia et al., 1998).

Figure 3-3 illustrates a Western blot of whole cell protein extract probed for FXR expression. This blot does confirm that FXR is expressed at protein level in these bladder cancer cells. This Western blot suggests that, when controlled for loading, all 4 cell lines may have similar expression of FXR. However, the mRNA expression suggests that expression of FXR in HT-1376, RT112 and EJ28 is reduced as compared to RT-4. These data suggest that bladder cancer cell lines express VDR and FXR mRNA and protein to varying levels.
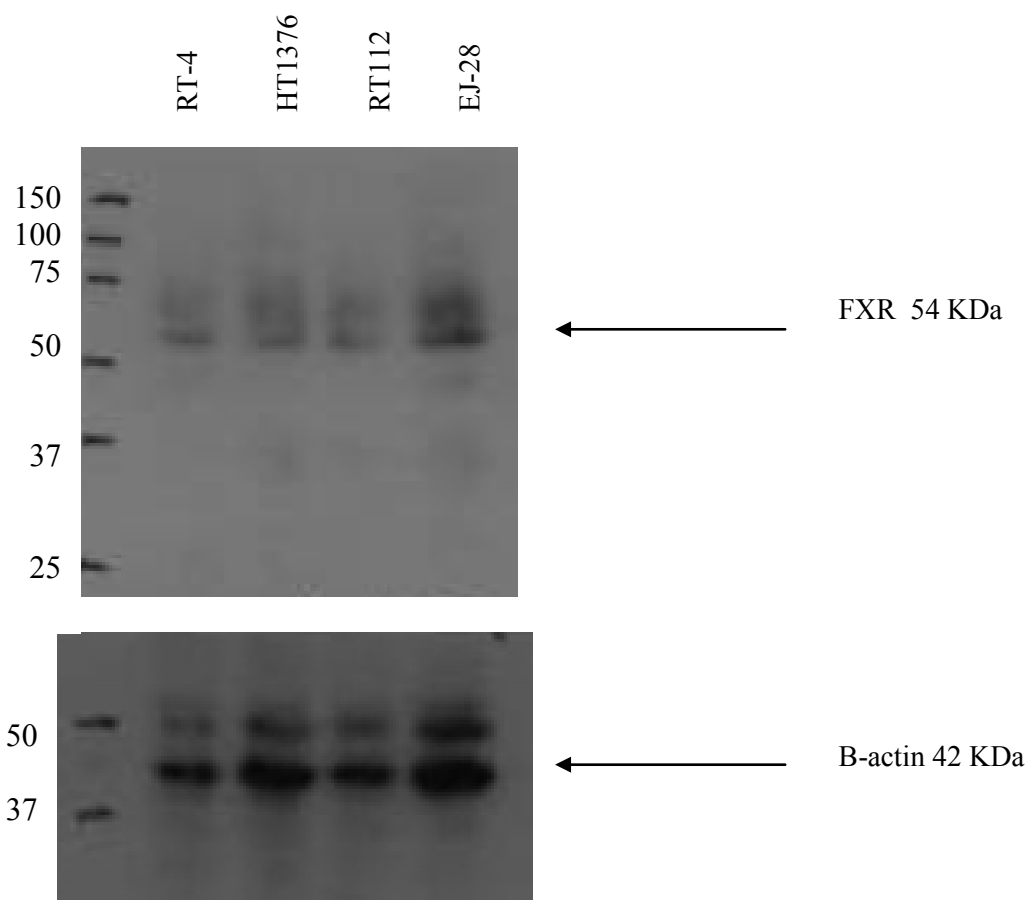
Figure 3.5: Western immunoblot for FXR. 3x10^6 cells were incubated in T25 flasks overnight and allowed to adhere and reach mid-exponential growth. Total cellular protein was extracted by adding RIPA buffer with protease inhibitor (Sigma). Western blot as per materials and methods. Monoclonal antibody against FXR was obtained from R&D Systems. The membrane was stripped and re-probed for β-actin (monoclonal antibody AC-15 Sigma).

3.3.4 Cell Sensitivity is Partly Correlated with Nuclear Receptor to Co-repressor Ratio

The co-repressor NCoR1 has significantly raised mRNA expression on RT-112 (1.6 fold) and EJ-28 (2.6 fold) cells as illustrated in section 3.3.2. This may lead to a raised ED50 for some of the NR ligands due to a shift in the equilibrium of the ligand bound nuclear receptor towards the repressor state i.e. bound to co-repressors and histone deacetylase enzymes which

would favour a transcriptionally silent state. One would expect the ratio of co-repressor expression to nuclear receptor to correlate with the ED50. Therefore, a raised relative level of nuclear receptor expression may alleviate the suppressive effect of the raised expression of NCoR1. To investigate whether NCoR1 over-expression may be correlated with the expression ratio of NCoR1 and each nuclear receptor ED_{50}, these values are given in table 3.2. This ratio is significantly correlated with ED_{50} values for EPA, ETYA and CDA. The correlation is difficult to assess for VDR and FXR as these dose response curves did not converge towards 50 % inhibition, hence an ED_{50} value was not generated. The NCoR1 to nuclear receptor ratio did not correlate with the ED50 for DHA, GW3965 and 22-HC. Also neither the nuclear receptor nor the NCoR1 expressions correlate with the ED50 values for the latter ligands (DHA, GW3965 and 22-HC).

		RT-4	EJ28	Correlation	
				r2 value	p-value
VDR (Vit D)	R exp		1	0.04425	
	NCoR:Recep		1	57.8229 **T**	
	ED50 **(nM)**		90	>100	
VDR (LCA)	R exp		1	0.04425	
	NCoR:Recep		1	57.8229	
	ED50 (mcM)		9.3	>100	
RARα	R exp		1	1.22702	
	NCoR:Recep		1	2.0855 **T**	
	ED50 (mcM)	ND	ND		
RARβ	R exp		1	0.22417	
	NCoR:Recep		1	11.415	
	ED50 (mcM)	ND	ND		
RXRα (9cisRA)	R exp		1	0.31986	
	NCoR:Recep		1	8.00023	
	ED50 (nM)	>100	>100		
RXRα (DHA)	ED50 (mcM)		89	95	
PPARα (EPA)	R exp		1	0.78752	
	NCoR:Recep		1	3.24937	
	ED50 (mcM)		105	130	0.904	0.049
PPARδ	R exp		1	0.47843	
	NCoR:Recep		1	5.34862 **T**	
	ED50 (mcM)	ND	ND		
PPARγ (ETYA)	R exp		1	0.03475	
	NCoR:Recep		1	73.6333	
	ED50 (mcM)		3.6	85	0.977	0.011
FXR (CDA)	R exp		1	0.00074	
	NCoR:Recep		1	3454.8	
	ED50 (mcM)		8.9	862	0.988	0.006
FXR (LCA)	R exp		1	0.00074	
	NCoR:Recep		1	3454.8	
	ED50 (mcM)		9.3	>100	
LXRα	R exp		1	0.61466	
	NCoR:Recep		1	4.16317	
LXRβ	R exp		1	2.3268	
	NCoR:Recep		1	1.09977	
(GW3965)	ED50 (mcM)		21	98	
(22-HC)	ED50 (mcM)		16	90	
HDAC inh (SAHA)	ED50 (mcM)		1.2	1.3	

Table 3.3: The four bladder cancer cell lines are arranged in their order of reducing differentiation. Total mRNA from RT-4 and EJ-28 was extracted, in triplicate, from mid-exponentially proliferating cells, and the levels of *NCOR1* and the indicated receptors was measured by Q-RT-PCR. From these values the fold changes of each target was determined in comparison to RT-4 cells. From these two values a ratio of the fold changes in levels of *NCOR1* to receptor mRNA is given (NCOR1:Recept), for each receptor. Parallel cultures were exposed to dose titration studies of the cognate ligands to generate sigmoidal dose-response curves from which the estimated dose required to inhibit proliferation by 50% (ED50) was calculated. The correlation between the NCOR1:Receptor ratio and the ED50 was measured and r2 and *p* values are indicated. T denotes those relationships that follow the same trend.

3.3.5 NCoR1 stable over-expression.

3.3.5.1 Confirmation of NCoR1 over-expression

Stable clones were isolated after transfection of RT-4 cells with either pcDNA3-NCoR1 plasmid or mock transfected with pcDNA3 empty vector (negative control). To confirm NCoR1 over-expression, we performed Q-RT-PCR for NCoR1 mRNA expression for the clones and normalised NCoR1 expression in over-expressing clones to the mean of the mock transfected clones.
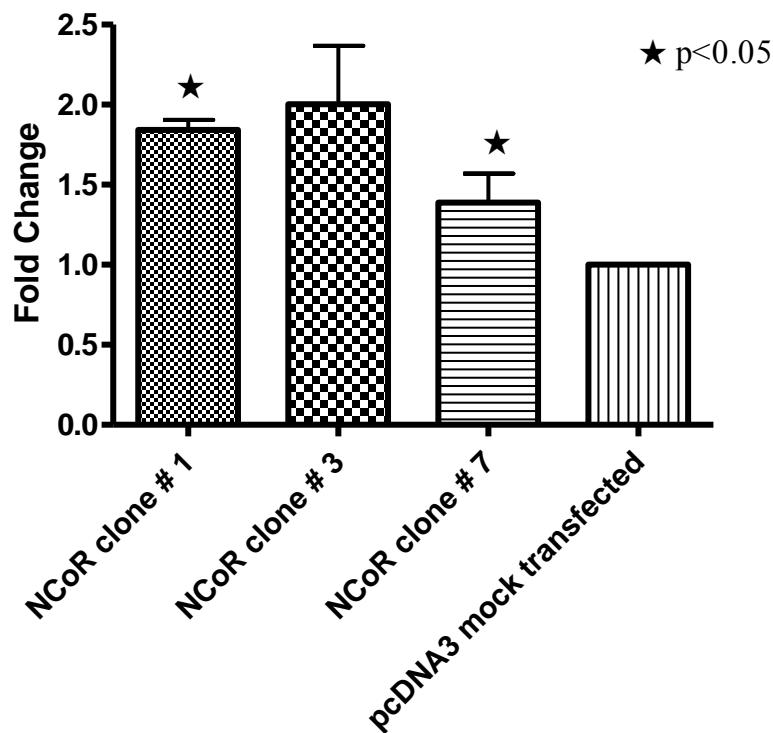
Figure 3.6: RNA was extracted from transfected cells in mid-exponential phase, reverse transcribed and q-RT-PCR performed for NCoR1 (18S as internal control). The fold changes are expressed as relative to the mean δCt of all of the mock transfected clones (pcDNA3 clones #1,5,6,7). The star signifies significant over-expression as tested by a one-tailed student's t-test.

Western blotting was performed for NCoR1 protein to confirm overexpression at the protein

level.
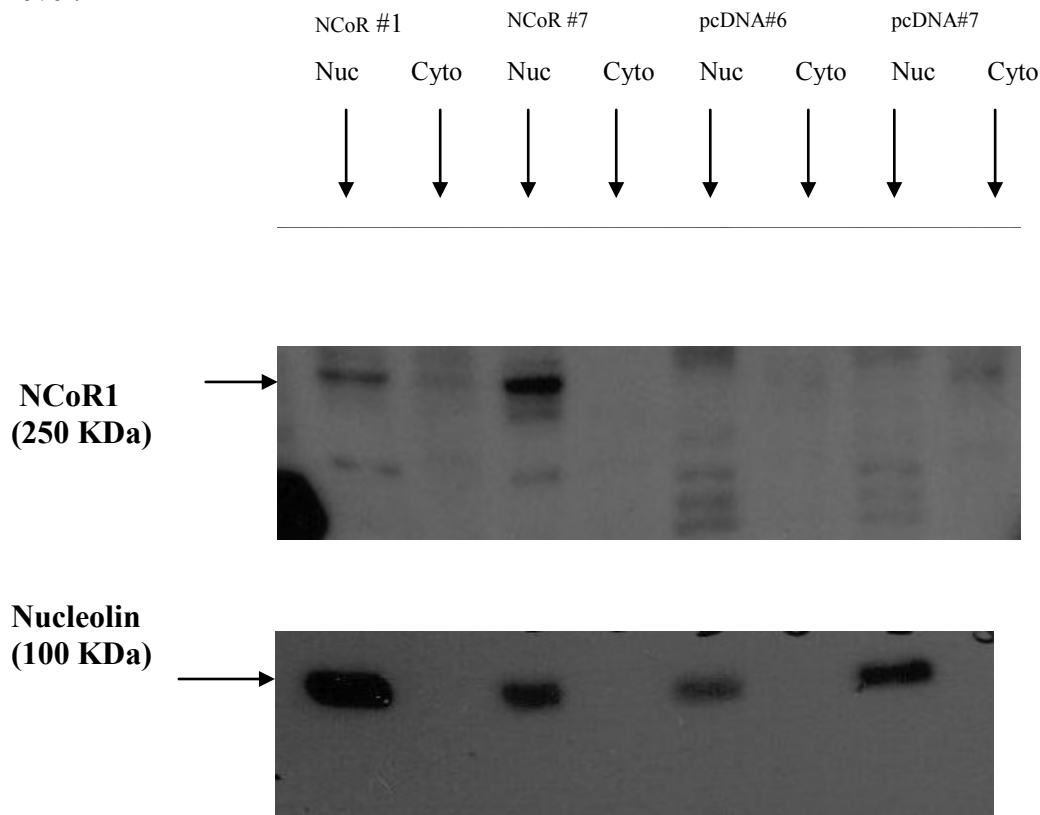
Figure 3.7: Western blot for NCoR1 in transfected clones. NCOR#1 and #7 are two clones stably expressing the transfected NCoR1. pcDNA#6 and #7 are mock transfected clones. Nuclear and cytoplasmic protein preparations were isolated from transfected cells (commercially available BioVision kit for the nuclear/cytoplasmic protein extraction was used). A polyclonal NCoR1 primary antibody (Abcam ab24552) was used to detect NCoR1. The immunoblot demonstrates a significant high molecular weight band in the nuclear fraction of clones NCoR#1 and #7 corresponding to the transfected NCoR1. The membrane was reprobed with nucleolin as a loading control.

The blot confirms presence of an appropriate weight band, corresponding to transfected

NCoR1, in the nuclear fractions of the NCoR1 transfected clones and not the mock

transfected clones. Expression is higher in NCoR # 7 as compared to NCoR #1 despite the

latter having higher mRNA expression for NCoR1 as per figure 3.6.

3.3.5.2 Over-expression of NCoR1 leads to reduced sensitivity to some NR ligands.

NCoR overexpressing clone # 7 and mock transfected pcDNA3 clone cells were treated with nuclear receptor ligands at 1, 10 and 100 μM concentrations for ETYA, CDA, LCA and SAHA and at 1, 10 and 100 nM for $1,25(OH)_2D_3$ and 9-cis RA. The ligands were incubated for 96 hours, with a re-dose at 48 hours as per section 2.3. There was a trend towards decreased sensitivity towards ligand with NCoR1 over-expression, best illustrated in figure 3.8 B, which shows the percentage suppression of cell growth at 10nM (Vit D and 9cisRA) and 10 μM (ETYA, CDA, LCA and SAHA).
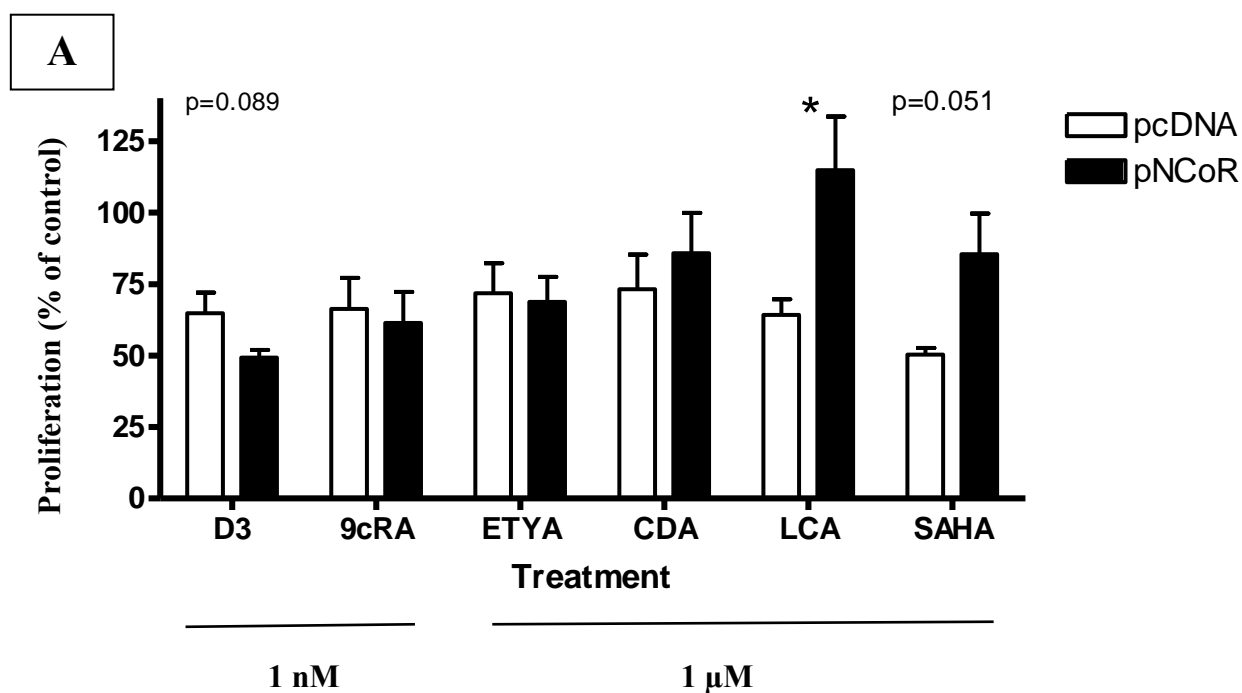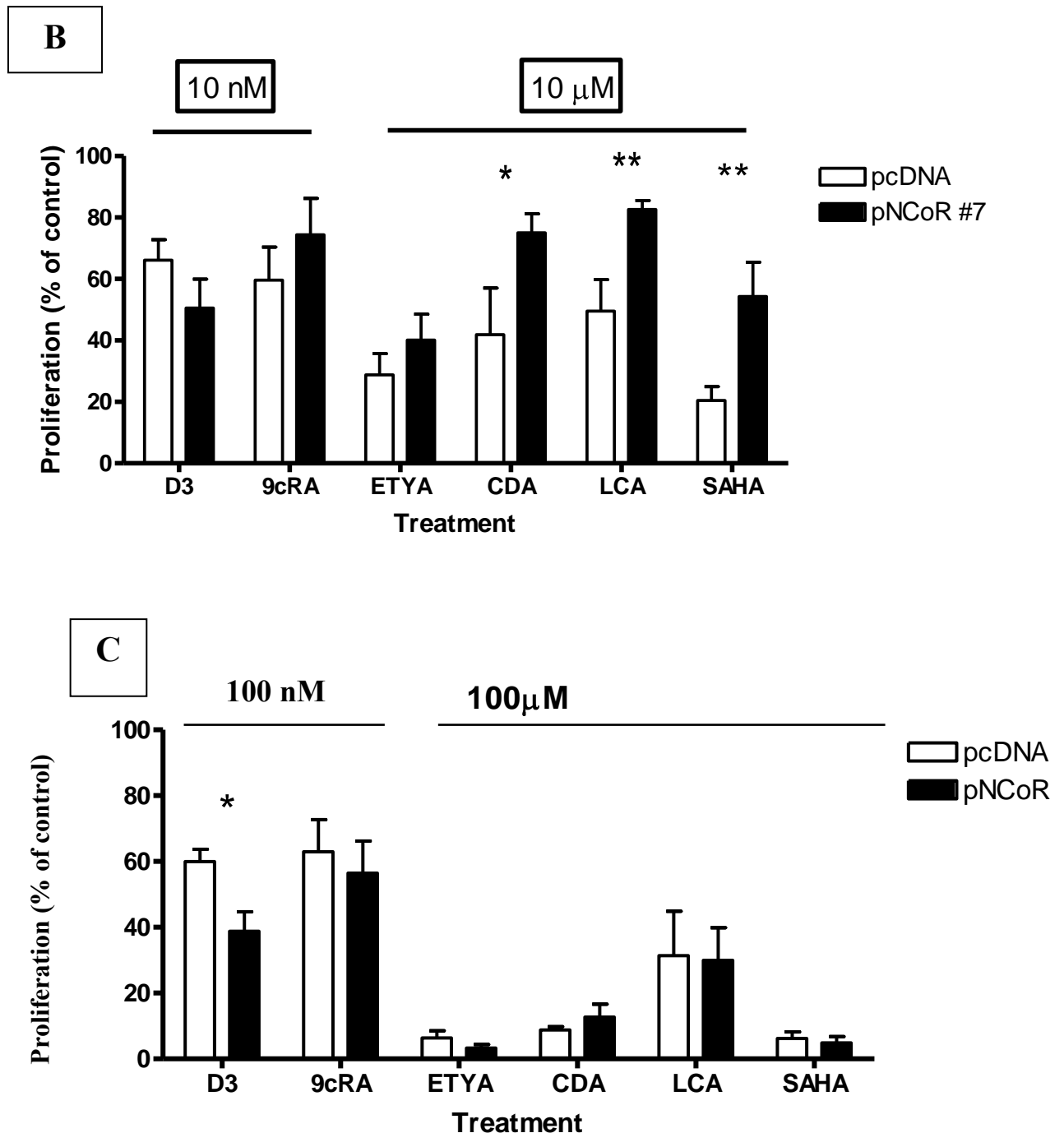
Figure 3.8: Sensitivity to inhibition of proliferation by treatment with the indicated NR ligands comparing RT-4 NCoR#7 and RT-4 pcDNA#6; 96 hour incubation with a re-dose at 48 hours; proliferation was measured using the ATP bioluminescent proliferation assay as detailed in materials and methods. A – 1 nM/μM, B – 10 nM/μM, C – 100 nM/μM. Each data point represents the mean value of three separate experiments each performed in triplicate wells; * indicates statistical significance at p<0.05 and ** at p<0.01 as tested by a one-tailed student's t-test..

Figure 3.8 B clearly shows reduced sensitivity in NCoR#7 cells as compared to mock transfected cells when treated with CDA, LCA and SAHA but not for $1,25(OH)_2D_3$, 9 cis RA and ETYA. This may suggest that NCoR1 selectively regulates FXR and the responses to HDAC inhibition but is not the co-repressor involved in the regulatory protein complexes with VDR, RXRs and PPARγ.

To recap, these experiments demonstrate a spectrum of sensitivity of the panel of bladder cancer cell lines towards a panel of NR ligands. The least sensitive cell line, EJ-28 over-expresses the co-repressor NCoR1 mRNA by 2.6 fold as compared to the most sensitive cell line RT-4. EJ-28 cells also over-express NCoR1 at the protein level as demonstrated in our publication (Abedin et al., 2009). Forced over-expression of NCoR1 in RT-4 cells resulted in reduced sensitivity to treatment with CDA, LCA and SAHA. The cellular model to explain these results hinges on nuclear receptors being bound to a repressor complex consisting of a multimeric protein complex which includes co-repressors such as NCoR1 as well as histone deacetylase enzymes that allosterically maintain a closed chromatin structure and hence suppress target gene transcription. Therefore, to test this model cells were treated subsequently with ED_{25} concentrations of NR ligands and SAHA in combination and running the proliferation assay to establish anti-proliferative responses.

3.3.6 Co-treatment of NR ligands with histone deacetylase inhibitor SAHA.

Treatment of the four cell lines with minimally active ED_{25} concentrations of the HDACi SAHA and ED_{25} concentrations of nuclear receptor ligands showed a range of additive behaviours. RT-4 has no strongly additive combinations whereas, every combination in EJ-28

and four out of five combinations in RT-112 cells are strongly additive. This indicates that the combination of NR ligand and SAHA lead to a statistically significantly larger inhibition of cell growth (p<0.05) than would be expected by the sum of the individual inhibitory effects of the NR ligand and SAHA. It is notable that the two cell lines that demonstrate the strongly additive inhibitory effect, RT-112 and EJ28 both over-express NCoR1 by 1.6 and 2.6 fold respectively. These results revealed that a raised expression of the co-repressor NCoR1 in RT-112 and EJ-28 cells, may be targeted pharmacologically with a histone deacetylase inhibitor. To further investigate this additive effect, the above experiment was repeated with NCoR1 over-expressing clones.

RT4

(a)

RT-112

★ < 0.05

(b)

HT-1376 Proliferation
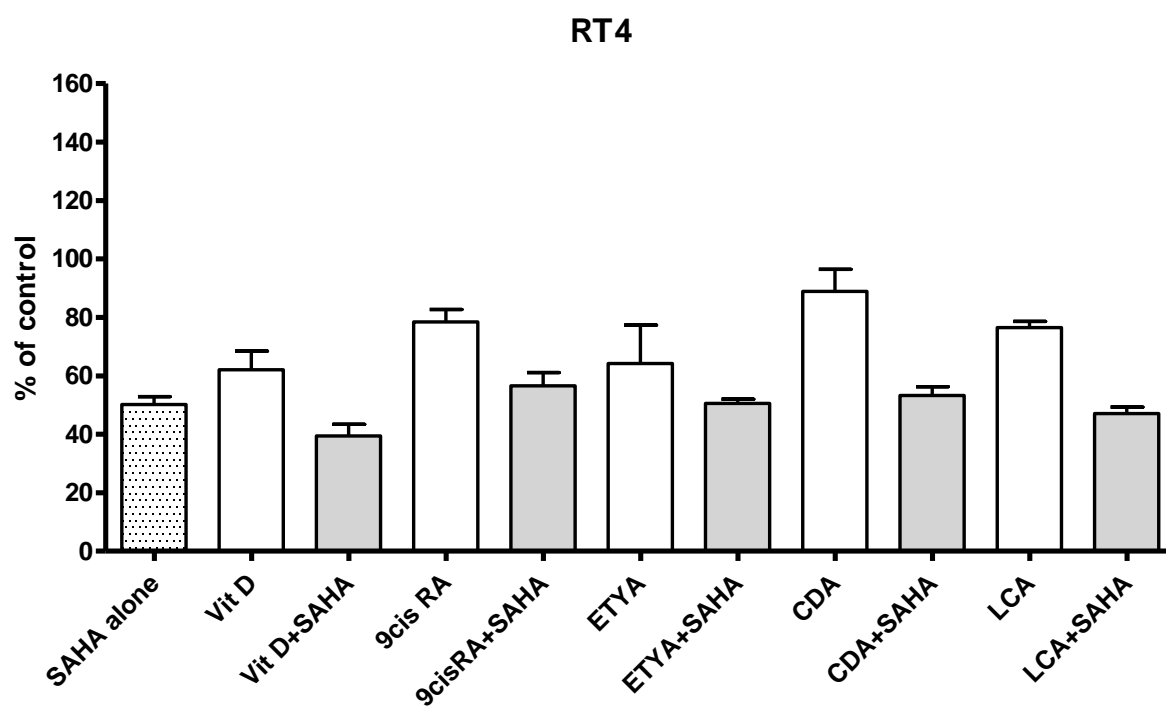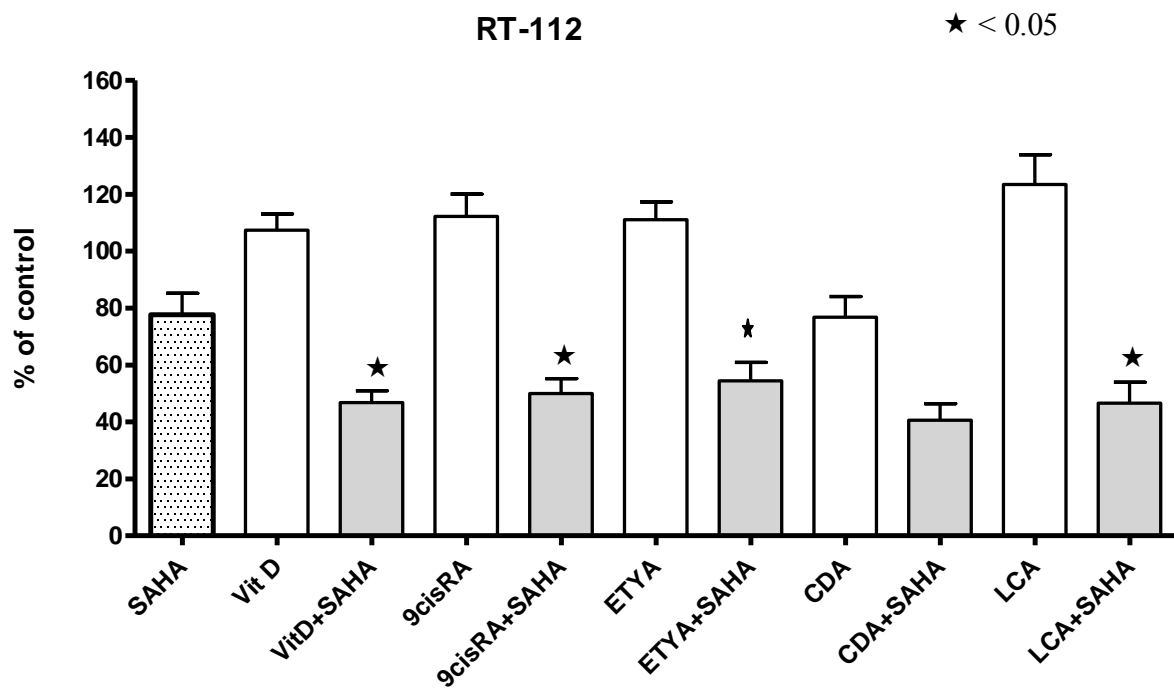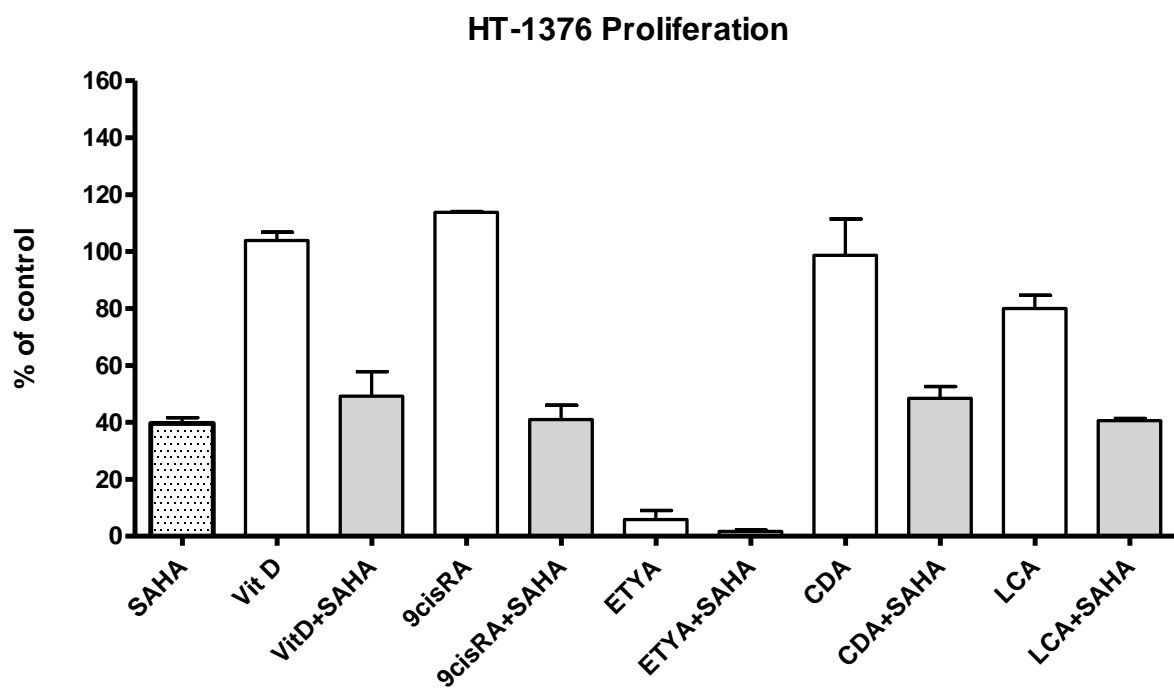
(c)
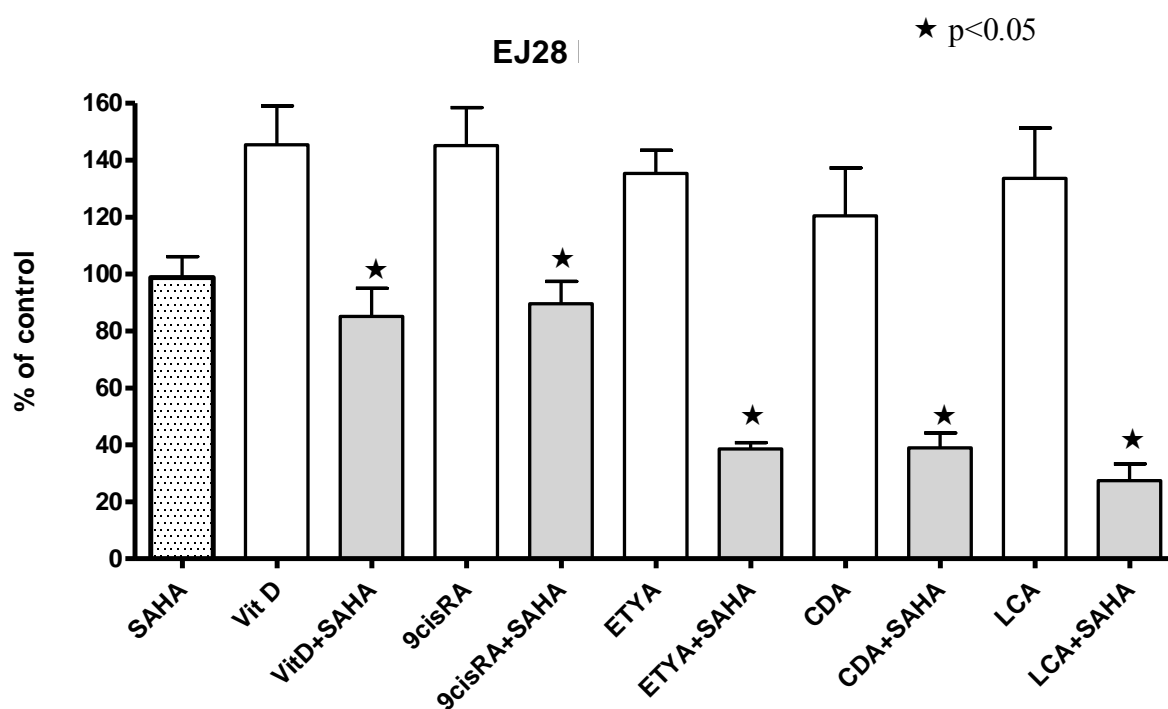
(d).

Figure 3.9 (a)-(d): Proliferation assays of cell lines treated by either ED$_{25}$ concentrations of NR ligand, SAHA or in combination in a 96 well format. Incubation for 96 hours with a re-dose at 48 hours. Y-axis denotes cell proliferation as percentage of negative control. * denotes strongly additive effect in combination i.e. the observed anti-proliferative effect is statistically significantly greater than that predicted from the sum of the individual effects of the NR ligand and SAHA alone; p<0.05 by the one tailed student's t-test.

3.3.7 Co-treatment of NCoR1 over-expressing clones with SAHA
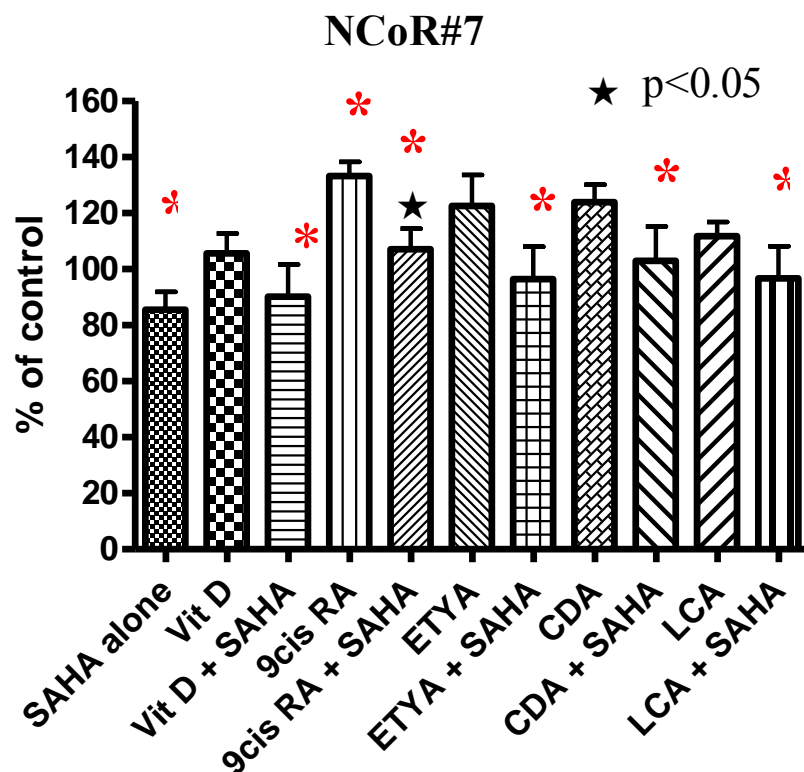
(a)
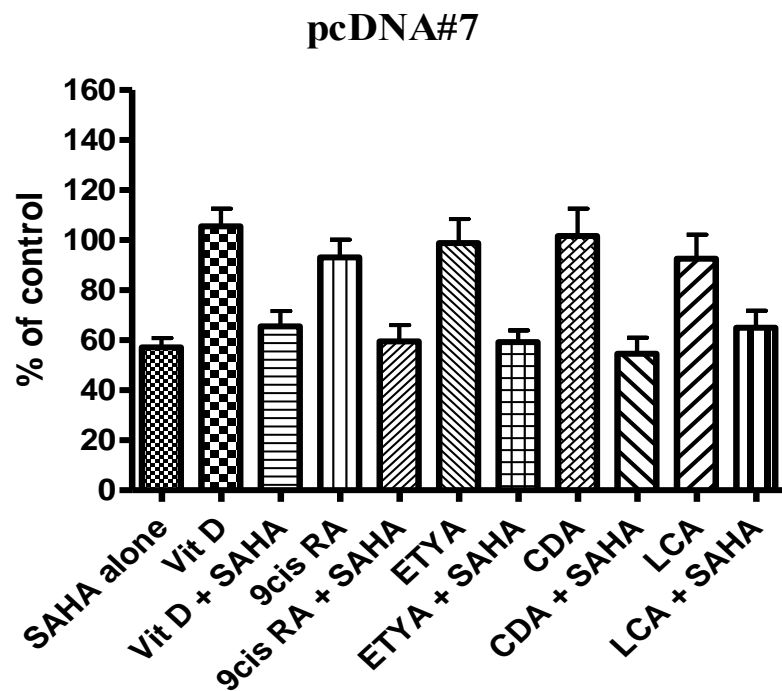
(b)

Figure 3.10 (a)-(b): Proliferation assays of NCoR1 over-expressing RT-4 clone (NCoR#7) and mock transfected clones (pcDNA#7) treated by ED$_{25}$ concentrations of either NR ligand, SAHA or in combination in a 96 well format. Incubation for 96 hours with a re-dose at 48 hours. Y-axis denotes cell proliferation as percentage of negative control. * denotes strongly additive effect in combination i.e. the observed anti-proliferative effect is statistically significantly greater than that predicted from the sum of the individual effects of the NR ligand and SAHA alone. * signifies treatments in the NCoR overexpressing clone#7 which exhibit statistically significant (p<0.05 one tailed student's t-test) reduced cell inhibition as compared to the same treatments in the mock transfected control pcDNA#7 clone.

The experiment illustrated in figure 3.9 (a) was repeated with the NCoR1 over-expressing clone#7 and the mock transfected clone #7. Figure 3.10 shows that the effect of over-expressing NCoR1 is to make the cells less sensitive to the treatments i.e. the degree of inhibition is reduced. For example, the degree of inhibition of the NCoR#7 clone when treated with SAHA alone is 14.5 % whereas in the mock transfected clone (pcDNA#7) it is 42.9 % i.e. the NCoR#7 over-expressing clone has lost sensitivity to SAHA. This may be expected as NCoR1 is a co-repressor, hence forced over-expression has enhanced its repressor role. Possibly reflecting this, there is no evidence of a strongly additive interaction between the NR ligands and this dose of SAHA.

When the cell inhibition in NCoR#7 clone was compared to the same treatments in the mock transfected control pcDNA clone#7 using the one tailed student's t-test, the treatments with SAHA appeared to lose inhibition and sensitivity in the NCoR over-expressing clone#7 (shown by * in figure 3.10 (a)). 9cis RA is the only individual treatment which led to a statistically significantly less inhibition in the NCoR#7 clone. Otherwise for 1,25(OH)$_2$D$_3$, ETYA, CDA and LCA, the individual treatment was not statistically different between the two clones however, the combined treatment with SAHA led to a significant loss of sensitivity in the NCoR#7 clone. The raised expression of NCoR1 has resulted in SAHA being less inhibitory.

3.4 Discussion

These data demonstrate varied responses to treatment with a panel of nuclear receptor ligands in four bladder cancer cell lines. This variability can to some extent be explained by the relative expression of the relevant nuclear receptors in the different cell lines. Therefore, the most sensitive cell line to $1\alpha,25(OH)_2D_3$ is RT-112 with an ED_{50} of 25 nM as compared to RT-4 (ED_{50} = 90 nM), HT-112 and EJ-28 (ED_{50} >100 nM). Correspondingly, the VDR expression in RT112 is 5.1 fold higher than RT4 and 14.5 fold and 127.5 fold higher than HT-1376 and EJ-28 cells respectively. In general, EJ28 cells have the lowest relative expression of the nuclear receptors tested. This is coupled with increased NCoR1 co-repressor expression which, in general, leads to the highest NCoR1: nuclear receptor ratio in EJ-28 cells. These cells, in most instances, also have the highest ED50 values, i.e. they are the least sensitive to the different ligands. For example, PPARα expression is 1.3 fold lower in EJ-28 cells as compared to RT-4 cells. However, this is coupled with an NCoR1 : PPARα ratio of 3.2 for EJ-28 which translates into a higher ED50 value (130 μM for EJ28 as compared to 105 μM for RT-4).

I have illustrated expression of the VDR and the FXR in bladder cancer cell lines at the protein level (figures 3.2 and 3.3). The expression of VDR in bladder cancer has been previously demonstrated via immuno-histochemistry on human bladder tumour tissue (Hermann and Andersen, 1997; Sahin et al., 2005). However, no previous references demonstrating FXR expression in the urinary bladder are apparent and therefore this is a novel finding. Bile acid conjugates have been demonstrated in urine from healthy volunteers. Goto et al have demonstrated the presence of acyl galactosides of deoxycholic acid in healthy human urine estimated at 20-100 ng/ml concentration (Goto et al., 2005). This bile acid is a known ligand for FXR (Makishima et al., 1999; Parks et al., 1999). Deoxycholic acid is

known to be a carcinogenic agent, indeed it has long been suggested as a promoter of colorectal cancer. Therefore, studies have shown higher levels in the faeces of colon cancer patients (Korpela et al., 1988), that it stimulates human colonic mucosal growth (Bartram et al., 1993) and stimulates growth of colonic cells in culture (Peiffer et al., 1997). Bile acid binding FXR has a number of well described cellular effects including the expression of the bile acid export pump (ABCB11) (Ananthanarayanan et al., 2001) and the multidrug resistance associated protein 2 (ABCC2) (Kast et al., 2002) and the expression of detoxifying enzymes such as CYP3A4 (Gnerre et al., 2004). These membrane pumps export the bile acids out of the cell and detoxifying enzymes degrade bile acids to less toxic derivatives. All of the above can lead to a model which can explain a possible physiological role for the expression of FXR in bladder urothelium. Therefore, FXR can sense potentially damaging bile acid conjugates in the urine which leads to expression of export pumps and detoxifying enzymes which protect the urothelial cells from the carcinogenic effects of these bile acids. There is intriguing evidence that VDR may also be involved in a similar role. Therefore, LCA bound to VDR can bind VDR response elements on the CYP3A4 promoter to also stimulate expression of this key detoxifying enzyme (Jurutka et al., 2005). These responses lead to protection of the bladder epithelial layer as it comes into contact with potentially damaging and carcinogenic substances in urine.

In order to support the suggestion that increased NCoR1 expression in RT-112 and EJ-28 cells may be related to reduced sensitivity to NR ligands, NCoR1 protein was over-expressed NCoR1 protein in RT-4 cells. The over-expressing clones demonstrated a significantly reduced sensitivity to CDA, LCA and SAHA (figure 3.8 b). This suggests a link between NCoR1 and responses to these ligands. Clearly, if the over-expression of NCoR1 in EJ-28

cells and responses to these ligands was a chance coincidence then over-expression in RT-4 would not have altered responsiveness in RT-4 cells. In other words, if NCoR1 was not a participant in the multi-meric protein repressor complex then its over-expression would not have altered responsiveness to the above ligands.

Figure 3.8 (a) and (c) demonstrate a dose dependent effect in the loss of sensitivity when NCoR1 is over-expressed. Therefore in fig 3.8 (a), clones are treated with 1 μM ETYA, CDA, LCA and SAHA; there is significant loss of sensitivity in LCA alone in the NCoR#7 clone. SAHA treatment exhibits a p-value of 0.051 i.e. this treatment approaches statistical significance. Figure 3.8 (c) exhibits inhibitory effects with 100 μM ETYA, CDA, LCA and SAHA treatment; none of these ligands exhibits significant loss of sensitivity. This is likely due to excessive cellular toxicity with a high dose of 100 μM; these treatments cause cell inhibition of greater than 80 % therefore this insult if likely to be too severe to be rescued by a raised expression of NCoR1.

Combination treatment of the tested nuclear receptor and SAHA (HDAC inhibitor) showed contrasting patterns of response (figure 3.9 (a) – (d)). RT-4 and HT-1376 display no strongly additive responses i.e. the addition of SAHA does not lead to significantly reduced cell numbers as compared to the expected combined response i.e. the sum of the effect of the NR ligand and SAHA alone. In RT-112, strongly additive effects are seen with $1,25(OH)_2D_3$, 9 cis RA, ETYA and LCA. However, in EJ-28 cells, strongly additive effects were seen with all of the ligands. This suggests that increased NCoR1 expression in RT-112 and EJ-28 cells (1.6 and 2.6 fold respectively, $p<0.05$) may be connected to this strongly additive response. However, these experiments were repeated with NCoR1 over-expressing clone #7 and mock transfected clone # 7 (figure 3.10) and did not show strongly additive responses apart from 9 cis RA. There can be two possible explanations for this. NCoR1 mRNA over-expression in

EJ-28 cells was 2.6 fold; we did not achieve this level of over-expression with the stably transfected clones (NCoR clone #1 was 1.84 fold and NCoR #7 was 1.39 fold, $p<0.05$). If a higher level of NCoR1 over-expression could be achieved then maybe we would have seen strongly additive responses. Intriguingly, RT-112 cells over-express NCoR1 by 1.6 fold i.e. less than EJ-28 cells and displayed strongly additive responses to 3 out of the 5 tested ligands. Also, the NCoR1 over-expressing cells are less sensitive to SAHA, therefore the dose of SAHA may be inadequate to elicit a strongly additive response and may need to be increased. This may suggest a spectrum of strongly additive response in proportion to the over-expression of NCoR1. An alternative explanation may be found in the ATP proliferation assay.

This assay estimates the number of cells present by measuring the total amount of ATP present. Therefore, when there is a reduction in cell numbers in response to treatment with an NR ligand +/- SAHA, the proliferation assay does not provide any insight to the mechanism leading to reduced cell numbers. A number of mechanisms could be responsible such as caspase dependent apoptosis, cell senescence, cell cycle arrest, non-apoptotic programmed cell death/paraptosis and autophagic cell death. There is evidence that the initiation of one or more of the above pathways is cell context dependent i.e. the response of two particular cell types to the same stimulus can lead to different mechanisms of cell death or growth arrest. This may occur in different cell lines derived from the same cancer type. An example may be the effect on different cells by treatment by the HDAC inhibitor, SAHA. This HDAC inhibitor, amongst other mechanisms, can cause the intrinsic pathway of apoptosis which is in part regulated by BCL-2 family members. Therefore, over-expression of BCL-2 or BCL-XL inhibits SAHA induced apoptosis in prostate cancer cells and inhibition of BCL-2 by the

chemical inhibitor HA14-1 increases apoptosis (Xu et al., 2006). The expression of BCL-2 may control the effect of treatment with SAHA, i.e. whether apoptosis occurs or not.

In the context of the strongly additive responses seen with co-treatment with NR ligands and SAHA in figure 3.9 (d), this response suggests that the combination of NR ligand and SAHA induces cellular pathways that do not occur with treatment with the individual agents. For example, the combination may induce apoptosis and cell cycle arrest or senescence or any other combination of cell death mechanism. Thereby, the combined treatment leads to a degree of cell death which is over and above that expected from the sum of the individual effects. When considering a separate cell line such as RT-4, this malignant cell line is likely to have widespread genomic and epigenetic differences as compared to EJ-28, not just in the expression of NCoR1 protein. These differences are likely to impact on the presence of functional cell death pathways. For example, the pro-apoptotic proteins BIM or BAX may be mutated in RT-4 which would attenuate the ability of this cell line to undergo apoptosis. Therefore, this lack of apoptosis may explain why a strongly additive response is not seen in RT-4.

To attempt to resolve this issue the following chapter will present data illustrating the cell-cycle effects on the four cell lines of treatment with LCA + /- SAHA, demonstrating that the cell lines do not have similar effects. This may be supportive of the proposal stated above.

Chapter 4 : Gene regulation in response to NR ligands.

4.1 Introduction

The previous chapter demonstrated a variety of anti-proliferative responses displayed in four bladder cancer cell lines towards a panel of nuclear receptor ligands (figures 3.9 (a)-(d)). There are a number of possible mechanisms for the variation in anti-proliferative responses, depending upon the contribution of cell-cycle arrest, programmed cell death processes and cell senescence. A key consideration to elucidating the mechanism of antiproliferative action is identification of the cohort of gene targets activated after treatment with ligand.

There are 17 gene families of cytochrome P450 enzymes in humans (Fukumori et al., 2007). These are membrane bound, heme containing mono-oxygenases which play a key detoxification role. The first 3 families, CYP1, CYP2 and CYP3 are known to metabolise drugs and xenobiotics (Pascussi et al., 2003). CYP3A4 is the most abundant Cyp P450 enzyme classically expressed in the liver and also expressed in small bowel epithelial cells. It plays a role in the metabolism of over 50 % of all drugs and xenobiotics by hydroxylation reactions (Wrighton et al., 1996), which convert them into water soluble metabolites for excretion via the urine and faeces.

Nuclear receptors act as sensors to many of these compounds to regulate the expression of CYP3A4. The Pregnane X receptor (PXR) is expressed in the liver and small intestine and is activated by endogenous compounds such as bile acids and exogenous substances such as the antibiotic rifampicin. Similar to VDR and FXR, PXR forms heterodimers with the retinoid x receptor (RXR) and upon activation, binds to response elements in the promoters of target genes. CYP3A4 is a key target gene; the PXR-RXR heterodimer binds via *ER6, DR3* and

DR4 repeat sequences in the promoter. Xie W et al have robustly proven that the nuclear receptor PXR (and its homologue SXR) is a xeno-sensor and is a regulator of CYP3A4 expression (and of its rat homologue Cyp3A23 and mouse homologue Cyp3a11) in response to appropriate inducers (Xie et al., 2000). They engineered PXR null mice and demonstrated lack of induction of Cyp3A enzymes by dexamethasone (Dex) and pregnenalone-16α-carbonitrile (PCN) which are rodent specific Cyp3A inducers. Only the Cyp3A enzyme was affected; induction of other CYPs such as Cyp 1A2 was intact in response to its inducer 3-methylcholanthrene. Dexamethasone, acting via the glucocorticoid receptor (GR), was also able to induce GR target gene hepatic tyrosine amino transferase. Hence, only Dex's action via the PXR was ablated.

4.2 Methods

- Propidium iodide cell staining and flow-cytometry for cell cycle analysis.
- Quantitative Real-time PCR (Q-RT-PCR)
- Q-RT-PCR$_m$ microfluidic arrays
- Affymetrix™ U133 plus 2 gene chip microarrays.

4.3 Results

4.3.1 Cell cycle effects of lithocholic acid +/- SAHA

To assess mechanistic details, one of the ligands, lithocholic acid (LCA), either alone or in combination with SAHA was chosen for cell cycle analysis (fig 4.1).
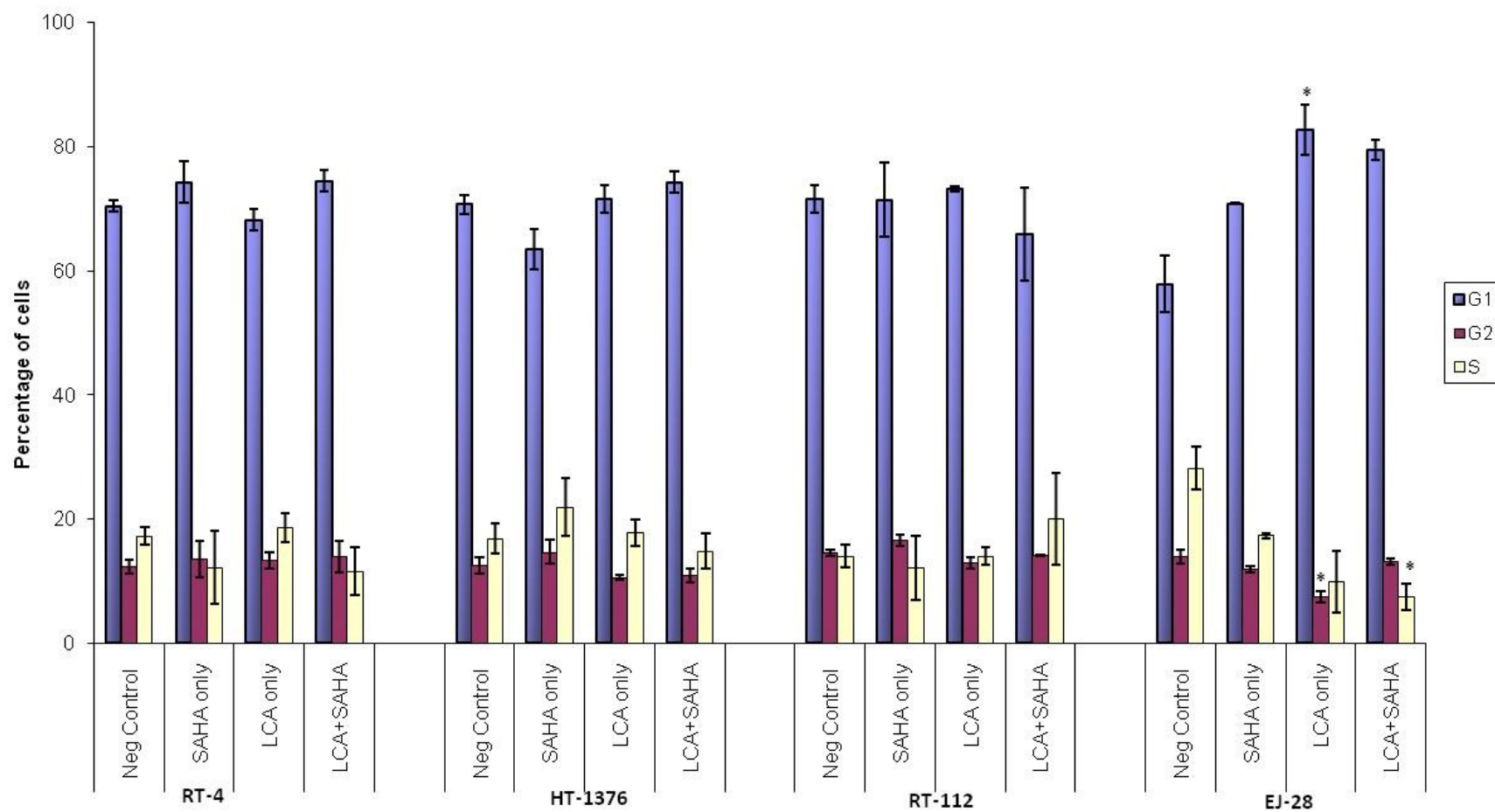
Figure 4.1: Cell cycle analysis using FACS (fluorescent activated cell sorting). $2x10^6$ cells were seeded in T25 flasks and allowed to adhere overnight. They were treated with LCA alone (ED50 dose; RT-4 20 µM, HT-1376 and EJ-28 100 µM, RT-112 50 µM) or in combination with SAHA (0.8 µM) and incubated for 96 hours with a re-dose at 48 hours. Total cells (both adherent and detached) were trypsinised, pelleted and washed in PBS. They were resuspended in FACS buffer (1% sodium citrate, 0.1% Triton X-100, 0.1 mM Na Cl and 10 µg/ml PI) and stained with PI. Cell cycle distribution was determined via flow cytometry analysis. Mean of triplicate independent experiments shown. Error bars show standard error. Statistical significance assessed with students t-test, * $p<0.05$ compared to negative control.

In EJ-28 cells, there is clear evidence of a G1/S cell cycle arrest with LCA treatment (mean percentage of cells in G1: 57.87 % +/- 4.55 for negative control as compared to 82.66 % +/- 4.06 for LCA treatment (p=0.03); mean percentage of cells in S phase is 28.22 % +/- 3.53 for negative control and 9.91 % +/- 5.01 for LCA treatment p=0.054). There is some evidence suggesting a G1/S phase cell-cycle arrest upon treatment with LCA + SAHA (mean percentage of cells in G1: negative control 57.87 % +/- 4.55, LCA+SAHA treatment 79.37 % +/- 1.61, p=0.51; mean percentage of cells in S phase: negative control 28.22 % +/- 3.53 as compared to LCA+SAHA treatment 7.49 % +/- 2.16, p=0.027) i.e. the reduction in cell number in S-phase is statistically significant even if the increase in cells in G1 phase upon treatment with LCA + SAHA is just short of reaching statistical significance. There is no evidence of a cell-cycle arrest in the other cell lines.

To investigate the cell cycle arrest in EJ28 cells, a Q-RT-PCR approach was used to investigate the expression of putative target genes that may underlie the anti-proliferative responses seen with LCA +/- SAHA treatment; p21$^{(wafl/cip1)}$ and CYP3A4 were chosen.

P21 $^{(Cip1/Wafl)}$ is a cyclin dependent kinase inhibitor which is a key anti-proliferative target of dietary derived nuclear receptors. Freedman LP et al first demonstrated the expression of p21$^{(wafl/cip1)}$ in response to $1\alpha,25(OH)_2D_3$, as well as the presence of a VDR response element within the p21 $^{(Cip1/Wafl)}$ promoter (Liu et al., 1996). Saramaki et al demonstrated in 2006, using chromatin immuno-presipitation, the presence of VDR response elements as well as $1\alpha,25(OH)_2D_3$ binding within the p21$^{Cip1/Wafl}$ promoter (Saramaki et al., 2006). There is evidence that lithocholic acid in combination with all trans retinoic acid can induce

oesophageal cells to express p21 $^{(Cip1/Waf1)}$ (Chang et al., 2007), hence there is circumstantial evidence suggesting that p21 $^{Cip1/Waf1}$ is a relevant potential target gene under these conditions.

4.3.2 Induction of *CDKN1A* (p21$^{(Waf1/Cip1)}$) post treatment with LCA+/- SAHA

Four bladder cancer cell lines were treated with LCA +/- SAHA at the same concentrations as used in figure 3.9, and mRNA was extracted at 6 hours post treatment. CDKN1A mRNA levels were measured using Q-RT-PCR. All four cell lines show significant induction of CDKN1A in at least the SAHA treatment. This is expected as CDKN1A is an established SAHA target gene (Gui et al., 2004).

RT-4 cells displayed the highest significant CDKN1A induction with all treatments [3.4 +/- 0.32 fold for SAHA, 2.28 +/- 0.31 fold for LCA and 4.62 +/- 0.30 fold for the combination treatment of LCA and SAHA]. Interestingly, in EJ-28 cells, SAHA induced nearly twice as much CDKN1A mRNA compared to control (1.91 +/- 0.16 fold) and the combination of LCA + SAHA induced 2.30 +/- 0.16 fold increased CDKN1A mRNA. These are statistically significant results. However, LCA treatment alone displayed no significant change in CDKN1A levels. This induction of CDKN1A mRNA reflects the G1 cell cycle arrest demonstrated in EJ-28 cells (figure 4.1). However, in figure 4.1, there is no statistically significant evidence of cell cycle arrest in RT-4 cells despite the larger induction of CDKN1A in these cells. Most likely, this reflects the difference in the time points (6 hours for CDKN1A and 96 hours for the cell cycle analysis).
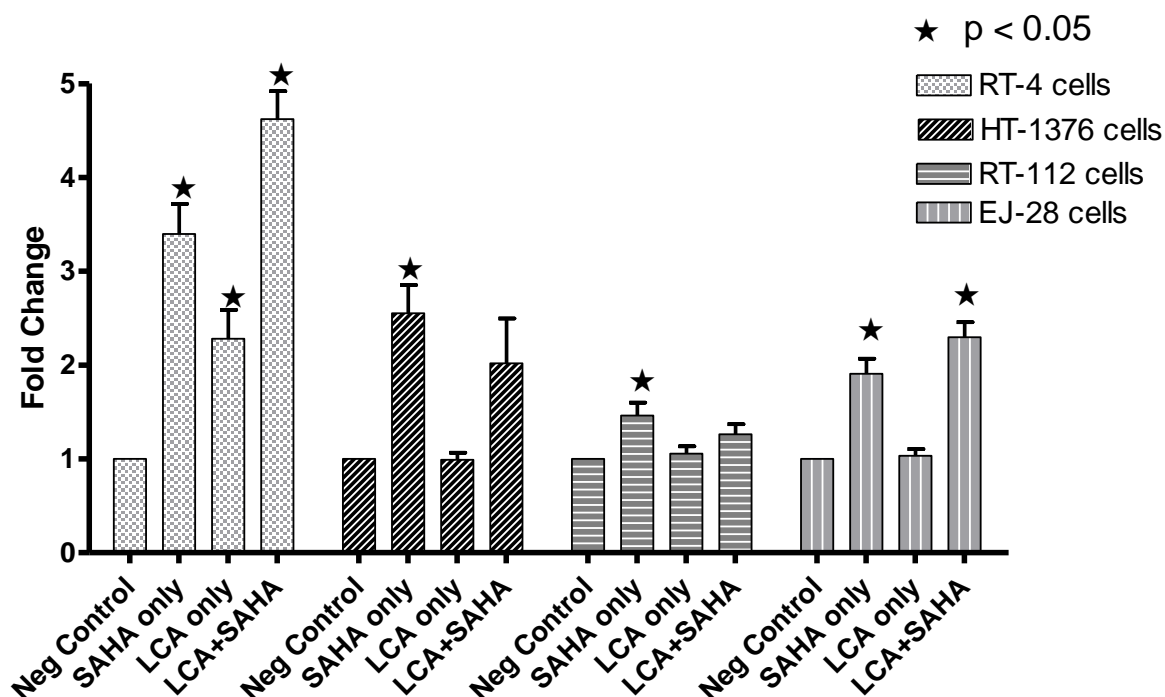
Figure 4.2: Induction of *CDKN1A(p21^{Waf1/Cip1})* after LCA+/- SAHA at 6 hours. Cells were treated with LCA (RT-4 20 μM, HT1376 and EJ-28 100 μM, RT-112 50 μM) +/- SAHA (0.8 μM) and total RNA isolated at 6 hours post treatment. After reverse transcription, Q-RT-PCR was conducted using *CDKN1A* primers and probes. Results from three independent experiments performed in triplicate are represented. Statistical significance was assessed by the students t-test (2-tail); *=p<0.05 compared to negative (untreated) control.

4.3.3 Induction of CYP3A4 after treatment with LCA +/- SAHA

The induction of CYP3A4 following treatment with LCA +/- SAHA was also investigated under the conditions above; illustrated in figure 4.3 below. In RT-4 cells, there was statistically significant induction of CYP3A4 mRNA in all three treatments [SAHA alone 2.47 +/- 0.64 fold; LCA alone 3.36 +/- 0.81 fold; LCA + SAHA 2.65 +/- 0.37 fold]. There was no evidence of additive induction with the combination treatment of LCA + SAHA. Both HT-1376 and RT-112 cells exhibited significant induction of CYP3A4 when treated with

LCA alone [1.80 +/- 0.35 fold and 2.01 +/- 0.50 fold respectively], but this was not altered significantly by LCA and SAHA treatments.

With EJ-28 cells, SAHA and LCA alone did not significantly induce CYP3A4 [1.37+/- 0.32 and 1.58 +/- 0.53 fold respectively], However, the combined treatment demonstrated significant induction by 3.42 +/- 1.02 fold (figure 4.3).

It is interesting that LCA induces CYP3A4 in all of the cell lines apart from EJ-28 (figure 4.3), which overexpresses NCoR1 by the highest amount (2.56 fold +/- 0.21 as compared to RT-112 cells which overexpress NCoR1 by 1.59 fold +/- 0.11). As previously demonstrated, FXR does induce CYP3A4 expression, therefore it is not surprising that LCA should increase CYP3A4 mRNA expression in RT-4, HT-1376 and RT-112. Perhaps increased NCoR1 expression in EJ28 cells, dampens the transactivation function of ligand bound FXR at response elements in the CYP3A4 promoter so transcription does not occur. The simultaneous addition of the HDAC inhibitor, SAHA may inhibit the bound histone deacetylases and either release or attenuate the inhibitory effect of NCoR1.
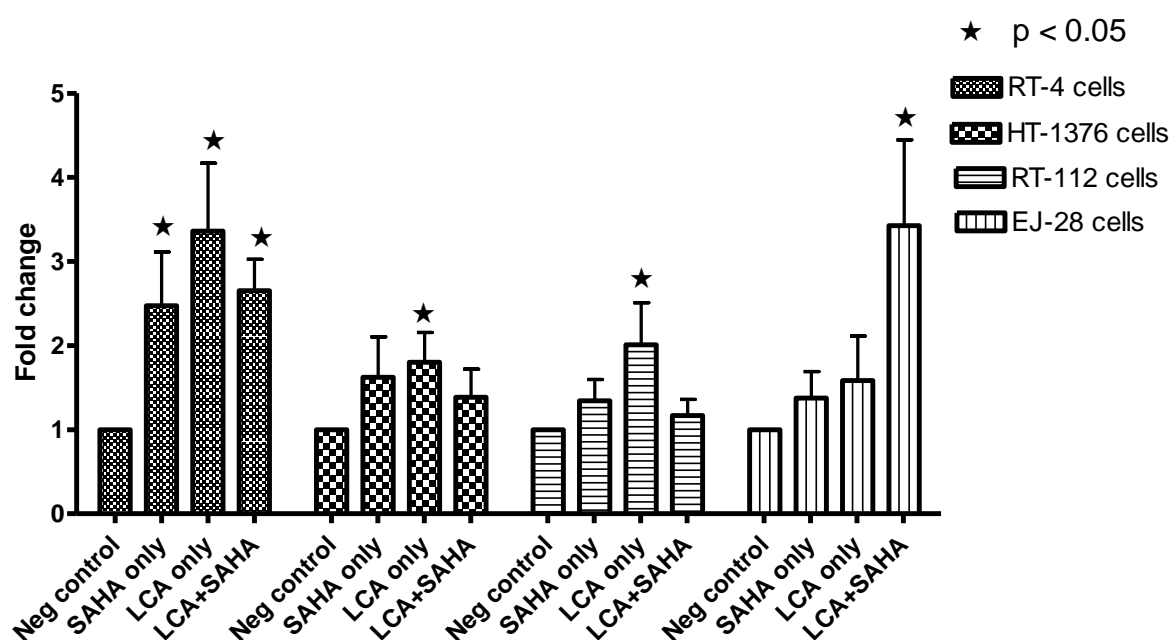
Figure 4.3: *CYP3A4* **induction after LCA +/- SAHA treatment at 6 hours. Cells were treated with LCA (RT-4= 20 μM, HT1376 and EJ-28= 100 μM, RT-112= 50 μM) +/- SAHA (0.8 μM) and total RNA isolated at 6 hours post treatment. After reverse transcription, Q-RT-PCR was conducted using *CYP3A4* primers and probes. Results from three independent experiments performed in triplicate are represented. Statistical significance was assessed by the students t-test (2-tail); *=p<0.05 compared to negative (untreated) control.**

There is some evidence that FXR acts as a regulator of CYP3A4 expression. Gnerre et al incubated Hep G2 liver cells with CDA or GW4064 (Gnerre et al., 2004). The former is a natural and the latter is a synthetic FXR ligand. Using Q-RT-PCR, they demonstrated a statistically significant increase in mouse Cyp3A4 expression after 24 hour incubation with 10 μM of GW4064. Gene reporter studies identified a highly FXR responsive fragment and further evidence from wild type, FXR^{-/-} and PXR [-/-] mice treated with intra-peritoneal injections of GW4064 add support to the concept that FXR is an activator of Cyp3A4 expression.

There is evidence to suggest that VDR is also a regulator of CYP3A4 expression. Human primary hepatocytes treated with $1\alpha\ 25\ (OH)_2\ D_3$ express CYP3A4 mRNA as detected by RT-PCR and Q-RT-PCR (15 fold) (Drocourt et al., 2002). Gel mobility shift assays have

demonstrated a band shift when VDR was incubated with the DR3 and ER6 response elements from the CYP3A4 distal enhancer and promoter regions respectively. Finally, when HepG2 hepatocyte cells were co-transfected with CYP3A4 promoter-reporter plasmids containing the DR3 or ER6 sequences as well as VDR, and treated with 1 nM 1α 25 $(OH)_2$ D_3, reporter gene activity was increased 12 and 40 fold respectively compared to control (Drocourt et al., 2002). Mice fed oral LCA demonstrated increased Cyp3A4 protein expression in the intestine (Matsubara et al., 2008). These authors have also demonstrated increased Cyp3A4 reporter activity in mice livers upon feeding with LCA provided the mice had adenovirally over-expressed VDR in their livers.

4.3.4 Target gene expression in NCoR1 transfectants

4.3.4.1 Expression of CDKN1A and CYP3A4 in NCoR1 transfectants

To investigate the possible role of NCoR1 expression on the expression of target genes, CDKN1A and CYP3A4, we treated NCoR stably overexpressing clones #1 and #7 and mock transfected control clones pcDNA#3 and #7 with 10 µM LCA and extracted mRNA at 4, 6, 8 and 24 hours. Subsequently, CDKN1A and CYP3A4 expression was measured using Q-RT-PCR.

Figure 4.4 illustrates the different CDKN1A expression patterns. Both pcDNA#6 and #7 have expression curves which lie above those of the NCoR overexpressing clones, which might be expected in view of elevated co-repressor expression. Indeed, CDKN1A expression in NCoR clone #1 is down regulated throughout the period of the time course experiment by as much as 0.63 fold +/- 0.027 at 8 hours. The fold change in CDKN1A expression in NCoR#1 and pcDNA#7 at 4 and 8 hours is statistically significantly different as detailed in Fig 4's legend.
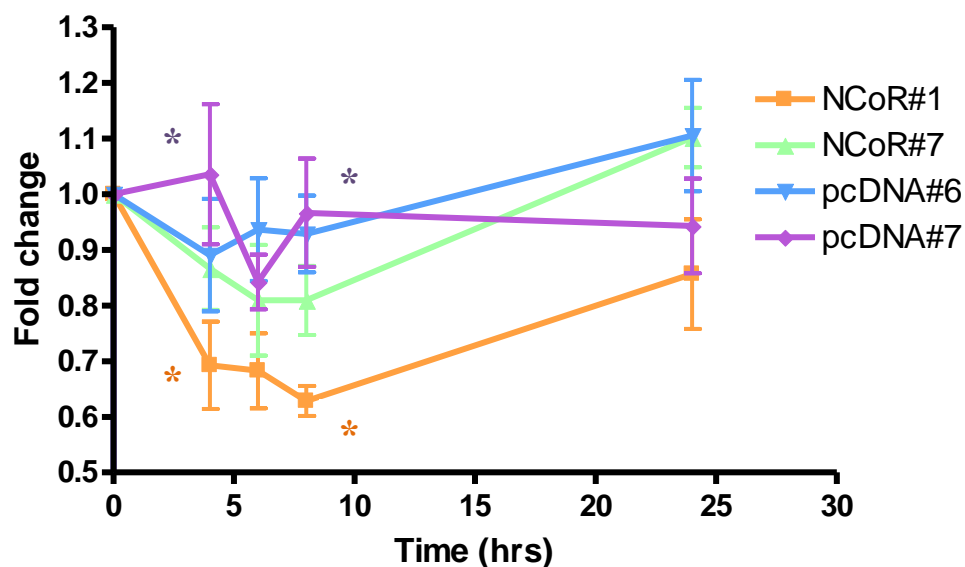
Figure 4.4: Time course experiment of expression of *CDKN1A* as measured by taqman Q-RT-PCR. Stably transfected cells (pNCoR overexpressing clones #1 and #7 and mock transfected pcDNA clones #6 and #7) were treated with LCA 10 μM and total RNA isolated at 4,6,8 and 24 hours post treatment. After reverse transcription, Q-RT-PCR was conducted using *CDKN1A (p21^(Cip1/Waf1))* primers and probes. Results from three independent experiments performed in triplicate are represented. There is a statistically significant difference (2 tailed t-test) in relative expression of *CDKN1A* in NCoR#1 and pcDNA#7 at 4 and 8 hrs (at 4 hrs mean fold change for pcDNA#7 = 1.04 and NCoR#1 = 0.69 p= 0.04; at 8 hrs mean fold change for pcDNA#7 = 0.97 and NCoR#1 = 0.63 p<0.05).

Figure 4.5 illustrates the expression of CYP3A4 in NCoR over-expressing and mock transfected clones in response to 10 μM LCA. In contrast to figure 4.4, NCoR clone #1 exhibits an early peak in CYP3A4 expression of 2.09 fold. Expression then falls to 0.86 fold at 8 hours and gradually rises to 1.76 fold at 24 hours. In comparison, NCoR clone #7 does not exhibit any peaks in expression at all, which gradually rises from baseline to 1.65 fold at 24 hours. Both pcDNA mock clones #6 and #7 have remarkably consistent patterns of CYP3A4 expression. However, unlike Figure 4.4, where pNCoR#1 has a clearly repressed pattern of CDKN1A as compared to pcDNA#6 and #7, in figure 4.5 CYP3A4 mRNA

expression is not clearly repressed across the different time points as compared to the mock control counterparts.
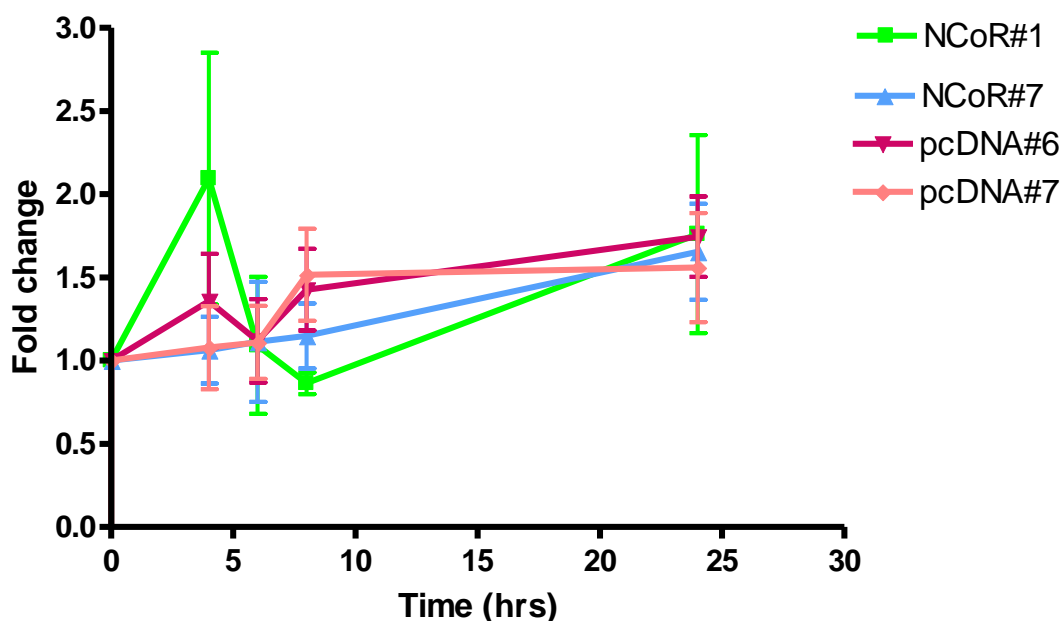
Figure 4.5: Time course experiment of CYP3A4 expression as measured by taqman qRT-PCR. Stably transfected cells (pNCoR overexpressing clones #1 and #7 and mock transfected pcDNA clones #6 and #7) were treated with LCA 10 μM and total RNA isolated at 4,6,8 and 24 hours post treatment. After reverse transcription, Q-RT-PCR was conducted using Cyp3A4 primers and probes. Results from three independent experiments performed in triplicate are represented. There is no statistically significant difference amongst the four cell lines.

4.3.4.2 NCoR1 overexpressing clones express different cohort of genes as compared to controls.

In order to extend the limited gene expression studies above, Applied Biosystems® microfluidic genecards (Q-RT-PCR$_m$) were used containing the primers and probes for 94

genes. These were selected by virtue of current experimental evidence suggesting their presence amongst the target genes of common nuclear receptors. These genes were divided into 9 functional groups; (1) Cell surface transporters, (2) Nuclear Receptors, (3) Nuclear receptor co-factors, (4) Metabolic enzymes, (5) Cell death regulators, (6) Transcription factors, (7) Histone modifiers, (8) Cell cycle regulators, (9) Signal transduction factors (eg. IGFBPs, MAPKs).

NCoR1 over-expressing clone#7 and mock transfected pcDNA clone #6 (RT-4 cells), were treated with 10 µM LCA and mRNA harvested by the standard Tri-reagent method at 6 hours incubation. 3.5 µg of RNA was assayed on the genecards, in triplicate.

Table 4.1: Fold changes in expression of genes, as measured by Taqman genecard.

GENE TARGET	BASAL FOLD CHANGE IN RT-4 pNCOR#7	REGULATED - COMMON		REGULATED - UNIQUE	
		RT-4 pcDNA#6	RT-4 pNCOR#7	RT-4 pcDNA#6	RT-4 pNCOR#7
Cell surface transporters					
ABCA1(20)	0.3				1.7
ABCB8		1.4	1.4		
ABCC3	0.8				1.5
Nuclear receptors					
DAX1	0.3				
PPARα(63)	0.3				
LXRβ	0.6			1.5	
PPARγ(64)	0.7				
THRB	0.7	1.5	1.6		
LXRα	0.8				1.4
RXRα				1.4	
ERα					1.4
ERβ	2.5				1.6
GR	1.5				1.7

RARα	0.6				1.6
VDR					1.7
FXR(65)				1.9	
Nuclear receptor co-factors					
PPARGC1A	0.2				
NCOR2(25)	0.5			1.4	
SIN3A	0.6			1.5	
NCOA3	0.6				
NCOA4	0.7				1.5
CRSP2	0.7				1.3
NCOA1		1.4	1.4		
NCOA2		1.5	1.6		
SIN3A		1.5	1.5		
TRIP15/Alien				1.3	
CRSP6				1.6	
CARM1	0.5			1.5	
PPARBP				1.7	
Metabolic enzymes					
CYP24A1(13, 66)	0.07				
SULT2A1(18, 67)	0.1			1.3	
ALOX5(68)	0.5	1.4	1.3		
CYP27B1(69)	0.7			1.6	
PTGS2(70)	1.3				1.8
ACADM(71)				2.1	
AKR1C1;AKR1C2-	1.7		1.5	1.6	
AKR1C3					1.5
Cell death regulators					
BAX	0.6				
CASP4	0.8			1.5	
Transcription factors					
MYB	0.4				
ID1	0.6				
CEBPA				1.5	

Gene					
GATA3	0.8			1.5	
YY1				1.4	
Histone modifiers					
HDAC6	0.4				
CARM1	0.5			1.6	
HDAC4	0.5	1.5	1.7		
HDAC3	0.6				1.3
HDAC1					1.4
SUV39H1					1.5
SIRT2					
PADI4					2.2
AOF2				1.5	
HDAC2				1.9	
HDAC7A				1.5	
HDAC6	0.4			1.5	
HDAC10				1.6	
Cell cycle regulators					
CDKN1A(21, 72)	0.5			1.2	
CDC2(73)	0.7				
CDKN1B(74, 75)	0.7			1.4	
RBBP4	0.6				
CCND1	0.8				
TP53	1.5				
G0S2(76)	4.3				
CCNE1		1.6	1.4		
CDK5		1.5	1.4		
CCNB1				1.5	
Signal transduction					
TGIF	0.5				
IKBKB	0.6	1.8	2.0		
EGFR		1.7	1.8		
CDH1(77)		1.8	1.6		
MAPKAPK2(14)					1.5
IGFBP3(78, 79)				1.4	

IGFBP5 (78, 79)				1.3	
MAPKAPK5	1.3			1.4	
IKBKG	1.4				

Total mRNA from the cells RT-4 pCDNA #6 and RT-4 pNCOR #7 was extracted from each clone, in triplicate, prior to Q-RT-PCR$_M$ analyses in duplicate wells per gene target, as indicated in the Materials and Methods. The full list of gene targets analysed is given in the Appendix 1; only those targets that have significantly different expression in RT-4 pNCOR #7 compared to RT-4 pcDNA#6 are listed above (Adj. *p* value < 0.01). Known gene targets of individual nuclear receptors are indicated.

4.3.4.3 Lithocholic acid induces a coordinated xenobiotic resistance response in bladder cancer cells.

Lithocholic acid is toxic to human cells; which have evolved complex protective mechanisms to protect against damage from exposure to this secondary bile acid. This is best characterised in hepatocytes (reviewed in (Elias and Mills, 2007)). LCA induces hepatocytes to hydroxylate this bile acid via Cyp3A4 or alternatively sulphate via the enzyme SULT2A1; these reactions lead to LCA detoxification and clearance. Coupled with detoxification, LCA is actively excreted out of hepatocytes and intestinal cells via MRP2 and MDR1, members of the ATP binding cassette transporter family of trans-membrane efflux pumps (ABC transporters). These are key components of a coordinated defence strategy against the xenobiotic LCA.

Lithocholic acid treatment in RT-4 cells stably over-expressing NCoR1 or mock transfected control plasmid induces a protective response towards this xenobiotic typified by upregulation of trans-membrane efflux pumps, detoxifying enzymes and cell-cycle arrest proteins (table 4.1).

MRP3, also known as ABCC3 is a member of the ABC transporter efflux pumps. These proteins span the cell membrane and export a wide variety of substances, including xenobiotics and bile acids out of the cell in an energy dependent manner. Lithocholic acid induces the RT-4 pNCoR#7 cells to upregulate ABCC3 expression by 1.5 fold. Teng et al demonstrated the increased expression of ABCC3 by two fold in the hepatoma cell line HuH7, by RT-PCR, when treated with 50 µM LCA for 24 hours (Teng et al., 2003). It is interesting that the induction of ABCC3 is only seen in the NCoR overexpressing clone, i.e. NCoR1 has a dose dependent effect to change the expression of ABCC3/MRP3. There may

be a negative regulator of MRP3 expression; raised NCoR1 levels may antagonise this regulator which in turn may release its inhibition on MRP3 expression.

ABCB8 is also an ATP binding cassette transporter membrane protein which is upregulated by 1.4 fold in both the mock transfected and RT-4 pNCoR#7 cells. There is no change in the basal expression of ABCB8 in RT-4 pNCoR#7 when compared to the mock transfected clone. ABCA1 is a third ATP binding cassette transporter which is downregulated at basal conditions in the RT-4 pNCoR#7 (by 0.3 fold) and when this clone of cells is treated with lithocholic acid, its expression is stimulated by 1.7 fold.

The ATP binding cassette transporters are described as being central players in the phenomenon of multixenobiotic resistance (MXR). This was initially described in the context of aquatic organisms such as mussels and sea urchins which are constantly exposed to toxins in polluted water and appear to express these trans-membrane transporters in their gills which actively pump a broad spectrum of toxins and xenobiotics out of cells (Smital et al., 2004). In the context of human liver cells, the FXR ligand and bile acid Chenodeoxycholic acid has been shown to upregulate expression of the ATP binding cassette transporters ABCB1, ABCC1 and ABCC2 at the mRNA level in the HepG2 cell line and primary hepatocytes and at protein level in HepG2 and Caco-2 cells (Martin et al., 2008).

On a second front, treatment of RT-4 transfected cells with LCA led to regulated expression of the detoxifying enzyme of the sulphotransferase family SULT2A1 (Elias and Mills, 2007; Falany, 1997). The latter is downregulated at basal level in the RT-4 pNCoR1#7 by 0.1 fold, however upon treatment with LCA, the mock transfected RT-4 pcDNA#6 upregulates SULT2A1 by 1.3 fold. SULT2A1 acts to sulphate conjugate hormones, drugs, bile acids and

xenobiotics, to convert them from hydrophobic to water soluble conjugates in an attempt to metabolise and excrete them via urine and faeces.

A third aspect of the coordinated response to exposure to LCA is expression of genes associated with cell cycle arrest. Therefore, the cyclin dependent kinase inhibitor CDKN1B/p27^{kip1} is induced by treatment with LCA (1.4 fold) and the basal expression in RT-4 pNCoR#7 is suppressed by 0.7 fold. A similar pattern is seen with CDKN1A (p21$^{waf1/cip1}$). In RT-4 pcDNA#1 the expression is marginally raised by 1.2 fold and the basal expression is suppressed by 0.5 fold in the RT-4 pNCoR#7. Hence, LCA induces expression of targets associated with a G1/S phase cell-cycle arrest. Overexpression of the co-repressor NCoR1 suppresses the anti-proliferative response elicited in the RT-4 cells by treatment with lithocholic acid (figure 3.8 B).

In the context of the cellular response to exposure to a xenobiotic, the RT-4 pcDNA#6 appear to stop dividing by inducing a cell-cycle arrest and then express genes encoding proteins that either pump toxic compounds out of the cell (e.g. members of the ATP binding cassette transporter family) or genes that encode proteins which metabolise xenobiotics and facilitate their excretion in urine (e.g. sulphotransferase enzymes).

4.3.4.4 Over-expression of NCoR1 in RT-4 cells leads to repression of NR target genes

Table 4.1 and Figure 4.6 illustrate the basal changes in gene expression in RT-4 NCoR#7 cells, i.e. the effects of NCoR1 overexpression. Apart from 9 genes (ERβ, GR, PTGS2,

AKRC1/AKRC2, CEBPA, TP53, G0S2, MAPKAPK5 and IKBKG) which are up-regulated, 37 genes are down-regulated. This is not surprising as NCoR1 acts as corepressor and hence, overexpression would be expected to dampen down target gene expression. However, the expected overall effect of the basal gene expression changes in RT-4 NCoR#7 would be to reduce sensitivity to a wide range of NRs by reducing their expression (DAX1, PPARα and γ, LXR α and β, THR β and RAR α) and to obtain a more pro-proliferative phenotype by suppressing expression if the pro-apoptotic protein BAX and the cell cycle inhibitors CDKN1A and CDKN1B. However, it is of interest that despite down-regulation of PPARγ in RT-4 NCoR#7 cells, treatment with ETYA does not lead to a statistically significant difference in proliferation between control RT-4 pcDNA and NCoR over-expressing cells as shown in Figure 3.8.

Multiple target genes are expressed or suppressed in response to treatment with LCA. Individual genes products may have interactions with each other which will affect the overall behaviour of the cells in question. In order to have a better understanding of the inter-related effects of the different target gene expression patterns, network diagrams were constructed from the Q-RT-PCR$_m$ data (and the Affymetrix™ genechip data as illustrated later) by utilising commercially available GeneGo™ network analysis software. This utilises previously published experimental data to generate networks between target genes demonstrated by the Q-RT-PCR$_m$ and gene array data.
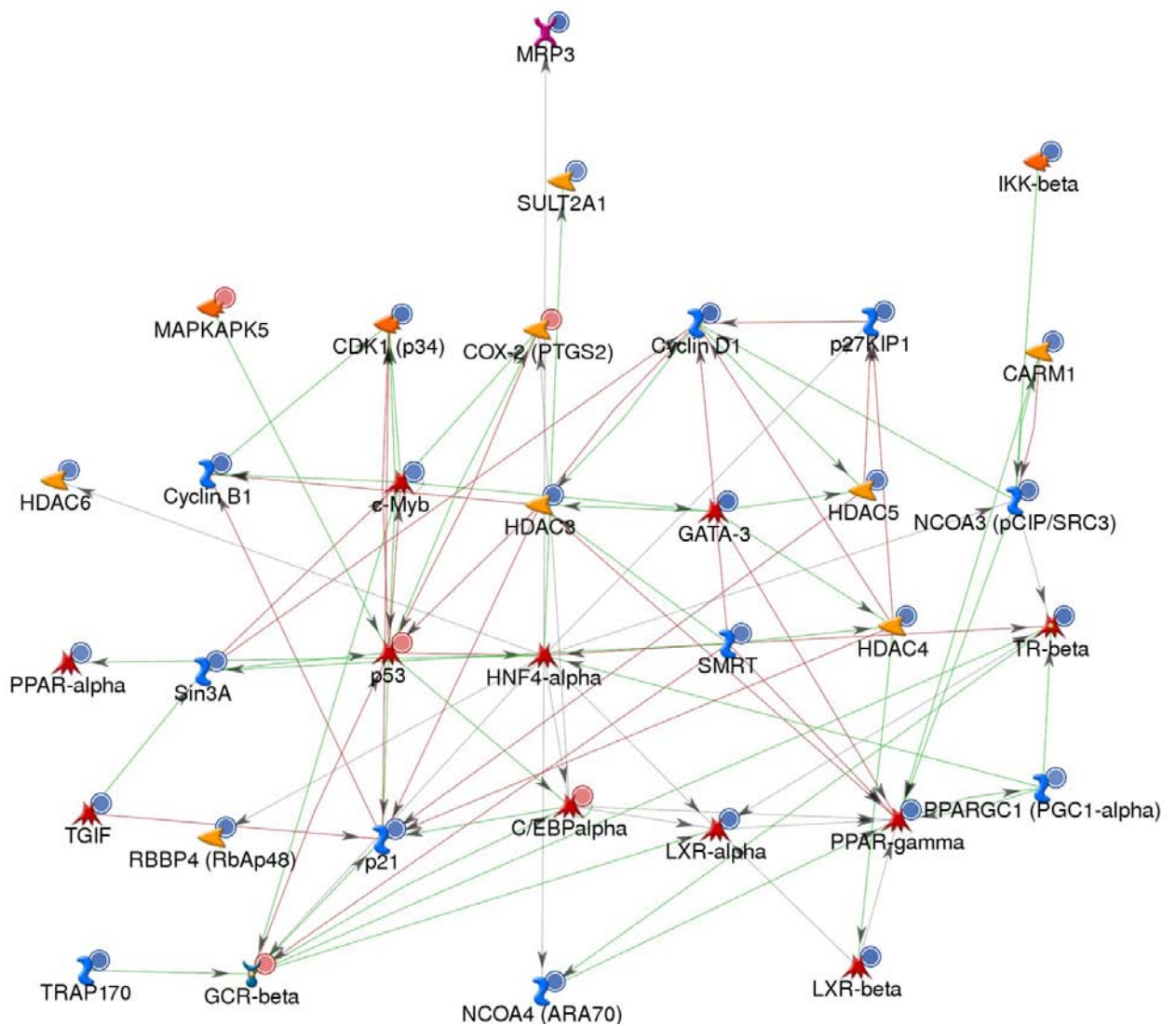
Figure 4.6: Network diagram of basal gene changes in pNCoR overexpressing clone #7 as compared to control mock transfected pcDNA clone #6. Stably transfected cells (pNCoR clone #7 and mock transfected pcDNA clone #6) were treated with LCA 10 μM and total RNA isolated at 6 hours post treatment. After reverse transcription of 3.5 μg of total RNA per sample, Q-RT-PCR$_m$ was conducted using the one-step QuantiTect Probe RT-PCR kit (Qiagen, http://www1.qiagen.com) directly on the custom-designed TaqMan® Low Density Arrays. Results from three independent experiments performed in duplicate are represented. Data was normalized to the internal control 18S and the pNCOR#7 samples calibrated to the pcDNA#6 samples using the δδCT method. The network diagram was generated using the GeneGo™ network analysis tools which use algorithms to build an interconnected network of interactions based on previously published experimental data. Green connectors indicated up-regulated targets. Red connectors indicate down-regulated gene targets. Gene targets with Red and Blue tags are up- and down-regulated in the network respectively. Network diagram generated by Dr. Moray Campbell.
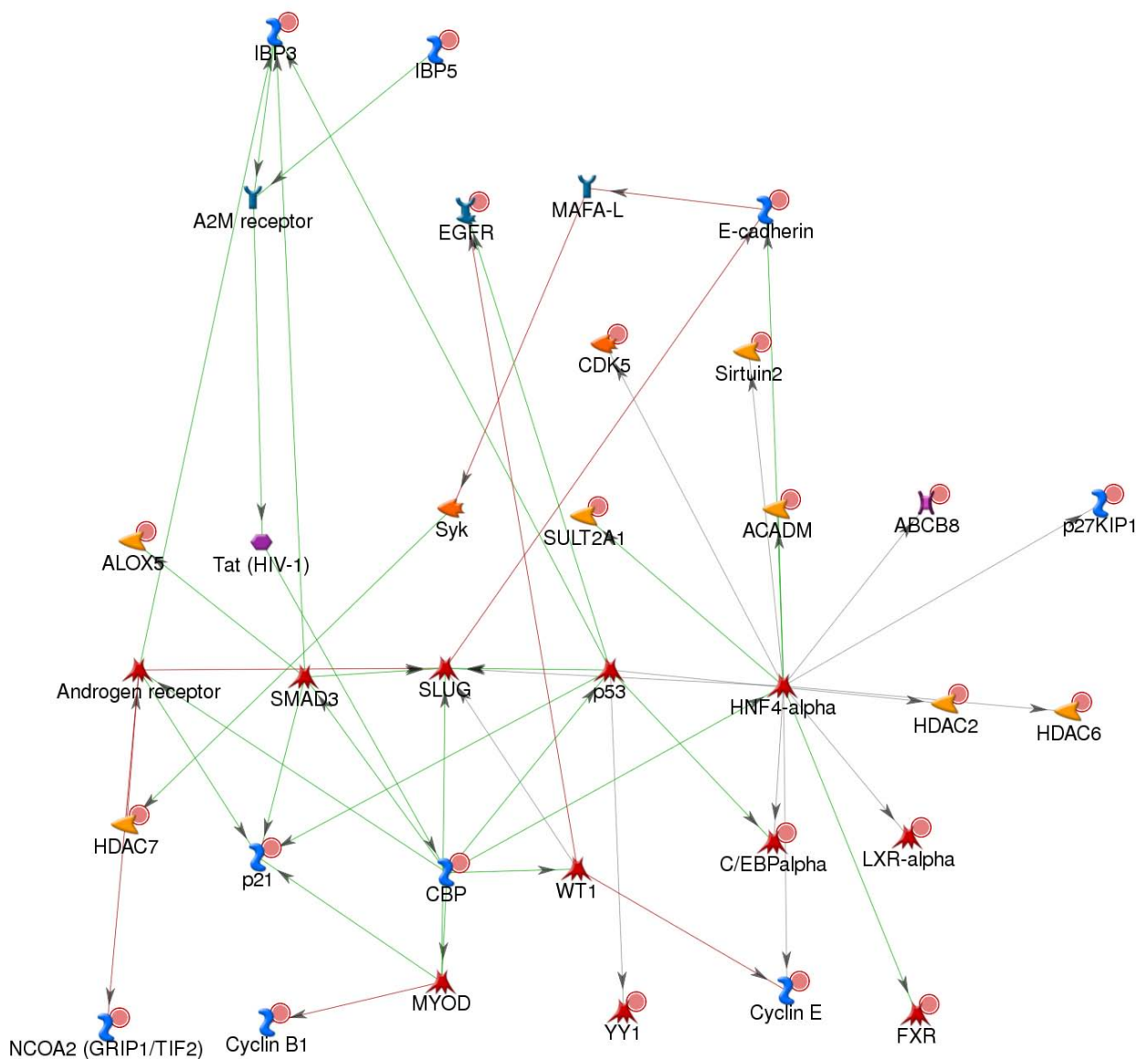
Figure 4.7: Network diagram of gene changes in control mock transfected pcDNA clone #6 on treatment with Lithocholic acid. Stably transfected cells (mock transfected pcDNA clone #6) were treated with LCA 10 µM and total RNA isolated at 6 hours post treatment. After reverse transcription of 3.5 µg of total RNA per sample, Q-RT-PCR$_m$ was conducted using the one-step QuantiTect Probe RT-PCR kit (Qiagen, http://www1.qiagen.com) directly on the custom-designed TaqMan® Low Density Arrays. Results from three independent experiments performed in duplicate are represented. Data was normalized to the internal control 18S and the treated samples calibrated to the untreated negative control samples using the δδCT method. The network diagram was generated using the GeneGo™ network analysis tools which use algorithms to build an interconnected network of interactions based on previously published experimental data. Green connectors indicated up-regulated targets. Red connectors indicate down-regulated gene targets. Gene targets with Red and Blue tags are up- and down-regulated in the network respectively. Network diagram generated by Dr. Moray Campbell.

Figure 4.8: Network diagram of gene changes on treating pNCoR overexpressing clone #7 with Lithocholic acid. Stably transfected cells (pNCoR clone #7) were treated with LCA 10 µM and total RNA isolated at 6 hours post treatment. After reverse transcription of 3.5 µg of total RNA per sample, Q-RT-PCR$_m$ was conducted using the one-step QuantiTect Probe RT-PCR kit (Qiagen, http://www1.qiagen.com) directly on the custom-designed TaqMan® Low Density Arrays. Results from three independent experiments performed in duplicate are represented. Data was normalized to the internal control 18S and the treated samples calibrated to the untreated negative control samples using the δδCT method. The network diagram was generated using the GeneGo™ network analysis tools which use algorithms to build an interconnected network of interactions based on previously published experimental data. Green connectors indicated up-regulated targets. Red connectors indicate down-regulated gene targets. Gene targets with Red and Blue tags are up- and down-regulated in the network respectively. Network diagram generated by Dr. Moray Campbell.

4.3.4.5 Hepatocyte Nuclear Factor 4 α (HNF4α) is the key regulator of the xenobiotic response.

Figure 4.7 illustrates the central position of the nuclear receptor HNF4α (Hepatocyte Nuclear Factor 4 α) in the network of gene transcriptional responses to treatment of pcDNA clone #6 with lithocholic acid. In contrast, figure 4.8 which shows gene expression changes in RT-4 NCoR#7 upon treatment with 10 μM LCA, does not indicate HNF4α as a central regulator, suggesting a connection between overexpression of NCoR1 and suppression of HNF4α regulated genes.

HNF4α is known to have a key role in regulating xenobiotic protective cellular responses. Tirona et al investigated the role of HNF4α in the context of the Pregnane-X-receptor (PXR) and induction of CYP3A4, the key cytochrome P450 xenobiotic enzyme, in hepatocytes (Tirona et al., 2003). They used a luciferase based promoter construct of the CYP3A4 proximal promoter along with the distal xenobiotic response enhancer module (XREM). The latter has been demonstrated to be responsible for PXR mediated Cyp3A4 induction in response to the antibiotic and PXR activator Rifampicin (Goodwin et al., 1999). This construct was used to transfect the liver cell line HepG2 which was co-transfected with a plasmid containing PXR as well as a variety of other nuclear receptors (FXR, LXR, VDR and HNF4α). This experiment was designed to assess the role of these latter nuclear receptors to potentiate PXR dependent CYP3A4 reporter plasmid activation. Only co-transfection of HNF4α led to augmented luciferase activity when the cells were treated with Rifampicin, suggesting a cooperative role for HNF4α in PXR dependent CYP3A4 activation.

Finally, Tirona et al generated mice with organ specific hepatic knockout of HNF4α. RT-PCR was used to measure Cyp3A4 mRNA from livers from such mice embryos; no Cyp3A4 mRNA was measured as compared to normal, control litter mates (Tirona et al., 2003). Adult

mice with hepatic HNF4α disruption using the Cre-Lox system have also been generated. These livers had approximately 50% less basal expression of CYP3A4. On treatment with PCN, the induction of Cyp3A4 is higher in wild type mice as compared to HNF4α knock out clones; there was no difference in PXR expression.

This paper provides evidence for HNF4α in augmenting the expression of the xenobiotic metabolising enzyme Cyp3A4 in response to signalling via the nuclear receptor PXR. HNF4α appears to bind a particular sequence in the enhancer module of the Cyp3A4 gene and appears to regulate the xenobiotic response in due to treatment with the PXR ligand PCN. In the context of the target gene network effects (fig 4.6 and 4.7), Tirona's paper provides evidence for two nuclear receptors, PXR and HNF4α to switch on the xenobiotic response enzyme Cyp3A4 in a cooperative fashion (Tirona et al., 2003). It is therefore possible that HNF4α may be playing a similar role when pNCoR1 or mock transfected RT-4 cells were treated with LCA.

4.3.5 Target gene expression of EJ-28 cells when treated with Lithocholic acid and a histone deacetylase inhibitor SAHA and assessed with Affymetrix™ U133 array.

Strongly additive anti-proliferative effects were demonstrated by treating EJ-28 cells with the nuclear receptor ligands ETYA, CDA or LCA in combination with the histone deacetylase inhibitor SAHA in figure 3.9(d). Also, as in figure 4.1, treating EJ-28 cells with LCA leads to a cell cycle arrest and when in combination with SAHA, the rise in proportion of cells in phase G1 approaches statistical significance (p=0.51); i.e. there is a suggestion of a cell-cycle arrest upon treating with the combination of LCA and SAHA. In order to investigate the genome wide expression of target genes associated with these effects, EJ-28 cells were treated

with 100 μmol of LCA +/- 0.8 μmol SAHA and hybridised the mRNA onto Affymetrix®
U133 genechips. The cells were treated for 6 hours before extracting RNA with a view to
studying the changes in gene expression directly regulated by the treatments.

4.3.5.1 Treatment of EJ-28 cells with LCA and SAHA produces a defined transcriptional response.

Figure 4.9 illustrates a network diagram of genes expressed uniquely when EJ-28 cells were
treated with LCA and SAHA (as compared to gene expression changes when EJ-28 cells
treated singly with LCA or SAHA). Remarkably, only a small cohort of 83 genes are uniquely
regulated out of a total of 33,000 gene sequences represented on the Affymetrix® U133
genechip. The genes thus regulated can be broadly divided into three groups based on their
predominant cellular function:

1. Genes that drive cell proliferation and progress through the cell cycle

2. Genes involved with transcription and post transcriptional mRNA processing.

3. Genes involved with repair of damaged cellular components.

Illustrative examples are detailed below:

Pro-proliferative genes

HB-EGF (Heparin binding EGF-like Growth factor)	↑	Growth Factor
N-RAS (neuroblastoma RAS viral oncogene homolog)	↓	G-protein, proto-oncogene
elf-5 (E74-like factor 5)	↓	ets domain transcription factor; involved in cell division and organ development eg. Lung development.

CDCA8 (cell division cycle associated 8)	↓	component of chromosomal passenger complex; required for stability of bipolar mitotic spindle.
CDC5L (cell division cycle 5 like)	↓	cell cycle regulator important For G2/M phase progression.

Transcription/post-transcriptional mRNA processing

SUPT16H (suppressor of Ty 16 homolog)	↓	subunit of the protein FACT; this interacts with histones H2A/H2B to cause nuceolosome disassembly prior to transcription.
PRPF4 (pre-mRNA processing factor 4 homologue)	↓	associates with spliceosomes involved with removal of introns from pre-mRNA.

Cellular repair:

PIMT (protein l-isoaspartyl methyltransferase)	↑	enzyme involved in repair of age damaged cellular proteins.

This data suggests a cellular response to treatment with the bile acid and FXR ligand LCA in combination with the histone deacetylase inhibitor SAHA, punctuated with inhibition of cell division, expression of transcriptional/post-transcriptional processing genes and expression of cellular reparative enzymes. This response has similarities to the previously demonstrated xenobiotic response in mock transfected RT-4 cells (section 4.3.4.3). Therefore, the cells appear to stop dividing when they are exposed to LCA in combination with SAHA, by reducing expression of the oncogene N-RAS and CDCA8 and CDC5L, both genes being important for cell division. The cells also express PIMT, an enzyme involved in repairing protein damage that may have been sustained during exposure to the xenobiotic LCA. This is analogous to the expression of SULT2A1 in the mock transfected RT-4 cells (figure 4.7) i.e.

this represents an enzyme-based cellular protection mechanism against the damaging effects of LCA.

The expression profile generally illustrates suppression of cellular proliferation however, contrasts with figure 4.1 which demonstrates a G1/S phase cell cycle arrest on treating EJ-28 cells with LCA and SAHA. The data above shows reduced expression of the protein CDC5L which is required for G2/M phase expression.
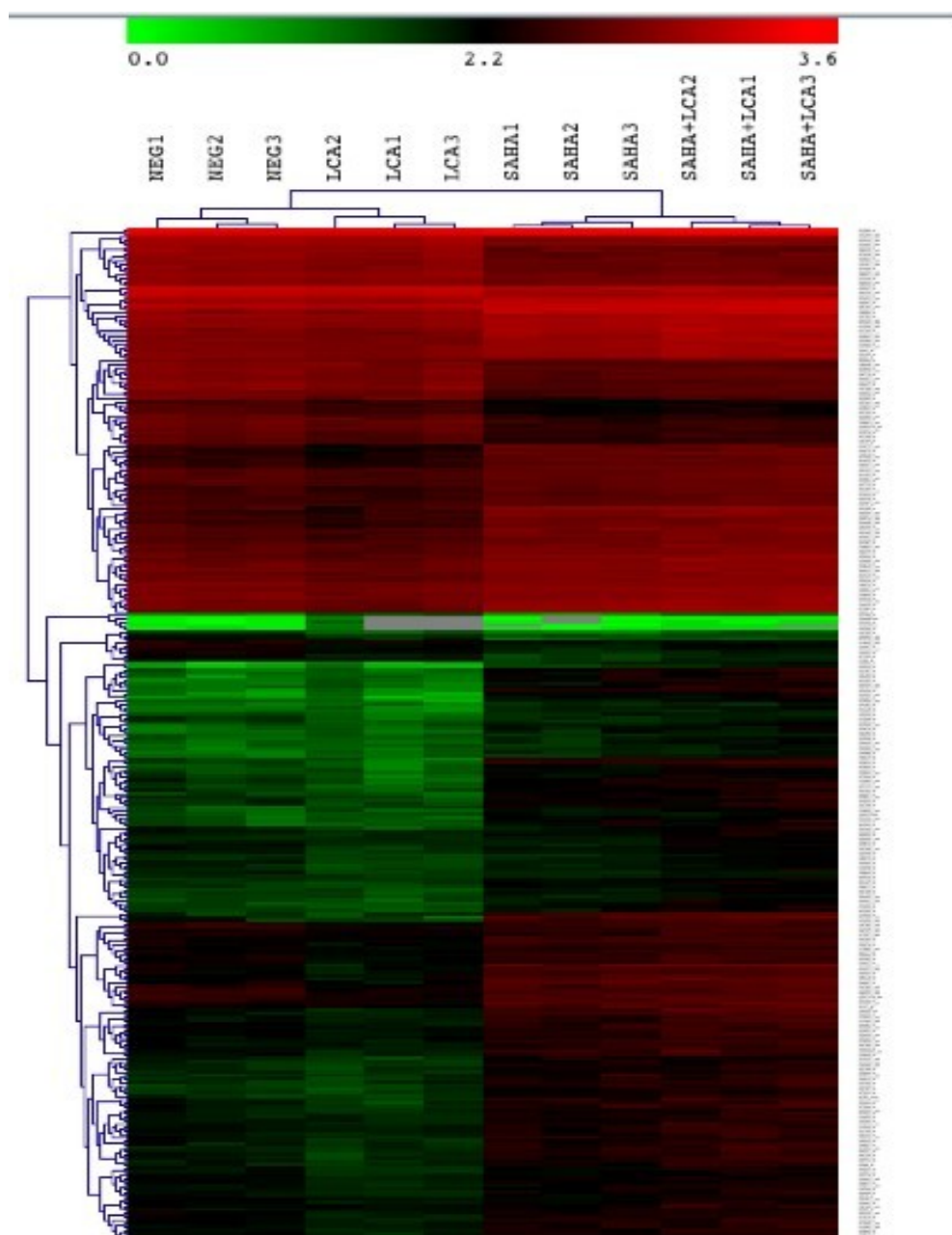
Figure 4.9: Heat map of the raw data from Affymetrix® U133 expression chip analysis. Cells were treated with LCA alone (100 μM), SAHA alone (0.8 μM) or LCA and SAHA in combination and total RNA extracted at 6 hours. This RNA was further purified using the RNeasy mini-kit using a RNAse free DNAses according to the manufacturers protocol (http://www1.qiagen.com). The RNA is reverse transcribed to double stranded cDNA which is then converted to biotin labelled cRNA as detailed in chapter 2. The cRNA is purified and fragmented before hybridisation to the Affymetrix U133 genechip arrays®. The results were analysed using the dChip software (http://biosun1.harvard.edu/complab/dchip/). Three independent experiments in triplicate were performed, in accordance with MIAME recommendations. Hybridisation was performed by Ms. Sim Sahota, research technician at Cancer Studies, Birmingham. Bioinformatic analysis performed by Dr. Sebastiano Battaglia.
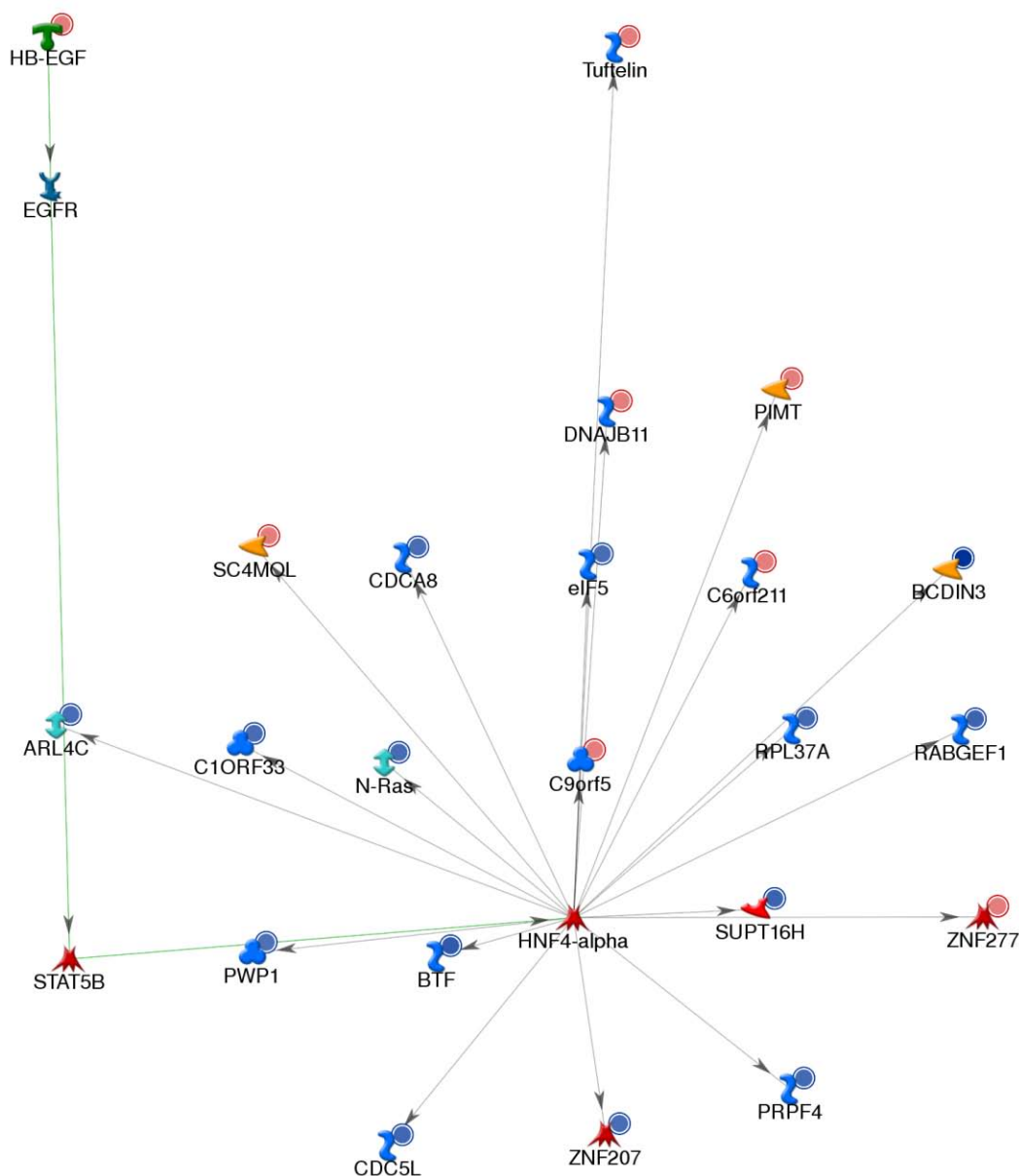
Figure 4.10: Network diagram of genes uniquely regulated by treatment with LCA + SAHA. EJ-28 cells, in the mid-exponential phase, were treated with 100 μM of LCA and 0.8 μM of SAHA and total RNA extracted at 6 hours. This RNA was further purified using the RNeasy mini-kit using a RNAse free DNAses according to the manufacturers protocol (http://www1.qiagen.com). The RNA is reverse transcribed to double stranded cDNA which is then converted to biotin labelled cRNA as detailed in chapter 2. The cRNA was purified and fragmented before hybridisation to the Affymetrix U133 genechip arrays®. The results were analysed using the dChip software (http://biosun1.harvard.edu/complab/dchip/). Three independent experiments in triplicate were performed. The network diagram was generated using the GeneGo™ network analysis tools which use algorithms to build an interconnected network of interactions based on previously published experimental data. Green connectors indicated up-regulated targets. Gene targets with Red and Blue tags are up- and down-regulated in the network. Downregulation of BCDIN3 and upregulation of ZNF277 was validated by demonstrating these changes in expression in EJ-28 cells treated with LCA following si-RNA silencing of NCoR1 expression (Abedin et al., 2009). This suggests that NCoR1 downregulation has a similar effect to treatment with the HDACi SAHA. Network diagram by Dr Moray Campbell.

4.4 Discussion

The cellular and gene transcriptional effects of treating bladder cancer cells with the xenobiotic lithocholic acid have been demonstrated under different cellular environments. A remarkably consistent theme emerges in terms of cellular response to exposure to the xenobiotic LCA, namely inhibition of the cell cycle and expression of a panel of genes whose common purpose is to limit the toxic effects of the xenobiotic to the cell. The latter set of genes include members of the ATP binding cassette superfamily of trans-membrane efflux pumps which act to pump out xenobiotics from the cell, enzymes that degrade and metabolise the xenobiotics by hydroxylation (CYP3A4) or sulphonation (SULT2A1); and finally genes that repair damage to cellular structure such as PIMT, which repairs cellular proteins.

4.4.1 LCA and the Cell Cycle

Increased expression of the cyclin dependent kinase inhibitor CDKN1A was demonstrated, in figure 4.2, in RT-4 and EJ-28 cells upon treatment with lithocholic acid with and without the HDAC inhibitor SAHA. There is evidence of bile acids inducing a G1/S cell cycle arrest in the prostate cancer cell line PC-3 (Choi et al., 2003). Choi et al have demonstrated a G1/S phase cell cycle arrest upon treatment with 100 µM of derivatives of CDA and ursodeoxycholic acid as determined by FACS analysis. This was associated with increased association of phosphorylated Rb (retinoblastoma protein) with E2F-1 protein as detected by immunoprecipitation with E2F-1 antibody and detected by Western blotting with anti-Rb antibody. Therefore, the sequestration of the E2F-1 transcription factor will prevent the cell from G1/S phase progression. This G1/S cell cycle arrest was further augmented by increased expression of CDKN1A (p21$^{Cip1/Waf1}$) upon treatment with 100 µM of bile acid derivatives as

demonstrated by Western blotting. Transient transfection of wild type p21$^{(Cip1/Waf1)}$ coupled with luciferase followed by demonstration of increased luminescence upon treatment with the bile acid derivatives (5.2 and 7.3 fold) provides suggestive evidence of bile acid derivatives leading to p21$^{Cip1/Waf1}$ expression. The authors demonstrate association of p21$^{Cip1/Waf1}$ with both Cdk-2 (cyclin dependent kinase-2) and PCNA (proliferating cell nuclear antigen) by immunoprecipitation of protein complexes with Cdk-2 and PCNA antibodies respectively following bile acid derivative treatment, and detection of bound p21$^{Cip1/Waf1}$ using a p21 antibody via Western blotting.

These experiments provide supportive evidence for the finding of a G1/S phase cell cycle arrest in EJ-28 cells upon treatment with lithocholic acid. However, it is unclear as to why a G1/S arrest is not demonstrated in RT-4 cells (figure 4.1) in view of increased expression of CDKN1A in this cell line on treatment with LCA +/- SAHA. This may be due to the effect of timing of the FACS analysis in relation to the dosing of LCA and SAHA.

It is striking that treatment with SAHA in figure 4.2 leads to a significant induction of CDKN1A in all of the four cell lines. CDKN1A is an established SAHA target gene; Richon et al reported treating the T24 bladder cancer cell line with SAHA which led to induction of p21$^{Cip1/Waf1}$ mRNA and protein. They went on to perform chromatin immunoprecipitation of T24 bladder cell line following SAHA treatment using an antibody against acetylated histones and followed with PCR of precipitated DNA with primers for the p21$^{Cip1/Waf1}$ promoter and demonstrated enriching of the p21$^{Cip1/Waf1}$ promoter with acetylated histones. Clearly, this suggests that the SAHA's HDACi activity is targeting the p21$^{Cip1/Waf1}$ promoter leading to mRNA induction (Richon et al., 2000).

4.4.2 LCA and Expression of Metabolic Enzymes

Cyp3A4 is the most abundantly expressed member of the cytochrome P450 family of xenobiotic metabolising enzymes; hence its expression in relation to LCA treatment of the four tested cell lines was investigated. Figure 4.3 illustrates significant Cyp3A4 induction in RT-4, HT-1376 and RT-112 cells after LCA treatment (RT-4 20 µM, HT1376 and RT-112 50 µM). Fukimori et al have demonstrated similar findings in LS180 human intestinal cells, albeit with higher fold increases in Cyp3A4 mRNA as measured by Q-RT-PCR. They treated LS180 cells with 10, 30 and 100 µM LCA for 6 hours and obtained 4, 16 and 20 fold induction of Cyp3A4 mRNA respectively. As discussed later in this chapter, the intestine, along with the liver play a key role in protecting the body from the toxic effects of LCA, in part by induction of metabolic enzymes such as Cyp3A4. Therefore, LS180 intestinal cells may have a higher capacity to express Cyp3A4 in view of their tissue of origin as compared to bladder cancer cells (Fukumori et al., 2007).

The Q-RT-PCR$_m$ genecard experiments were designed to reveal the gene expression signatures on LCA treatment of RT-4 cells stably transfected to over-express NCoR1 or mock-transfected [as illustrated in figures 4.6 – 4.8] have revealed a key omission (table 4.1). I have previously demonstrated CYP3A4 mRNA induction in RT-4 cells upon treatment with SAHA (0.8 µM), LCA (20 µM) and the combination of LCA+SAHA for 6 hours (figure 4.3), however, treatment of RT-4 p NCoR#7 transfected and mock pcDNA#6 clones with LCA (10 µM) for 6 hours did not lead to CYP3A4 induction as measured by microfluidic Q-RT-PCR$_m$ gene cards (table 4.1). The mock transfected clones would conventionally be expected to behave as the wild type RT-4 cells. The lack of Cyp3A4 induction may be due to the lower

concentration of LCA used in the Q-RT-PCR$_m$ experiment as compared to figure 4.3 (10μM as compared to 20 μM).

The Q-RT-PCR$_m$ genecard transcriptional profile of pNCoR#7 and pcDNA#6 clones has demonstrated differential expression of the metabolic enzyme SULT2A1 and ALOX5. Both these enzymes show reduced expression in the basal state in pNCoR#7 clone as compared to the control pcDNA#6 (0.1 and 0.5 fold respectively). SULT2A1 is a member of the sulfotransferase family and catalyses the addition of sulphate groups by conjugation to steroid hormones, drugs, xenobiotics and bile acids. This increases the solubility of bile acids and thereby facilitates excretion via faeces or urine (Elias and Mills, 2007). ALOX-5 (or arachidonate 5 lipoxygenase) catalyses the production of leukotrienes (important inflammatory mediators) from arachidonic acid. Rodriguez-Ortigosa studied the relationship between ALOX-5, leukotrienes and bile salt excretion in isolated, perfused rat livers (Rodriguez-Ortigosa et al., 1995). In this model system, they demonstrated increased expression of ALOX-5 mRNA in the rat livers when they were perfused with the bile acid taurocholate. This was associated with increased de novo production of leukotrienes within the liver and was followed by increased bile acid excretion within bile. Therefore, by some as yet undetermined mechanism, there appears to be a possible role for leukotriene production via ALOX-5 in increasing bile acid excretion from hepatocytes. There may be a similar mechanism within the bladder cancer cell model as a means of protection from the increased exposure to LCA.

Over-expression of NCoR1 in the pNCoR#7 clones suppresses the basal expression of both SULT2A1 and ALOX-5 as noted above, however, treatment with LCA causes a modest induction of these enzymes in the pcDNA#6 control clone by 1.3 and 1.4 fold respectively.

SULT2A1 is not induced when pNCoR#7 cells are treated with LCA suggesting a role for transcriptional suppression by NCoR1.

4.4.3 LCA and Expression of ABC Transporters

The ATP binding cassette family of transporters represents a large protein family expressed in both eukaryotes and prokaryotes, which act as trans-membrane pumps which transport specific molecules across intra and extracellular membranes in an energy dependent fashion. These proteins have two trans-membrane domains composed of α helices with between 6-11 trans-membrane spanning regions. These proteins have one or two ATP binding domains on the cytosolic surface which release energy from ATP hydrolysis which drives the protein conformational change enabling the trans-membrane transfer. These proteins have been implicated in a wide range of biological processes such as multi-drug resistance in cancer and in bacterial cells, physiological processes such as transport across the gut or the blood-brain barrier and transport across intracellular organelles such as peroxisomes.

The membrane transporters MRP3 (multi-drug resistance protein 3) and ABCA 1 are downregulated in the pNCoR#7 cells (0.8 and 0.3 fold respectively) in the basal state, suggesting a repressive effect of NCoR1 over-expression. Upon treatment with LCA, these are not induced in the pcDNA#6 control cells. However, the transporter ABCB8 is upregulated by 1.4 fold. When pNCoR#7 cells are treated with LCA, both MRP3 and ABCA1 demonstrate increased mRNA expression of 1.5 and 1.7 fold respectively.

ABC transporters play a key role in the known mechanisms of limiting intracellular levels of LCA by actively transporting the bile acid out of cells and this is the likely role of the ABC transporters induced in pcDNA#6 and pNCoR#7 clones upon treatment with LCA.

MRP 3 gene promoter has been shown to be transcriptionally induced by VDR and RXR in response to treatment with $1\alpha,25(OH)_2D_3$ and LCA. McCarthy et al cloned a 5 Kb regulatory region of the mouse MRP-3 promoter into a luciferase expression plasmid and co-transfected this into Hep G2 hepatoma cells with an RXR expression vector and a variety of relevant bile acid sensing nuclear receptors such as CAR, FXR, PPAR α, PXR and VDR. These cells were treated with the relevant NR ligands; significant reporter activation was seen with VDR co-transfection when treated with $1\alpha,25(OH)_2D_3$ (6-7 fold with 1 nM) or LCA (4.5 fold with 10 µM) (McCarthy et al., 2005).

There is little evidence to show a transcriptional link between the ABCA1 gene and LCA apart from Sporstøl's study which appears to demonstrate reduced ABCA1 mRNA expression (39 % with 5 µM and 85 % with 25 µM LCA) and protein expression as assessed by Western blotting, in Hep G2 cells in response to LCA treatment (Sporstol et al., 2005). The authors performed an ABCA1 gene reporter experiment by transient transfection into HepG2 cells; there was a reduced promoter activity by 43 % with 25 µM of LCA. With co-transfection with PXR and RXR expression vectors, this suppression of promoter activity with 25 µM of LCA increased to 80 %. This result appears to contradict with the apparent induction of ABCA1 mRNA in pNCoR#7 cells. It is possible that the raised NCoR1 level may inhibit possible PXR signalling which Sporstøl et al appear to suggest is inhibitory towards ABCA1 expression (Sporstol et al., 2005).

4.4.4 A Coordinated Xenobiotic Protective Response in the Bladder

The bladder transitional cell urothelium is exposed to xenobiotics in urine. Significant quantities of bile acids are found in human urine in the presence of bile duct obstruction or

cholestasis. However, Goto et al have demonstrated galactoside conjugates of the bile acids cholic and deoxycholic acid in urine from healthy subjects (Goto et al., 2005). The carcinogenic potential of these bile acid derivatives are unclear however, protection of the urothelium from potentially toxic bile acid derivatives may provide the selective advantage for development and maintainance of a coordinated protective response to these xenobiotics. Therefore, the urothelial cell first stops cell division and initiates a cell cycle arrest when exposed to these chemicals. DNA replication and cell division are a particularly vulnerable time for cells to endure geno-toxic injury. Cell-cycle arrest allows the cell to clear the xenobiotic effectively or alternatively undergo apoptosis if it is unable to do so to avoid proliferation of urothelial cells with genetic mutations. A well established example of such a coordinated protective response exists in the liver.

4.4.5 The Hepatocellular Protective Response to Xenobiotics

The liver has a strategic position at the cross-roads of the alimentary tract and the systemic circulation. Therefore, all substances, including xenobiotics absorbed from the small bowel are transported to the liver via the hepatic portal vein. The mechanism of LCA handling provides an example of a coordinated protective response employed by hepatocytes to handle this potentially toxic xenobiotic. Indeed, this mechanism is only present in humans and chimpanzees which can handle LCA; New Zealand white rabbits fed a 0.5 % dietary concentration of LCA have a 14 day mortality of 50 % as they lack the ability to sulphate LCA which is a key detoxifying step (Elias and Mills, 2007).

Levels of lithocholic acid are sensed in hepatocytes by VDR and FXR and probably other nuclear receptors such as PXR. The two most important target detoxifying genes are Cyp3A4 and SULT2A1. Cyp3A4 hydroxylates LCA and increases aqueous solubility and hence

increases excretion in urine. SULT2A1, via sulphonation of LCA, increases solubility in bile and water and hence excretion via faeces. Sulphonation of LCA also reduces reuptake of LCA in the colon via the entero-hepatic circulation. These detoxifying steps are coordinated with active pumping of LCA and its conjugates out of the cell, via the ABC transporters MDR1 and MRP2 and is also linked with regulation of bile acid synthesis. FXR binds bile acids (CDA, LCA and Cholic acid) and represses transcription of the enzyme cholesterol 7 α hydroxylase which is the rate limiting enzyme in bile acid synthesis (Elias and Mills, 2007). Hence this is an important example in which the separate actions of bile acid sensing, detoxifying enzymes, transmembrane pumps and bile acid synthesis enzymes are regulated in concert to achieve the overall aim of hepato-cellular protection from a toxic compound.

Chapter 5 : Discussion

5.1 Summary

5.1.1 Expression of nuclear receptors in non-classical tissue sites

Figure 3.3 demonstrates the expression of a panel of nuclear receptors and co-repressors at the mRNA level in the four bladder cancer cell lines (RT-4, RT-112, HT1376 and EJ-28). These nuclear receptors have defined classical physiological roles in other organ systems rather than the urinary bladder. For example, VDR is expressed in the small bowel, the kidney and skin in relation to its classical role in regulating calcium reabsorption from the gastro-intestinal tract and maintaining serum calcium levels. However, this nuclear receptor has been demonstrated in diverse tissues such as the breast (Friedrich et al., 1998), the prostate (Kivineva et al., 1998b; Krill et al., 2001) and the bladder (Hermann and Andersen, 1997; Sahin et al., 2005) and has demonstrable anti-proliferative roles by upregulating genes such as p21$^{(Waf1/Cip1)}$ (Saramaki et al., 2009; Saramaki et al., 2006a).

5.1.2 Bladder cancer cell lines display a spectrum of anti-proliferative responses towards a panel of nuclear receptor ligands

Table 3.2 demonstrates the ED50 values for a panel of nine nuclear receptor ligands towards the four bladder cancer cell lines RT-4, RT-112, HT-1376 and EJ-28. Eight ligands display a range of ED50 values; 9 cis-RA does not demonstrate a dose-response curve which crosses 50 %, hence an ED50 cannot be determined. EJ-28 cells are least sensitive five of the remaining eight ligands (1α,25(OH)$_2$D$_3$, LCA, EPA, ETYA, CDCA). This particular cell line also has

the highest expression of the co-repressor NCoR1 (fig 3.3) which may be responsible for the reduced sensitivity towards these NR ligands.

5.1.3   Forced over-expression of NCoR1 leads to reduced sensitivity towards CDA, LCA and SAHA

In order to test the hypothesis that overexpression of NCoR1 in EJ28 cells may be responsible for the reduced sensitivity to some NR ligands, NCoR1 was stably over-expressed in RT-4 cells which is the most sensitive amongst the four cell lines (table 3.2). When the NCoR1 over-expressing clone#7 and mock transfected control clone were treated with 10 μM for 96 hours with a re-dose at 48 hours, there was a statistically significant reduction in the anti-proliferative response to CDA, LCA and SAHA (figure 3.8B). There was no difference in anti-proliferative response between the two clones when treated with $1\alpha,25(OH)_2D_3$, 9cis RA or ETYA. This may be due to the presence of another co-repressor in the NR complex associated with these ligands.

5.1.4   Co-treatment with HDAC inhibitor SAHA leads to a cooperative anti-proliferative response in cells which over-express NCoR1

I hypothesised that co-treatment of the bladder cancer cell lines with a histone deacetylase inhibitor, SAHA would target the co-repressor complex as HDACs co-locate with co-repressors and lead to a closed chromatin structure via deacetylation. Figure 3.9 (a)-(d) illustrate cell proliferation as % of control when the four cell lines were treated with ED25 doses of a panel of NR ligands. Interestingly, RT-112 and EJ-28, both cells which over-express NCoR1, demonstrate a strongly additive anti-proliferative effect when co-treated with

NR (except CDA in RT-112 cells) and SAHA. This may be due to increased HDAC association with the NRs secondary to raised NCoR1 expression, which may make these two cell lines (RT-112 and EJ28) more susceptible to cell death by the NR ligands in combination with SAHA.

5.1.5 LCA induces a G1/S phase cell cycle arrest in EJ-28 cells

In order to assess the mechanism of the anti-proliferative response to one of the NRs (LCA) +/- SAHA, cell cycle FACS analysis was performed as illustrated in fig 4.1. This demonstrates a clear G1/S phase cell cycle arrest when EJ-28 cells are treated with LCA. When EJ-28 are treated with LCA and SAHA in combination, there is a trend towards statistical significant accumulation of cells in G1 phase and reduction of cells in S phase, i.e. G1/S arrest. However, there is no statistical evidence of cell cycle arrest in any of the other three cell lines with LCA +/- SAHA.

5.1.6 Induction of CDKN1A (p21$^{(Waf1/Cip1)}$) and CYP3A4 upon treatment with LCA +/- SAHA

As described above, treatment with NR ligands, with or without SAHA, produces a spectrum of anti-proliferative responses. In order to investigate whether these are associated with expression of particular anti-proliferative genes, I initially measured the expression of CDKN1A which is a $1\alpha,25(OH)_2D_3$ target gene (Saramaki et al., 2009) and has also been shown to be upregulated in response to derivatives of bile acids such as CDA and ursodeoxycholic acid (Choi et al., 2003a).

Figure 4.2 illustrates expression of CDKN1A as assessed by Q-RT-PCR. SAHA induces a statistically significant rise in CDKN1A mRNA in all four cell lines; this is not surprising as it is a known SAHA target gene (Gui et al., 2004). In RT-4 cells, both LCA as well as LCA + SAHA induce a significant CDKN1A mRNA induction however, in EJ-28 cells, only the combined treatment of LCA + SAHA leads to CDKN1A expression.

CYP3A4 is the most abundant of the cytochrome p450 enzymes and is involved in detoxification of bile acids as well as xenobiotics and drugs. Hence, I investigated its expression in the bladder cancer cells in response to the secondary bile acid LCA. Figure 4.3 illustrates the induction of CYP3A4 mRNA using Q-RT-PCR. LCA treatment leads to a statistically significant induction in CYP3A4 mRNA in RT-4, HT-1376 and RT-112 cells but not EJ-28. LCA has been previously demonstrated to induce CYP3A4 induction in intestinal and liver cells (Fukumori et al., 2007; Matsubara et al., 2008) as well as in mice (Matsubara et al., 2008). The lack of induction in EJ-28 cells may be due to the over-expression of NCoR1 which may lead to a closed chromatin conformation around the CYP3A4 promoter. Interestingly, co-treatment with LCA + SAHA in EJ-28 cells does lead to significant CYP3A4 mRNA induction; SAHA may be antagonising the elevated NCoR1's co-repressor effect.

5.1.7 LCA induces a xenobiotic protective response in RT-4 cells

RT-4 cells stably transfected to overexpress NCoR1 (pNCoR#7) as well as mock transfected RT-4 cells (pcDNA#6) were treated with LCA (10μM) for 6 hours and changes in mRNA expression were investigated via Q-RT-PCR microfluidic arrays (figures 4.7 and 4.8). There are three groups of genes which display changes in expression with LCA: the ATP-binding

153

cassette transporter family of trans-membrane efflux pumps, detoxifying enzymes and cell-cycle arrest proteins. pNCoR#7 cells induce expression of ABCC3, ABCB8 and ABCA1 upon exposure to LCA; pcDNA#6 also expresses ABCB8 on LCA treatment.

SULT2A1 is a detoxifying enzyme belonging to the sulphotransferase family and plays a key role in detoxifying xenobiotics in the liver. In pNCoR#7 cells, this enzyme is down-regulated under basal conditions as compared to pcDNA#6, no doubt due to the enhanced repressor effect of NCoR1 overexpression. When pcDNA#6 cells are treated with LCA, SULT2A1 expression is increased which is probably in an effort to detoxify this bile acid.

The cell cycle arrest proteins CDKN1B/p27^{kip1} and CDKN1A / p21$^{waf1/cip1}$ are both suppressed in their basal expression in pNCoR#7 clones and upon treatment with LCA, their expression is increased in the pcDNA#6 clone by 1.4 and 1.2 fold respectively.

In the context of the cellular response to exposure to a xenobiotic, the RT-4 pcDNA#6 appear to stop dividing by inducing a cell-cycle arrest and then express genes encoding proteins that either pump toxic compounds out of the cell (e.g. members of the ATP binding cassette transporter family) or genes that encode proteins which metabolise xenobiotics and facilitate their excretion in urine (e.g. sulphotransferase enzymes).

5.2 Future Studies

5.2.1 Measurement of VDR, FXR and NCoR1 expression in human samples

Chapter 3 describes expression of a panel of nuclear receptors and co-repressors at the mRNA level (figure 3.3) and the expression of VDR (figure 3.4) and FXR (fig 3.5) at the protein level in the panel of four bladder cancer cell lines. These immortalised cell lines are a model system for bladder cancer. It is possible that the culture conditions of these cells may alter the spectrum of genes expressed by the cell lines as compared to the original bladder tumours that they were derived from; hence it is imperative that expression of the nuclear receptors and co-repressors are verified in a representative cohort of primary bladder cancer tissue. It would also be possible to assess expression in bladder biopsy samples from patients undergoing surgery for benign prostatic disease such as benign prostatic hyperplasia. This can act as an age matched normal control tissue as there are no established non-malignant bladder epithelial cell lines.

5.2.2 Chromatin Immunoprecipitation

I have demonstrated induction of CDKN1A in all four cell lines (RT-4, RT-112, HT137 and EJ-28) upon treatment with SAHA alone, in RT-4 cells upon treatment with LCA alone and in RT-4 and EJ-28 cells upon treatment with LCA and SAHA combined (figure 4.2). I have surmised that LCA is binding either VDR or FXR and is binding to its relevant response elements in the CDKN1A (p21$^{(Cip1/Waf1)}$) promoter. The traditional approaches to demonstrate binding of a nuclear receptor to a target gene promoter involved gene reporter assays or alternatively using recombinant NR DNA binding domains to enrich for DNA sequences from

libraries of random sequences. However, these approaches are hampered by numerous problems. Firstly, NR binding to a promoter sequence occurs outside the context of chromatin therefore, in vivo binding sites may differ from in vitro sites as chromatin compaction and relaxation may hide or reveal particular NR binding sites in vivo. Also, in the in vitro conditions, protein conformations of the NR DNA binding domains may be different from the vivo native conformation which may lead to differing NR/DNA binding (Massie and Mills, 2008).

These limitations are overcome via chromatin immunoprecipitation which involves treatment of cells with the particular NR ligand followed by treatment with formaldehyde which chemically cross-links DNA-protein interactions by forming covalent bonds between the exocyclic amino groups and the endocyclic imino groups of DNA bases and the α-amino groups of amino acids as well as the nitrogen side chains of lysines, arginines and histidines (Kuo and Allis, 1999). This cross-linking 'fixes' any NR-DNA interaction for further analysis. The chromatin extract is sonicated to break-up the cross-linked DNA/protein into small DNA fragments with attached proteins. This allows the DNA to be handled more easily during the incubation with specific antibody to the protein in question (VDR or FXR in our current example). The antibody incubation step immuno-precipitates DNA sequences bound to the protein in question. The antibody-protein/DNA complexes are eluted and the cross-likages are reversed by incubation in a NaCl solution incubated at 65°C (Kuo and Allis, 1999). This DNA can then be analysed in a variety of ways. Conventional PCR or Q-RT-PCR may be performed provided primer sequences are used for candidate binding regions, for example in the p21$^{(Cip1/Waf1)}$ promoter region. The immune-precipitated DNA would always be compared to the background genomic DNA to assess the degree of enrichment by immune-precipitation.

The above approach necessitates investigating transcription factor binding against a particular target gene sequence which can be amplified by a PCR reaction. Alternative strategies for an unbiased approach to identifying target binding sequences involve the ChIP on chip approach and ChIP sequencing (Zecchini and Mills, 2009).

ChIP on chip describes amplifying and fluorescent labelling the DNA fragments isolated from a round on chromatin immunoprecipitation and hybridising to a DNA microarray. Total genomic DNA is also hybridised to the microarray after labelling with a different fluorescent probe and acts as a control. Therefore, the fluorescent signals from the ChIP DNA fragments which correspond to the transcription factor binding sites would generate a significantly higher signal as compared to the total genomic DNA control (Zecchini and Mills, 2009). This technique allows for genome wide screening for nuclear receptor binding sites and allows for generation of network diagrams similar to figures 4.6-4.9 which provide a genome wide view of the disparate effects of binding of a particular nuclear receptor to its target sequences.

ChIP sequencing involves processing of DNA fragments generated from ChIP via a high throughput parallel whole genome sequencing platform such as Solexa, Roche/454 and ABI SOLiD. After a round of ChIP, the DNA fragments generated are purified and adapters are tagged to the ends of the DNA fragments. Adapters are short sequences of DNA which can be used to bind the DNA fragments to the sequencing platform. The tagged fragments are amplified and simultaneously sequenced. The analysis software will then align the different DNA fragments to the known genomic sequence and identify the identity of the fragments. This method of post ChIP analysis has the advantage of not being limited by the spacing between probes, which occurs in ChIP on chip analysis (Zecchini and Mills, 2009).

Journal publications related to this thesis

1.　　　"Elevated NCOR1 disrupts a network of dietary-sensing nuclear receptors in bladder cancer cells." **Abedin SA**, Thorne J, Battaglia S, Maguire O, Hornung L, Doherty AP, Mills IG, Campbell MJ. *Carcinogenesis* 2009 Mar;30(3):449-56. Epub 2009 Jan 6.

2.　　　"Epigenetic corruption of VDR signalling in malignancy." **Abedin SA**, Banwell CM, Colston KW, Carlberg C, Campbell MJ. *AntiCancer Research*. July 2006. 26:2557-2566.

3.　　　"Vitamin D and Cancer". Campbell MJ and **Abedin SA**. *Expert Reviews in Endocrinology and Metabolism*. 2006;1(2):219-231.

Published Abstracts

1.　　　"Targeting Farnesoid X receptor in bladder cancer cells." **Abedin SA**, Thorne J, Battaglia S, Doherty AP, Wallace DM, Campbell MJ. *BJU Int*. June 2008;101 (Supplement 5):43.

2. "Targeting novel nuclear receptors with histone deacetylase inhibitor combination therapy in bladder cancer." **Abedin SA**, Veerakumarasivam A, Kelly J, Neal DE, Mills I, Campbell MJ. *Eur Urol Suppl* 2006;5(2):36.

3. "Epigenetic corruption of dietary sensing on bladder cancer cells." **Abedin SA,** Veerakumarasivam A, Wallard M, Mills IG, Neal DE, Kelly J, Campbell MJ. *Proceedings of the AACR* 2005 Apr;46:820.

Conference Proceedings

1.   "Targeting Farnesoid X receptor in bladder cancer cells." **Abedin SA**, Thorne J, Battaglia S, Doherty AP, Wallace DM, Campbell MJ. *Annual Scientific Meeting of the British Association of Urological Surgeons*. Manchester. U.K. June 2008.

2.   "Targeting novel nuclear receptors with histone deacetylase inhibitor combination therapy in bladder cancer." **Abedin SA**, Veerakumarasivam A, Kelly J, Neal D, Mills I, Campbell M. *Annual Congress of the European Association of Urology*. Paris, France. April 2006.

3.   "Epigenetic corruption of dietary signals in bladder cancer." **Abedin SA**, Kelly J, Neal DE, Mills IG, Campbell MJ. *National Cancer Research Institute*. Annual Meeting. ICC, Birmingham, UK. Oct 2005.

4.   "Epigenetic corruption of dietary sensing capacity in bladder cancer cells." **Abedin SA**, Veerakumarasivam A, Wallard M, Mills IG, Neal DE, Kelly J, Campbell MJ. *American Association of Cancer Research*. Annual Meeting. Anaheim, California, USA 2005.

5.   "Epigenetic disruption in epithelial cancers of nuclear receptor mediated dietary sensing." Campbell MJ, **Abedin SA**, Gommersall LM, Banwell CM, Mills IG, Peehl DM, Colston KW, Turner BT. *The Alan Wolffe EMBO Conference on Chromatin and Epigenetics*. Heidelberg, Germany 2005.

6.   "Environmental sensing capacity by VDR and related nuclear receptors." **Abedin SA**, Veerakumarasivam A, Mills IG, Neal DE, Kelly JD, Campbell MJ. *2nd Symposium on Vitamin D Analogs in Cancer Prevention and Therapy*. Lübeck, Germany. May 2005.

7.   "Co-repressor complexes as targets for epigenetic therapy." Gommersall LM, Coulter HSO **Abedin SA**, Peehl DM, Doherty AP, James ND Campbell MJ. *British Prostate Group/British Association of Urologic Surgeons Joint Meeting* **2004**

Appendix 1

List of genes on Q-RT-PCRm genecard

Gene Symbol	Alternative names	Common name	LocusLink Gene Name
Cell surface transporters			
ABCA1	ABC-1, ABC1, CERP, FLJ14958, HDLDT1,	ABCA1	ATP-binding cassette, sub-family A (ABC1), member 1,Gene hCG1789838 Celera Annotation
ABCB8	MABC1; M-ABC1; EST328128	ABCB8	ATP-binding cassette, sub-family B (MDR/TAP), member 8,Gene hCG18685 Celera Annotation
ABCC3	MLP2; MRP3; ABC31;	ABCC3	ATP-binding cassette, sub-family C (CFTR/MRP), member 3,Gene hCG29634 Celera Annotation
ABCG2	MRX; MXR; ABCP; BCRP; BMDP; MXR1;	ABCG2	ATP-binding cassette, sub-family G (WHITE), member 2,Gene hCG37696 Celera Annotation
Nuclear receptors			
AR	NR3C4, AIS, DHTR, HUMARA, TFM	AR	androgen receptor (dihydrotestosterone receptor; testicular feminization; Kennedy disease),Gene hCG15093 Celera Annotation
ESR1		ERα	estrogen receptor 1,Gene hCG1811630 Celera Annotation
ESR2	NR3A2,Erb; ESRB; ESTRB;; ERα-BETA;	ERß	estrogen receptor 2 (ER beta),Gene hCG21449 Celera Annotation
NR0B1	NROB1, AHC; AHX; AHCH; DAX1;	DAX1	nuclear receptor subfamily 0, group B, member 1,Gene hCG15520 Celera Annotation

	DAX-1;		
NR1H2		LXRβ	nuclear receptor subfamily 1, group H, member 2,Gene hCG22944 Celera Annotation
NR1H3		LXRα	nuclear receptor subfamily 1, group H, member 3,Gene hCG25179 Celera Annotation
NR1H4	BAR; FXR; HRR1; HRR-1; RIP14	FXR	nuclear receptor subfamily 1, group H, member 4,Gene hCG20893 Celera Annotation
NR1I2	BXR; PAR; PRR; PXR; SAR; SXR; ONR1;	PXR	nuclear receptor subfamily 1, group I, member 2,Gene hCG21777 Celera Annotation
NR1I3	CAR; CAR1; MB67; CAR-SV1; CAR-SV4;	CAR	nuclear receptor subfamily 1, group I, member 3,Gene hCG1766510 Celera Annotation
NR3C1	GR	GR	nuclear receptor subfamily 3, group C, member 1 (glucocorticoid receptor),Gene hCG37601 Celera Annotation
PPARA		PPARα	Peroxisome proliferative activated receptor, alpha,Gene hCG41801 Celera Annotation
PPARD	FAAR; NUC1; NUCI; NR1C2; PPAR-beta	PPARδ	Peroxisome proliferative activated receptor, delta,Gene hCG17666 Celera Annotation
PPARG	NR1C3; PPARG1; PPARG2; HUMPPARG	PPARγ	Peroxisome proliferative activated receptor, gamma,Gene hCG26772 Celera Annotation
RARA	RAR; NR1B1	RARα	retinoic acid receptor, alpha,Gene hCG2007196 Celera Annotation
RARB,	HAP; RRB2; NR1B2	RARβ	retinoic acid receptor, beta,Gene hCG26863 Celera Annotation
RARG		RARγ	retinoic acid receptor, gamma,Gene hCG31521 Celera Annotation
RXRA		RXRα	retinoid X receptor, alpha,Gene hCG18150 Celera Annotation
RXRB	NR2B2; DAUDI6; RCoR-1; H-2RIIBP	RXRβ	retinoid X receptor, beta,Gene hCG2042227 Celera Annotation
THRB	THR1;NR1A2; THRB1; THRB2; ERBA-BETA	THRB	thyroid hormone receptor, beta (erythroblastic leukemia viral (v-erb-a) oncogene homolog 2, avian),Gene hCG15525 Celera Annotation
VDR	NR1I1	VDR	vitamin D (1,25- dihydroxyvitamin D3) receptor,Gene hCG27705 Celera Annotation

Nuclear receptor co-factors			
COPS2	CSN2; SGN2; ALIEN; TRIP15	ALIEN/TRIP 15	COP9 constitutive photomorphogenic homolog subunit 2 (Arabidopsis),Gene hCG41786 Celera Annotation
CREBBP	CBP	CBP	CREB binding protein (Rubinstein-Taybi syndrome),Gene hCG16633 Celera Annotation
CRSP2	EXLM1; MED14; DRIP150; TRAP170;	DRIP150/ TRAP170	cofactor required for Sp1 transcriptional activation, subunit 2, 150kDa,Gene hCG18523 Celera Annotation
CRSP6	MED17; CRSP77; DRIP80; TRAP80;	TRAP80/DR IP80	cofactor required for Sp1 transcriptional activation, subunit 6, 77kDa,Gene hCG20933 Celera Annotation
NCOA1	SRC1; NCoA-1; RIP160; F-SRC-1;	NCoA1/RIP 160	nuclear receptor coactivator 1,Gene hCG21379 Celera Annotation
NCOA2	TIF2; GRIP1; NCoA-2;	NCo-A2	nuclear receptor coactivator 2,Gene hCG18449 Celera Annotation
NCOA3	AIB1; RAC3; SRC3; pCIP;CAGH16;	NCOA3	nuclear receptor coactivator 3,Gene hCG44065 Celera Annotation
NCOA4	RFG; ELE1; PTC3; ARA70;	NCoA4	nuclear receptor coactivator 4,Gene hCG1982904 Celera Annotation
NCOR2	SMRT; SMRTE; TRAC1; TNRC14;	SMRT/NCO R2	nuclear receptor co-repressor 2,Gene hCG25303 Celera Annotation
PPARBP	PBP; MED1;RB18A; CRSP200; DRIP205; DRIP230;; TRAP220;	DRIP/ TRAP220	PPAR binding protein,Gene hCG1818520 Celera Annotation
PPARGC1A	LEM6; PGC1; PGC1A; PGC-1(alpha)	PPARGC1	Peroxisome proliferative activated receptor, gamma, coactivator 1, alpha,Gene hCG1811770 Celera Annotation
SIN3A	FLJ90319; KIAA0700; DKFZP434K2235	SIN3A/KIAA	SIN3 homolog A, transcription regulator (yeast),Gene hCG2005450 Celera Annotation

Metabolic enzymes			
ACADM	MCAD; ACAD1; MCADH	ACADM	acyl-Coenzyme A dehydrogenase, C-4 to C-12 straight chain,Gene hCG22915 Celera Annotation
AKR1C1/2	C9; DD1; DDH; DDH1; H-37; MBAB; HAKRC; MGC8954; 2-ALPHA-HSD; 20-ALPHA-HSD; DD; DD2; BABP;	AKR1C1/2	aldo-keto reductase family 1, member C1 (dihydrodiol dehydrogenase 1; 20-alpha (3-alpha)-hydroxysteroid dehydrogenase),aldo-keto reductase family 1, member C2 (dihydrodiol dehydrogenase 2; bile acid binding protein; 3-alpha hydroxysteroid dehydrogenase, type III),Gene hCG1773822 Celera Annotation
AKR1C3	DD3; HAKRB; HAKRe; HA1753; HSD17B5; hluPGFS; KIAA0119	AKR1C3	aldo-keto reductase family 1, member C3 (3-alpha hydroxysteroid dehydrogenase, type II),Gene hCG19343 Celera Annotation
ALOX5		ALOX5	arachidonate 5-lipoxygenase,Gene hCG18416 Celera Annotation
APOA1	MGC117399	APOA1	apolipoprotein A-I,Gene hCG41332 Celera Annotation
CYP24A1	P450-CC24	Cyp24	Cytochrome P450, family 24, subfamily A, polypeptide 1,Gene hCG37130 Celera Annotation
CYP27B1		Cyp27	Cytochrome P450, family 27, subfamily B, polypeptide 1,Gene hCG2014568 Celera Annotation
CYP3A4	HLP; CP34; CYP3A; NF-25; P450C3;	Cyp3A4	Cytochrome P450, family 3, subfamily A, polypeptide 4,Gene hCG17094 Celera Annotation
PTGS1	COX1; COX3; PHS1; PCOX1; PGHS1;	COX-1	prostaglandin-endoperoxide synthase 1 (prostaglandin G/H synthase and cyclooxygenase),Gene hCG31046 Celera Annotation
PTGS2	COX-2; PHS-2; PGG/HS; PGHS-2	COX-2	prostaglandin-endoperoxide synthase 2 (prostaglandin G/H synthase and cyclooxygenase),Gene hCG39885 Celera Annotation
SULT2A1		SULT2A	sulfotransferase family, cytosolic, 2A, dehydroepiandrosterone (DHEA)-preferring, member 1,Gene hCG201431 Celera Annotation
Cell death			

regulators			
BAX	Bax zeta	BAX	BCL2-associated X protein,Gene hCG1811614 Celera Annotation
CASP4	TX; ICH-2; Mih1/TX; ICEREL-II; ICE(rel)II	CASP4	caspase 4, apoptosis-related cysteine peptidase,Gene hCG40121 Celera Annotation
Transcription factors			
CEBPA	CEBP; C/EBP-alpha	C/EBPa	CCAAT/enhancer binding protein (C/EBP), alpha,Gene hCG20142 Celera Annotation
GATA3	HDR	GATA3	GATA binding protein 3,Gene hCG23634 Celera Annotation
ID1	ID	ID1	inhibitor of DNA binding 1, dominant negative helix-loop-helix protein
MYB		MYB	v-myb myeloblastosis viral oncogene homolog (avian),Gene hCG32380 Celera Annotation
SNAI1	SNA; SNAH; SLUGH2;	SNAI1	snail homolog 1 (Drosophila),Gene hCG37886 Celera Annotation
YY1	DELTA; NF-E1; UCRBP; YIN-YANG-1	YY1	YY1 transcription factor,Gene hCG25023 Celera Annotation
Histone modifiers			
AOF2	LSD1; BHC110; KIAA0601	LSD1/KIAA	amine oxidase (flavin containing) domain 2,Gene hCG38847 Celera Annotation
CARM1	PRMT4	CARM	coactivator-associated arginine methyltransferase 1,Gene hCG29972 Celera Annotation
HDAC1		HDAC1	histone deacetylase 1,Gene hCG41610 Celera Annotation
HDAC2	RPD3; YAF1	HDAC2	histone deacetylase 2,Gene hCG21384 Celera Annotation
HDAC3		HDAC3	histone deacetylase 3,Gene hCG42506 Celera Annotation
HDAC4	HD4; HDACA; HA6116; HDAC-A;	HDAC4	histone deacetylase 4,Gene hCG22188 Celera Annotation

HDAC5		HDAC5	histone deacetylase 5,Gene hCG1991411 Celera Annotation
HDAC6		HDAC6	histone deacetylase 6,Gene hCG19817 Celera Annotation
HDAC7A	HGNC	HDAC7	histone deacetylase 7A,Gene hCG27711 Celera Annotation
HDAC10	HDAC10	HDAC10	histone deacetylase 10,Gene hCG31857 Celera Annotation
PADI4	PAD; PDI4; PDI5; PADI5	PADI4	peptidyl arginine deiminase, type IV,Gene hCG25125 Celera Annotation
SET7	SET7; SET9; SET7/9; FLJ21193;	SET7/KIAA	SET domain-containing protein 7,Gene hCG37951 Celera Annotation
SIRT2		SIRT2	sirtuin (silent mating type information regulation 2 homolog) 2 (S. cerevisiae),Gene hCG1997264 Celera Annotation
SIRT6		SIRT6	sirtuin (silent mating type information regulation 2 homolog) 6 (S. cerevisiae),Gene hCG2004101 Celera Annotation
SUV39H1		SUV39A	Suppressor of variegation 3-9 homolog 1 (Drosophila),Gene hCG19814 Celera Annotation
Cell cycle regulators			
CCNB1		Cyclin B1	cyclin B1,Gene hCG27173 Celera Annotation
CCND1	BCL1; PRAD1; U21B31; D11S287E	Cyclin D1	cyclin D1 (PRAD1: parathyroid adenomatosis 1),Gene hCG2016647 Celera Annotation
CCNE1		Cyclin E1	cyclin E1,Gene hCG20435 Celera Annotation
CDC2		CDC2	Cell division cycle 2, G1 to S and G2 to M,Gene hCG40242 Celera Annotation
CDH1	UVO; CDHE; ECAD; LCAM; Arc-1; CD324	Arc-1/CDH1	cadherin 1, type 1, E-cadherin (epithelial),Gene hCG28201 Celera Annotation
CDK5		CDK5	cyclin-dependent kinase 5,Gene hCG18690 Celera Annotation
CDKN1A	P21; CIP1; WAF1; CDKN1; MDA-6;	P21$^{(waf1/cip1)}$	cyclin-dependent kinase inhibitor 1A (p21, Cip1),Gene hCG15367 Celera Annotation
CDKN1B	KIP1; CDKN4; P27KIP1	P27$^{(kip1)}$	cyclin-dependent kinase inhibitor 1B (p27, Kip1),Gene hCG27692 Celera Annotation

CDKN2A	p16	P16$^{(ink4a)}$	cyclin-dependent kinase inhibitor 2A (melanoma, p16, inhibits CDK4),Gene hCG28309 Celera Annotation
G0S2		G0S2	G0/G1switch 2,Gene hCG1641564 Celera Annotation
GADD45A		GADD45α	growth arrest and DNA-damage-inducible, alpha,Gene hCG21703 Celera Annotation
TP53		P53	tumor protein p53 (Li-Fraumeni syndrome),Gene hCG42016 Celera Annotation
RBBP4	NURF55; RBAP48	RBBP4	retinoblastoma binding protein 4,Gene hCG2032433 Celera Annotation
Signal transduction			
EGFR	ERBB; mENA; ERBB1	EGFR	epidermal growth factor receptor (erythroblastic leukemia viral (v-erb-b) oncogene homolog, avian),Gene hCG1811404 Celera Annotation
IGFBP1	AFBP; IBP1; PP12; IGF-BP25; hIGFBP-1	IGFBP1	insulin-like growth factor binding protein 1,Gene hCG2003734 Celera Annotation
IGFBP3		IGFBP3	insulin-like growth factor binding protein 3,Gene hCG1735376 Celera Annotation
IGFBP5	IBP5	IGFBP5	insulin-like growth factor binding protein 5,Gene hCG16384 Celera Annotation
IKBKB		IKKB	inhibitor of kappa light polypeptide gene enhancer in B-cells, kinase beta,Gene hCG17395 Celera Annotation
IKBKG		IKKG	inhibitor of kappa light polypeptide gene enhancer in B-cells, kinase gamma,Gene hCG2003089 Celera Annotation
MAPK4	ERK3; Erk4; PRKM4; p63MAPK	MAPK4	mitogen-activated protein kinase 4,Gene hCG23688 Celera Annotation
MAPKAPK2		MAPKAP2	mitogen-activated protein kinase-activated protein kinase 2,Gene hCG22205 Celera Annotation
MAPKAPK5		MAPKAPK5	mitogen-activated protein kinase-activated protein kinase 5,Gene hCG40141 Celera Annotation
TGFB2		TGFB2	transforming growth factor, beta 2,Gene hCG24906 Celera Annotation
TGIF	HPE4	TGIF	TGFB-induced factor (TALE family homeobox),Gene hCG1994498 Celera Annotation

Appendix 2

List of genes uniquely regulated by LCA + SAHA on Affymetrix U133 genechip array after 6 hours treatment.

Probe Set	Fold Change	Probe Set	Fold Change	Probe Set	Fold Change
ADNP	-1.63	EIF5	-1.47	PROCR	1.6
ARF6	-1.77	EIF5	-1.57	PRPF4	-1.6
ARL4C	-1.52	FAM131A	2.12	PTBP1	-1.66
BCLAF1	-2.12	FLJ12529	-1.58	PWP1	-1.36
BICD2	1.66	FSCN1	2.07	RAD21	-1.7
BRD2	-1.55	FUS	-1.62	RBM22	-1.54
BRD2	-1.56	FUS	-1.85	RBM22	-1.58
C14orf32	-1.42	GABARAPL2	1.35	RELA	-1.38
C14orf4	-1.46	HBEGF	1.48	RIN2	-1.78
C1orf43	-1.46	HN1L	-1.39	RPL37A	-1.65
		HSPA1A ///			
C1orf52	1.57	HSPA1B	1.62	RTF1	1.7
C6orf211	2.15	IL18	1.82	SAP30	1.85
C9orf5	1.43	IRF2BP2	-1.45	SC4MOL	1.59
CASC3	-1.66	LOC440983	-1.9	SHOC2	1.48
CBL	1.8	MCM2	-1.52	SMARCD1	-1.74
CDC5L	-1.68	MCM7	-1.39	SNX9	-1.49
CDCA8	-1.45	MEPCE	-3.54	SNX9	-1.56
COIL	-1.94	MLF1	1.63	STXBP1	1.96
CPOX	1.93	MPDU1	-1.7	SUPT16H	-1.85
CTF8	-1.58	MRPS10	-1.5	TBPL1	1.89
DHX15	-1.39	MRPS10	-1.61	TGIF1	-1.47
DKFZP686M0199	-1.37	MRTO4	-1.52	TM2D2	1.59
DNAJB11	1.43	MSL-1	-1.98	TMEM189	1.98
DUSP5	1.68	NOL11	-1.35	TMEM41B	1.57
EID2	1.65	NRAS	-1.52	TSR1	-1.43
EIF1	-1.46	NUP43	1.42	TUFT1	2.25
EIF1	-1.47	PCMT1	1.37	UBLCP1	1.8
EIF1	-1.53	POGK	-2.02	VAT1	1.42
EIF3A	-1.43	PPP2R1A	-1.43	WSB2	-1.57
		PRKAR1A	-1.65	ZFR	-1.39
				ZNF207	-1.49
				ZNF277	2.33
				ZNF313	1.64

Reference List

Abedin,S.A., Thorne,J.L., Battaglia,S., Maguire,O., Hornung,L.B., Doherty,A.P., Mills,I.G., and Campbell,M.J. (2009). Elevated NCOR1 disrupts a network of dietary-sensing nuclear receptors in bladder cancer cells. Carcinogenesis *30*, 449-456.

Ananthanarayanan,M., Balasubramanian,N., Makishima,M., Mangelsdorf,D.J., and Suchy,F.J. (2001). Human bile salt export pump promoter is transactivated by the farnesoid X receptor/bile acid receptor. J. Biol. Chem. *276*, 28857-28865.

Archer,S.Y., Meng,S., Shei,A., and Hodin,R.A. (1998). p21(WAF1) is required for butyrate-mediated growth inhibition of human colon cancer cells. Proc. Natl. Acad. Sci. U. S. A *95*, 6791-6796.

Augustine,A., Hebert,J.R., Kabat,G.C., and Wynder,E.L. (1988). Bladder cancer in relation to cigarette smoking. Cancer Res. *48*, 4405-4408.

Banwell,C.M., MacCartney,D.P., Guy,M., Miles,A.E., Uskokovic,M.R., Mansi,J., Stewart,P.M., O'Neill,L.P., Turner,B.M., Colston,K.W., and Campbell,M.J. (2006). Altered nuclear receptor corepressor expression attenuates vitamin D receptor signaling in breast cancer cells. Clin. Cancer Res. *12*, 2004-2013.

Bartram,H.P., Scheppach,W., Schmid,H., Hofmann,A., Dusel,G., Richter,F., Richter,A., and Kasper,H. (1993). Proliferation of human colonic mucosa as an intermediate biomarker of carcinogenesis: effects of butyrate, deoxycholate, calcium, ammonia, and pH. Cancer Res. *53*, 3283-3288.

Bell,D.A., Taylor,J.A., Paulson,D.F., Robertson,C.N., Mohler,J.L., and Lucier,G.W. (1993). Genetic risk and carcinogen exposure: a common inherited defect of the carcinogen-metabolism gene glutathione S-transferase M1 (GSTM1) that increases susceptibility to bladder cancer. J. Natl. Cancer Inst. *85*, 1159-1164.

Brockmoller,J., Cascorbi,I., Kerb,R., Sachse,C., and Roots,I. (1998). Polymorphisms in xenobiotic conjugation and disease predisposition. Toxicol. Lett. *102-103*, 173-183.

Burch,J.D., Rohan,T.E., Howe,G.R., Risch,H.A., Hill,G.B., Steele,R., and Miller,A.B. (1989). Risk of bladder cancer by source and type of tobacco exposure: a case-control study. Int. J. Cancer *44*, 622-628.

Chambers,A.E., Banerjee,S., Chaplin,T., Dunne,J., Debernardi,S., Joel,S.P., and Young,B.D. (2003). Histone acetylation-mediated regulation of genes in leukaemic cells. Eur. J. Cancer *39*, 1165-1175.

Chang,C.L., Lao-Sirieix,P., Save,V., De La Cueva,M.G., Laskey,R., and Fitzgerald,R.C. (2007). Retinoic acid-induced glandular differentiation of the oesophagus. Gut *56*, 906-917.

Chatterjee,S.J., George,B., Goebell,P.J., avi-Tafreshi,M., Shi,S.R., Fung,Y.K., Jones,P.A., Cordon-Cardo,C., Datar,R.H., and Cote,R.J. (2004). Hyperphosphorylation of pRb: a mechanism for RB tumour suppressor pathway inactivation in bladder cancer. J. Pathol. *203*, 762-770.

Cheskis,B.J., Greger,J., Cooch,N., McNally,C., Mclarney,S., Lam,H.S., Rutledge,S., Mekonnen,B., Hauze,D., Nagpal,S., and Freedman,L.P. (2008). MNAR plays an important role in ERa activation of Src/MAPK and PI3K/Akt signaling pathways. Steroids *73*, 901-905.

Choi,Y.H., Im,E.O., Suh,H., Jin,Y., Yoo,Y.H., and Kim,N.D. (2003). Apoptosis and modulation of cell cycle control by synthetic derivatives of ursodeoxycholic acid and chenodeoxycholic acid in human prostate cancer cells. Cancer Lett. *199*, 157-167.

Chomczynski,P. and Mackey,K. (1995). Substitution of chloroform by bromo-chloropropane in the single-step method of RNA isolation. Anal. Biochem. *225*, 163-164.

Chomczynski,P. and Sacchi,N. (1987). Single-step method of RNA isolation by acid guanidinium thiocyanate-phenol-chloroform extraction. Anal. Biochem. *162*, 156-159.

Cole,P., Hoover,R., and Friedell,G.H. (1972). Occupation and cancer of the lower urinary tract. Cancer *29*, 1250-1260.

Cote,R.J., Dunn,M.D., Chatterjee,S.J., Stein,J.P., Shi,S.R., Tran,Q.C., Hu,S.X., Xu,H.J., Groshen,S., Taylor,C.R., Skinner,D.G., and Benedict,W.F. (1998). Elevated and absent pRb expression is associated with bladder cancer progression and has cooperative effects with p53. Cancer Res. *58*, 1090-1094.

Crouch,S.P., Kozlowski,R., Slater,K.J., and Fletcher,J. (1993). The use of ATP bioluminescence as a measure of cell proliferation and cytotoxicity. J. Immunol. Methods *160*, 81-88.

Czerniak,B., Cohen,G.L., Etkind,P., Deitch,D., Simmons,H., Herz,F., and Koss,L.G. (1992). Concurrent mutations of coding and regulatory sequences of the Ha-ras gene in urinary bladder carcinomas. Hum. Pathol. *23*, 1199-1204.

Drocourt,L., Ourlin,J.C., Pascussi,J.M., Maurel,P., and Vilarem,M.J. (2002). Expression of CYP3A4, CYP2B6, and CYP2C9 is regulated by the vitamin D receptor pathway in primary human hepatocytes. J. Biol. Chem. *277*, 25125-25132.

Echchgadda,I., Song,C.S., Roy,A.K., and Chatterjee,B. (2004). Dehydroepiandrosterone sulfotransferase is a target for transcriptional induction by the vitamin D receptor. Mol. Pharmacol. *65*, 720-729.

Elias,E. and Mills,C.O. (2007). Coordinated defence and the liver. Clin. Med. *7*, 180-184.

Faivre,E.J. and Lange,C.A. (2007). Progesterone receptors upregulate Wnt-1 to induce epidermal growth factor receptor transactivation and c-Src-dependent sustained activation of Erk1/2 mitogen-activated protein kinase in breast cancer cells. Mol. Cell Biol. *27*, 466-480.

Falany,C.N. (1997). Enzymology of human cytosolic sulfotransferases. FASEB J. *11*, 206-216.

Filardo,E.J., Quinn,J.A., Bland,K.I., and Frackelton,A.R., Jr. (2000). Estrogen-induced activation of Erk-1 and Erk-2 requires the G protein-coupled receptor homolog, GPR30, and occurs via trans-activation of the epidermal growth factor receptor through release of HB-EGF. Mol. Endocrinol. *14*, 1649-1660.

Finlay,C.A., Hinds,P.W., Tan,T.H., Eliyahu,D., Oren,M., and Levine,A.J. (1988). Activating mutations for transformation by p53 produce a gene product that forms an hsc70-p53 complex with an altered half-life. Mol. Cell Biol. *8*, 531-539.

Finnin,M.S., Donigian,J.R., Cohen,A., Richon,V.M., Rifkind,R.A., Marks,P.A., Breslow,R., and Pavletich,N.P. (1999). Structures of a histone deacetylase homologue bound to the TSA and SAHA inhibitors. Nature *401*, 188-193.

Friedrich,M., Rafi,L., Tilgen,W., Schmidt,W., and Reichrath,J. (1998). Expression of 1,25-dihydroxy vitamin D3 receptor in breast carcinoma. J. Histochem. Cytochem. *46*, 1335-1337.

Fukumori,S., Murata,T., Taguchi,M., and Hashimoto,Y. (2007). Rapid and drastic induction of CYP3A4 mRNA expression via vitamin D receptor in human intestinal LS180 cells. Drug Metab Pharmacokinet. *22*, 377-381.

Gallagher,S.R. and Desjardins,P.R. (2008). Quantitation of DNA and RNA with absorption and fluorescence spectroscopy. Curr. Protoc. Protein Sci. *Appendix 3*, Appendix.

George,B., Datar,R.H., Wu,L., Cai,J., Patten,N., Beil,S.J., Groshen,S., Stein,J., Skinner,D., Jones,P.A., and Cote,R.J. (2007). p53 gene and protein status: the role of p53 alterations in predicting outcome in patients with bladder cancer. J. Clin. Oncol. *25*, 5352-5358.

Glaser,K.B., Staver,M.J., Waring,J.F., Stender,J., Ulrich,R.G., and Davidsen,S.K. (2003). Gene expression profiling of multiple histone deacetylase (HDAC) inhibitors: defining a common gene set produced by HDAC inhibition in T24 and MDA carcinoma cell lines. Mol. Cancer Ther. *2*, 151-163.

Gnerre,C., Blattler,S., Kaufmann,M.R., Looser,R., and Meyer,U.A. (2004). Regulation of CYP3A4 by the bile acid receptor FXR: evidence for functional binding sites in the CYP3A4 gene. Pharmacogenetics *14*, 635-645.

Goodwin,B., Hodgson,E., and Liddle,C. (1999). The orphan human pregnane X receptor mediates the transcriptional activation of CYP3A4 by rifampicin through a distal enhancer module. Mol. Pharmacol. *56*, 1329-1339.

Goto,T., Shibata,A., Sasaki,D., Suzuki,N., Hishinuma,T., Kakiyama,G., Iida,T., Mano,N., and Goto,J. (2005). Identification of a novel conjugate in human urine: bile acid acyl galactosides. Steroids *70*, 185-192.

Grossmann,C., Freudinger,R., Mildenberger,S., Husse,B., and Gekle,M. (2008). EF domains are sufficient for nongenomic mineralocorticoid receptor actions. J. Biol. Chem. *283*, 7109-7116.

Gubler,U. and Hoffman,B.J. (1983). A simple and very efficient method for generating cDNA libraries. Gene *25*, 263-269.

Gui,C.Y., Ngo,L., Xu,W.S., Richon,V.M., and Marks,P.A. (2004). Histone deacetylase (HDAC) inhibitor activation of p21WAF1 involves changes in promoter-associated proteins, including HDAC1. Proc. Natl. Acad. Sci. U. S. A *101*, 1241-1246.

Hanahan,D. and Weinberg,R.A. (2000). The hallmarks of cancer. Cell *100*, 57-70.

Hermann,G.G. and Andersen,C.B. (1997). Transitional cell carcinoma express vitamin D receptors. Scand. J. Urol. Nephrol. *31*, 161-166.

Hitomi,T., Matsuzaki,Y., Yokota,T., Takaoka,Y., and Sakai,T. (2003). p15(INK4b) in HDAC inhibitor-induced growth arrest. FEBS Lett. *554*, 347-350.

Huang,L. and Pardee,A.B. (2000). Suberoylanilide hydroxamic acid as a potential therapeutic agent for human breast cancer treatment. Mol. Med. *6*, 849-866.

Javitt,N.B., Budai,K., Miller,D.G., Cahan,A.C., Raju,U., and Levitz,M. (1994). Breast-gut connection: origin of chenodeoxycholic acid in breast cyst fluid. Lancet *343*, 633-635.

Jurutka,P.W., Thompson,P.D., Whitfield,G.K., Eichhorst,K.R., Hall,N., Dominguez,C.E., Hsieh,J.C., Haussler,C.A., and Haussler,M.R. (2005). Molecular and functional comparison of 1,25-dihydroxyvitamin D(3) and the novel vitamin D receptor ligand, lithocholic acid, in activating transcription of cytochrome P450 3A4. J. Cell Biochem. *94*, 917-943.

Kast,H.R., Goodwin,B., Tarr,P.T., Jones,S.A., Anisfeld,A.M., Stoltz,C.M., Tontonoz,P., Kliewer,S., Willson,T.M., and Edwards,P.A. (2002). Regulation of multidrug resistance-associated protein 2 (ABCC2) by the nuclear receptors pregnane X receptor, farnesoid X-activated receptor, and constitutive androstane receptor. J. Biol. Chem. *277*, 2908-2915.

Khanim,F.L., Gommersall,L.M., Wood,V.H., Smith,K.L., Montalvo,L., O'Neill,L.P., Xu,Y., Peehl,D.M., Stewart,P.M., Turner,B.M., and Campbell,M.J. (2004). Altered SMRT levels disrupt vitamin D3 receptor signalling in prostate cancer cells. Oncogene *23*, 6712-6725.

Kirkali,Z., Chan,T., Manoharan,M., Algaba,F., Busch,C., Cheng,L., Kiemeney,L., Kriegmair,M., Montironi,R., Murphy,W.M., Sesterhenn,I.A., Tachibana,M., and Weider,J. (2005). Bladder cancer: epidemiology, staging and grading, and diagnosis. Urology *66*, 4-34.

Kivineva,M., Blauer,M., Syvala,H., Tammela,T., and Tuohimaa,P. (1998). Localization of 1,25-dihydroxyvitamin D3 receptor (VDR) expression in human prostate. J. Steroid Biochem. Mol. Biol. *66*, 121-127.

Knudson,A.G., Jr. (1971). Mutation and cancer: statistical study of retinoblastoma. Proc. Natl. Acad. Sci. U. S. A *68*, 820-823.

Kolch,W., Kotwaliwale,A., Vass,K., and Janosch,P. (2002). The role of Raf kinases in malignant transformation. Expert. Rev. Mol. Med. *4*, 1-18.

Korpela,J.T., Adlercreutz,H., and Turunen,M.J. (1988). Fecal free and conjugated bile acids and neutral sterols in vegetarians, omnivores, and patients with colorectal cancer. Scand. J. Gastroenterol. *23*, 277-283.

Krill,D., DeFlavia,P., Dhir,R., Luo,J., Becich,M.J., Lehman,E., and Getzenberg,R.H. (2001). Expression patterns of vitamin D receptor in human prostate. J. Cell Biochem. *82*, 566-572.

Kumar,P., Wu,Q., Chambliss,K.L., Yuhanna,I.S., Mumby,S.M., Mineo,C., Tall,G.G., and Shaul,P.W. (2007). Direct Interactions with G alpha i and G betagamma mediate nongenomic signaling by estrogen receptor alpha. Mol. Endocrinol. *21*, 1370-1380.

Kuo,M.H. and Allis,C.D. (1999). In vivo cross-linking and immunoprecipitation for studying dynamic Protein:DNA associations in a chromatin environment. Methods *19*, 425-433.

Levin,E.R. (2008). Rapid Signaling by Steroid Receptors. Am. J. Physiol Regul. Integr. Comp Physiol.

Lin,H.Y., Chen,C.S., Lin,S.P., Weng,J.R., and Chen,C.S. (2006). Targeting histone deacetylase in cancer therapy. Med. Res. Rev. *26*, 397-413.

Liu,M., Lee,M.H., Cohen,M., Bommakanti,M., and Freedman,L.P. (1996). Transcriptional activation of the Cdk inhibitor p21 by vitamin D3 leads to the induced differentiation of the myelomonocytic cell line U937. Genes Dev. *10*, 142-153.

LOWRY,O.H., ROSEBROUGH,N.J., FARR,A.L., and RANDALL,R.J. (1951). Protein measurement with the Folin phenol reagent. J. Biol. Chem. *193*, 265-275.

Makishima,M., Okamoto,A.Y., Repa,J.J., Tu,H., Learned,R.M., Luk,A., Hull,M.V., Lustig,K.D., Mangelsdorf,D.J., and Shan,B. (1999). Identification of a nuclear receptor for bile acids. Science *284*, 1362-1365.

Martin,P., Riley,R., Back,D.J., and Owen,A. (2008). Comparison of the induction profile for drug disposition proteins by typical nuclear receptor activators in human hepatic and intestinal cells. Br. J. Pharmacol. *153*, 805-819.

Massie,C.E. and Mills,I.G. (2008). ChIPping away at gene regulation. EMBO Rep. *9*, 337-343.

Matsubara,T., Yoshinari,K., Aoyama,K., Sugawara,M., Sekiya,Y., Nagata,K., and Yamazoe,Y. (2008). Role of vitamin D receptor in the lithocholic acid-mediated CYP3A induction in vitro and in vivo. Drug Metab Dispos. *36*, 2058-2063.

McCarthy,T.C., Li,X., and Sinal,C.J. (2005). Vitamin D receptor-dependent regulation of colon multidrug resistance-associated protein 3 gene expression by bile acids. J. Biol. Chem. *280*, 23232-23242.

Messing,E.M., Young,T.B., Hunt,V.B., Gilchrist,K.W., Newton,M.A., Bram,L.L., Hisgen,W.J., Greenberg,E.B., Kuglitsch,M.E., and Wegenke,J.D. (1995). Comparison of bladder cancer outcome in men undergoing hematuria home screening versus those with standard clinical presentations. Urology *45*, 387-396.

Miller,C.W., Morosetti,R., Campbell,M.J., Mendoza,S., and Koeffler,H.P. (1997). Integrity of the 1,25-dihydroxyvitamin D3 receptor in bone, lung, and other cancers. Mol. Carcinog. *19*, 254-257.

Mitsiades,C.S., Mitsiades,N.S., McMullan,C.J., Poulaki,V., Shringarpure,R., Hideshima,T., Akiyama,M., Chauhan,D., Munshi,N., Gu,X., Bailey,C., Joseph,M., Libermann,T.A., Richon,V.M., Marks,P.A., and Anderson,K.C. (2004). Transcriptional signature of histone deacetylase inhibition in multiple myeloma: biological and clinical implications. Proc. Natl. Acad. Sci. U. S. A *101*, 540-545.

Miyamoto,H., Shuin,T., Torigoe,S., Iwasaki,Y., and Kubota,Y. (1995). Retinoblastoma gene mutations in primary human bladder cancer. Br. J. Cancer *71*, 831-835.

Moch,H., Sauter,G., Moore,D., Mihatsch,M.J., Gudat,F., and Waldman,F. (1993). p53 and erbB-2 protein overexpression are associated with early invasion and metastasis in bladder cancer. Virchows Arch. A Pathol. Anat. Histopathol. *423*, 329-334.

Morrison,A.S. (1984). Advances in the etiology of urothelial cancer. Urol. Clin. North Am. *11*, 557-566.

Morrison,A.S. and Cole,P. (1976). Epidemiology of bladder cancer. Urol. Clin. North Am. *3*, 13-29.

Nakata,S., Yoshida,T., Horinaka,M., Shiraishi,T., Wakada,M., and Sakai,T. (2004). Histone deacetylase inhibitors upregulate death receptor 5/TRAIL-R2 and sensitize apoptosis induced by TRAIL/APO2-L in human malignant tumor cells. Oncogene *23*, 6261-6271.

Nangia,A.K., Butcher,J.L., Konety,B.R., Vietmeier,B.N., and Getzenberg,R.H. (1998). Association of vitamin D receptors with the nuclear matrix of human and rat genitourinary tissues. J. Steroid Biochem. Mol. Biol. *66*, 241-246.

Neal,D.E., Sharples,L., Smith,K., Fennelly,J., Hall,R.R., and Harris,A.L. (1990). The epidermal growth factor receptor and the prognosis of bladder cancer. Cancer *65*, 1619-1625.

Niku,S.D., Stein,P.C., Scherz,H.C., and Parsons,C.L. (1994). A new method for cytodestruction of bladder epithelium using protamine sulfate and urea. J. Urol. *152*, 1025-1028.

Nimmanapalli,R., Fuino,L., Stobaugh,C., Richon,V., and Bhalla,K. (2003). Cotreatment with the histone deacetylase inhibitor suberoylanilide hydroxamic acid (SAHA) enhances imatinib-induced apoptosis of Bcr-Abl-positive human acute leukemia cells. Blood *101*, 3236-3239.

Okkels,H., Sigsgaard,T., Wolf,H., and Autrup,H. (1997). Arylamine N-acetyltransferase 1 (NAT1) and 2 (NAT2) polymorphisms in susceptibility to bladder cancer: the influence of smoking. Cancer Epidemiol. Biomarkers Prev. *6*, 225-231.

Oren,M., Maltzman,W., and Levine,A.J. (1981). Post-translational regulation of the 54K cellular tumor antigen in normal and transformed cells. Mol. Cell Biol. *1*, 101-110.

Pan,L.N., Lu,J., and Huang,B. (2007). HDAC inhibitors: a potential new category of anti-tumor agents. Cell Mol. Immunol. *4*, 337-343.

Parks,D.J., Blanchard,S.G., Bledsoe,R.K., Chandra,G., Consler,T.G., Kliewer,S.A., Stimmel,J.B., Willson,T.M., Zavacki,A.M., Moore,D.D., and Lehmann,J.M. (1999). Bile acids: natural ligands for an orphan nuclear receptor. Science *284*, 1365-1368.

Parsons,C.L., Greenspan,C., and Mulholland,S.G. (1975). The primary antibacterial defense mechanism of the bladder. Invest Urol. *13*, 72-78.

Pascussi,J.M., Gerbal-Chaloin,S., Drocourt,L., Maurel,P., and Vilarem,M.J. (2003). The expression of CYP2B6, CYP2C9 and CYP3A4 genes: a tangle of networks of nuclear and steroid receptors. Biochim. Biophys. Acta *1619*, 243-253.

Peart,M.J., Smyth,G.K., van Laar,R.K., Bowtell,D.D., Richon,V.M., Marks,P.A., Holloway,A.J., and Johnstone,R.W. (2005). Identification and functional significance of genes regulated by structurally different histone deacetylase inhibitors. Proc. Natl. Acad. Sci. U. S. A *102*, 3697-3702.

Pedram,A., Razandi,M., and Levin,E.R. (2006). Nature of functional estrogen receptors at the plasma membrane. Mol. Endocrinol. *20*, 1996-2009.

Pedram,A., Razandi,M., Sainson,R.C., Kim,J.K., Hughes,C.C., and Levin,E.R. (2007). A conserved mechanism for steroid receptor translocation to the plasma membrane. J. Biol. Chem. *282*, 22278-22288.

Peiffer,L.P., Peters,D.J., and McGarrity,T.J. (1997). Differential effects of deoxycholic acid on proliferation of neoplastic and differentiated colonocytes in vitro. Dig. Dis. Sci. *42*, 2234-2240.

Perissi,V. and Rosenfeld,M.G. (2005). Controlling nuclear receptors: the circular logic of cofactor cycles. Nat. Rev. Mol. Cell Biol. *6*, 542-554.

Peter,S. (1978). The junctional connections between the cells of the urinary bladder in the rat. Cell Tissue Res. *187*, 439-448.

Poggi,M.M., Johnstone,P.A., and Conner,R.J. (2000). Glycosaminoglycan content of human bladders. a method of analysis using cold-cup biopsies. Urol. Oncol. *5*, 234-237.

Prout,G.R., Jr., Barton,B.A., Griffin,P.P., and Friedell,G.H. (1992). Treated history of noninvasive grade 1 transitional cell carcinoma. The National Bladder Cancer Group. J. Urol. *148*, 1413-1419.

PROUT,G.R. and MARSHALL,V.F. (1956). The prognosis with untreated bladder tumors. Cancer *9*, 551-558.

Razandi,M., Alton,G., Pedram,A., Ghonshani,S., Webb,P., and Levin,E.R. (2003a). Identification of a structural determinant necessary for the localization and function of estrogen receptor alpha at the plasma membrane. Mol. Cell Biol. *23*, 1633-1646.

Razandi,M., Pedram,A., Greene,G.L., and Levin,E.R. (1999). Cell membrane and nuclear estrogen receptors (ERs) originate from a single transcript: studies of ERalpha and ERbeta expressed in Chinese hamster ovary cells. Mol. Endocrinol. *13*, 307-319.

Razandi,M., Pedram,A., Merchenthaler,I., Greene,G.L., and Levin,E.R. (2004). Plasma membrane estrogen receptors exist and functions as dimers. Mol. Endocrinol. *18*, 2854-2865.

Razandi,M., Pedram,A., Park,S.T., and Levin,E.R. (2003b). Proximal events in signaling by plasma membrane estrogen receptors. J. Biol. Chem. *278*, 2701-2712.

Richon,V.M., Sandhoff,T.W., Rifkind,R.A., and Marks,P.A. (2000). Histone deacetylase inhibitor selectively induces p21WAF1 expression and gene-associated histone acetylation. Proc. Natl. Acad. Sci. U. S. A *97*, 10014-10019.

Risch,A., Wallace,D.M., Bathers,S., and Sim,E. (1995). Slow N-acetylation genotype is a susceptibility factor in occupational and smoking related bladder cancer. Hum. Mol. Genet. *4*, 231-236.

Rodriguez-Ortigosa,C.M., Vesperinas,I., Qian,C., Quiroga,J., Medina,J.F., and Prieto,J. (1995). Taurocholate-stimulated leukotriene C4 biosynthesis and leukotriene C4-stimulated choleresis in isolated rat liver. Gastroenterology *108*, 1793-1801.

Sahin,M.O., Canda,A.E., Yorukoglu,K., Mungan,M.U., Sade,M., and Kirkali,Z. (2005). 1,25 Dihydroxyvitamin D(3) receptor expression in superficial transitional cell carcinoma of the bladder: a possible prognostic factor? Eur. Urol. *47*, 52-57.

Saiki,R.K., Scharf,S., Faloona,F., Mullis,K.B., Horn,G.T., Erlich,H.A., and Arnheim,N. (1985). Enzymatic amplification of beta-globin genomic sequences and restriction site analysis for diagnosis of sickle cell anemia. Science *230*, 1350-1354.

Saramaki,A., Banwell,C.M., Campbell,M.J., and Carlberg,C. (2006). Regulation of the human p21(waf1/cip1) gene promoter via multiple binding sites for p53 and the vitamin D3 receptor. Nucleic Acids Res. *34*, 543-554.

Saramaki,A., Diermeier,S., Kellner,R., Laitinen,H., Vaisanen,S., and Carlberg,C. (2009). Cyclical chromatin looping and transcription factor association on the regulatory regions of the p21 (CDKN1A) gene in response to 1alpha,25-dihydroxyvitamin D3. J. Biol. Chem. *284*, 8073-8082.

Sasakawa,Y., Naoe,Y., Sogo,N., Inoue,T., Sasakawa,T., Matsuo,M., Manda,T., and Mutoh,S. (2005). Marker genes to predict sensitivity to FK228, a histone deacetylase inhibitor. Biochem. Pharmacol. *69*, 603-616.

Sauter,G., Moch,H., Moore,D., Carroll,P., Kerschmann,R., Chew,K., Mihatsch,M.J., Gudat,F., and Waldman,F. (1993). Heterogeneity of erbB-2 gene amplification in bladder cancer. Cancer Res. *53*, 2199-2203.

Silverman,D.T., Alguacil,J., Rothman,N., Real,F.X., Garcia-Closas,M., Cantor,K.P., Malats,N., Tardon,A., Serra,C., Garcia-Closas,R., Carrato,A., Lloreta,J., Samanic,C.,

Dosemeci,M., and Kogevinas,M. (2008). Does increased urination frequency protect against bladder cancer? Int. J. Cancer *123*, 1644-1648.

Smital,T., Luckenbach,T., Sauerborn,R., Hamdoun,A.M., Vega,R.L., and Epel,D. (2004). Emerging contaminants--pesticides, PPCPs, microbial degradation products and natural substances as inhibitors of multixenobiotic defense in aquatic organisms. Mutat. Res. *552*, 101-117.

Sporstol,M., Tapia,G., Malerod,L., Mousavi,S.A., and Berg,T. (2005). Pregnane X receptor-agonists down-regulate hepatic ATP-binding cassette transporter A1 and scavenger receptor class B type I. Biochem. Biophys. Res. Commun. *331*, 1533-1541.

Stenzl,A., Hennenlotter,J., and Schilling,D. (2008). Can we still afford bladder cancer? Curr. Opin. Urol. *18*, 488-492.

Swales,K.E., Korbonits,M., Carpenter,R., Walsh,D.T., Warner,T.D., and Bishop-Bailey,D. (2006). The farnesoid X receptor is expressed in breast cancer and regulates apoptosis and aromatase expression. Cancer Res. *66*, 10120-10126.

Taylor,J.A., Umbach,D.M., Stephens,E., Castranio,T., Paulson,D., Robertson,C., Mohler,J.L., and Bell,D.A. (1998). The role of N-acetylation polymorphisms in smoking-associated bladder cancer: evidence of a gene-gene-exposure three-way interaction. Cancer Res. *58*, 3603-3610.

Teng,S., Jekerle,V., and Piquette-Miller,M. (2003). Induction of ABCC3 (MRP3) by pregnane X receptor activators. Drug Metab Dispos. *31*, 1296-1299.

Thorne,J. and Campbell,M.J. (2008). The vitamin D receptor in cancer. Proc. Nutr. Soc. *67*, 115-127.

Tirona,R.G., Lee,W., Leake,B.F., Lan,L.B., Cline,C.B., Lamba,V., Parviz,F., Duncan,S.A., Inoue,Y., Gonzalez,F.J., Schuetz,E.G., and Kim,R.B. (2003). The orphan nuclear receptor HNF4alpha determines PXR- and CAR-mediated xenobiotic induction of CYP3A4. Nat. Med. *9*, 220-224.

Walz,T., Haner,M., Wu,X.R., Henn,C., Engel,A., Sun,T.T., and Aebi,U. (1995). Towards the molecular architecture of the asymmetric unit membrane of the mammalian urinary bladder epithelium: a closed "twisted ribbon" structure. J. Mol. Biol. *248*, 887-900.

Wong,C.W., McNally,C., Nickbarg,E., Komm,B.S., and Cheskis,B.J. (2002). Estrogen receptor-interacting protein that modulates its nongenomic activity-crosstalk with Src/Erk phosphorylation cascade. Proc. Natl. Acad. Sci. U. S. A *99*, 14783-14788.

Wrighton,S.A., Vandenbranden,M., and Ring,B.J. (1996). The human drug metabolizing cytochromes P450. J. Pharmacokinet. Biopharm. *24*, 461-473.

Xie,W., Barwick,J.L., Downes,M., Blumberg,B., Simon,C.M., Nelson,M.C., Neuschwander-Tetri,B.A., Brunt,E.M., Guzelian,P.S., and Evans,R.M. (2000). Humanized xenobiotic response in mice expressing nuclear receptor SXR. Nature *406*, 435-439.

Xu,W., Ngo,L., Perez,G., Dokmanovic,M., and Marks,P.A. (2006). Intrinsic apoptotic and thioredoxin pathways in human prostate cancer cell response to histone deacetylase inhibitor. Proc. Natl. Acad. Sci. U. S. A *103*, 15540-15545.

Xu,W.S., Parmigiani,R.B., and Marks,P.A. (2007). Histone deacetylase inhibitors: molecular mechanisms of action. Oncogene *26*, 5541-5552.

Zecchini,V. and Mills,I.G. (2009). Putting chromatin immunoprecipitation into context. J. Cell Biochem. *107*, 19-29.

Zhang,X.D., Gillespie,S.K., Borrow,J.M., and Hersey,P. (2004). The histone deacetylase inhibitor suberic bishydroxamate regulates the expression of multiple apoptotic mediators and induces mitochondria-dependent apoptosis of melanoma cells. Mol. Cancer Ther. *3*, 425-435.

Zhuang,S.H., Schwartz,G.G., Cameron,D., and Burnstein,K.L. (1997). Vitamin D receptor content and transcriptional activity do not fully predict antiproliferative effects of vitamin D in human prostate cancer cell lines. Mol. Cell Endocrinol. *126*, 83-90.